Universidad Zaragoza
1542

Trabajo Fin de Máster

Análisis de los Gráficos de Poincaré y desarrollo de Interfaz Gráfica de Usuario para el estudio de la Variabilidad del Ritmo Cardíaco en niños asmáticos

Poincaré Plot Analysis and Graphical User Interface development for the study of Heart Rate Variability in asthmatic children

Autor

Javier Milagro Serrano

Director

Jari Viik

Ponente

Raquel Bailón Luesma

Escuela de Ingeniería y Arquitectura

Julio 2016

RESUMEN

El asma es una enfermedad respiratoria crónica, que provoca inflamación y estrechamiento de las vías respiratorias. Aunque se trata de una enfermedad que puede afectar a personas de cualquier edad, suele desarrollarse durante la infancia. A pesar de ello y de que el diagnóstico de asma en adultos ha sido extensamente estudiado y estandarizado, todavía no existe un método clínico para el diagnóstico prematuro de asma en niños, lo que dota a este proceso de un carácter subjetivo que depende de los criterios del médico que realiza el estudio. El desarrollo de un método estandarizado para el diagnóstico de asma en niños es un tema de alto interés clínico, ya que tanto el número de niños asmáticos como la gravedad del asma que padecen se ha incrementado drásticamente en los últimos años, hasta el punto de que actualmente el asma se considera la enfermedad crónica más común durante la infancia en Estados Unidos.

Uno de los síntomas más comunes entre los pacientes asmáticos es la hiper-reactividad broquial, y varias fuentes bibliográficas han relacionado la patofisiología del asma con un funcionamiento anómalo del sistema nervioso autónomo, que es el responsable de los mecanismos de bronco-constricción. El sistema nervioso autónomo es la rama del sistema nervioso central implicada en el control de las acciones involuntarias, como respirar, hacer la digestión o incluso de modificar el ritmo cardiaco. Dentro del sistema nervioso autónomo pueden distinguirse dos ramas principales: el sistema nervioso simpático, que es el encargado de preparar al cuerpo para afrontar una situación de peligro o estrés, y el sistema nervioso parasimpático, cuya misión es llevar al cuerpo a un estado de relajación o calma. El correcto balance entre la acción de estos sistemas opuestos es fundamental para mantener nuestro organismo en un estado de homeostasis.

El sistema nervioso autónomo es también el encargado de controlar el ritmo cardíaco, que no es constante de latido a latido sino que es objeto de pequeñas variaciones en función de la actividad nerviosa de los sistemas simpático y parasimpático. Estas variaciones son lo que se conoce como variabilidad del ritmo cardíaco. El análisis de la variabilidad del ritmo cardíaco ha despertado un enorme interés científico en las últimas décadas debido a que, al estar dicha variabilidad regulada por el sistema nervioso autónomo, a partir de ella puede extraerse la actividad simpática y parasimpática subyacente. Como tanto la variabilidad del ritmo cardíaco como los mecanismos de bronco-constricción se rigen por la actividad del sistema nervioso autónomo, las alteraciones en el funcionamiento del sistema parasimpático relacionadas con la patogénesis del asma podrían verse reflejadas en la variabilidad del rimo cardíaco. De este modo, podría encontrarse en la variabilidad del ritmo cardíaco una fuente fiable de información acerca de los procesos subyacentes implicados en la aparición del asma.

El análisis de la variabilidad del ritmo cardíaco se ha desarrollado tradicionalmente tanto en el dominio temporal como en el dominio frecuencial. Mientras que los métodos para el análisis en el dominio temporal son computacionalmente simples, los métodos para el análisis en el dominio de la frecuencia proporcionan información sobre el origen de las variaciones observadas en el ritmo cardíaco (actividad simpática o parasimpática). Sin embargo, en los últimos años ha sido ampliamente aceptada la hipótesis de que el sistema cardiovascular presenta un comportamiento no lineal, lo que implica que los métodos clásicos en los dominios del tiempo y la frecuencia no estarías representado correctamente los procesos que generan

dicho comportamiento. De este modo, se considera que el empleo de técnicas no lineales podría proporcionar una descripción mucho más exacta del comportamiento del sistema cardiovascular. En esta línea, existen muchas fuentes en la bibliografía que proponen la aplicación de diferentes técnicas no lineales para el análisis de la variabilidad del ritmo cardiaco. En este trabajo, el método empleado es el conocido como gráfico de Poincaré.

El gráfico de Poincaré, también llamado mapa de retorno o de Lorentz, es una técnica derivada de la dinámica de sistemas no lineales, y constituye una herramienta visual y cuantitativa en la que la forma del gráfico permite clasificar el funcionamiento del sistema cardiovascular en diferentes clases, atendiendo al grado y tipo de enfermedad del paciente estudiado. Básicamente, el gráfico de Poincaré es generado mediante la representación de cada intervalo RR (el periodo temporal entre latidos consecutivos) como una función del intervalo RR previo. A pesar de las características no lineales intrínsecas en este método, los índices extraídos a partir de él han demostrado presentar una alta correlación con los parámetros temporales y frecuenciales clásicos, lo que indica que no se está aprovechando el comportamiento no lineal del mismo.

De este modo, los objetivos del presente trabajo pueden resumirse en los siguientes puntos:

- Analizar en detalle los orígenes del gráfico de Poincaré y su relación con los parámetros clásicos en el análisis de la variabilidad del ritmo cardíaco con el propósito de proponer nuevos parámetros que reflejen características no lineales adicionales.
- Aplicar estos nuevos índices al grupo de estudio, compuesto por varios pacientes de entre 3 y 7 años, para intentar clasificarlos en función del riesgo de padecer asma que presentan.
- Debido a que el gráfico de Poincaré es comúnmente definido como una herramienta de carácter visual y cuantitativo, se propone también el desarrollo de una interfaz gráfica de usuario, que permita estudiar las diferentes características de los gráficos de manera sencilla y que permita una comparación rápida con los parámetros clásicos en el estudio de la variabilidad del ritmo cardíaco.

La base de datos utilizada en el presente trabajo está compuesta por 34 pacientes con edades de entre 3 y 7 años, todos ellos transferidos a la Unidad Pediátrica de Alergias del Hospital Universitario de Helsinki debido a síntomas recurrentes o persistentes en la sección inferior del tracto respiratorio. Los pacientes fueron clasificados en tres grupos diferentes atendiendo al riesgo de padecer asma (es importante tener en cuenta que esta clasificación no es en base al diagnóstico positivo o negativo de padecer asma, sino a términos probabilísticos de padecerla en un futuro): alto riesgo, bajo riesgo y un tercer grupo de pacientes bajo tratamiento (corticoesteroides inhalados).

A pesar de que la duración de las señales disponibles varía entre 9 y 19 horas cada una, en este trabajo se han estudiado sólo los segmentos correspondientes al periodo nocturno, cuando los pacientes están durmiendo. Esto es debido a que la tos y otros síntomas relacionados con episodios asmáticos son más frecuentes durante la noche o de madrugada, debido a una disminución de la función pulmonar en estos periodos.

Todas las señales fueron adquiridas utilizando dispositivos especialmente adaptados y diseñados por la Universidad Tecnológica de Tampere (Finlandia). Dichos dispositivos disponen

de cuatro electrodos que fueron simétricamente dispuestos en la sección proximal de los brazos y en el tórax. La frecuencia de muestreo utilizada por los dispositivos es de 256 Hz.

En cuanto a los métodos empleados, el primer paso es la definición de los nuevos parámetros que se van a extraer a partir de los gráficos de Poincaré (el estudio detallado de los orígenes de este método y de la relación de los parámetros que se obtienen a partir del gráfico con los parámetros clásicos empleados en el análisis de la variabilidad del ritmo cardíaco pueden consultarse en el apartado 3.4 de la memoria). Atendiendo a la naturaleza visual de esta herramienta, en este trabajo se proponen dos nuevos parámetros: el ángulo del gráfico y la evolución temporal de su forma.

El primero de los parámetros propuestos es el ángulo del gráfico de Poincaré que, en condiciones normales, es de 45^{o} debido a la acción opuesta de las ramas simpática y parasimpática del sistema nervioso autónomo. La hipótesis subyacente a la definición de este parámetros es que cambios prolongados en el tiempo en el ritmo cardíaco (tanto aceleración como deceleración del ritmo cardíaco medio) podrían provocar una variación en el ángulo del gráfico, pudiendo ser un indicador de episodios asmáticos. Para la obtención del ángulo del gráfico se utiliza un algoritmo de descomposición en valores singulares (SVD, por sus siglas en inglés).

El siguiente parámetro propuesto es la evolución temporal de la forma del gráfico de Poincaré. A pesar de que la forma de este tipo de gráficos ya ha sido estudiada, demostrándose válida como estratificadora de ciertas enfermedades cardiovasculares, este análisis de ha desarrollado siempre de manera visual en la literatura, y siempre considerando periodos largos de señal. Lo que se propone en este trabajo es el análisis automático de la forma del gráfico de Poincaré generado a partir de segmentos de sólo cinco minutos de duración, con incrementos temporales de un minuto, lo que nos permite evaluar la evolución temporal del gráfico minuto a minuto. El valor numérico asignado para cada forma observada (llamado *Sh* en la memoria y cuya definición puede observarse en la ecuación 5.3) tiene dos componentes fundamentales: la relación entre la desviación típica en las direcciones perpendicular y paralela a la línea de identidad del gráfico, que constituye una medida de como de circular es la forma observada, y la relación entre las desviaciones estándar en la dirección perpendicular a la línea de identidad del gráfico en el 30% y el 70% de la longitud del mismo, que representa una medida de simetría. La variación en el tiempo de este parámetro *Sh* podría ofrecer información adicional a aquella proporcionada por los parámetros clásicos extraídos a partir del gráfico de Poincaré.

Otra técnica implementada en este trabajo e intrínsecamente relacionada con los gráficos de Poincaré es un método de filtrado basado en clusters (conocido como DBSCAN por sus siglas en inglés), así como una versión más avanzada del mismo (EDBSCAN) que plantean la posibilidad de eliminar latidos ectópicos (latidos que no tienen origen en el nodo sinusal y que, por lo tanto, no representan la actividad del sistema nervioso autónomo) en el dominio de los gráficos de Poincaré. El algoritmo EDBSCAN se implementa en este trabajo en combinación con otro método de filtrado mucho más simple, conocido como *Square filter*, que se aplica también en el domino de los gráficos de Poincaré, y que consiste en establecer unos límites pasados los cuales un latido no tiene sentido fisiológico, por lo que debe ser eliminado del estudio posterior.

En lo referente al análisis de los resultados y de los métodos estadísticos empleados, pueden distinguirse varias fases. En primer lugar, todas las señales fueron interpoladas a 1000 Hz para poder ser utilizadas en el software Biosigbrowser (desarrollado por el grupo BSICoS de la Universidad de Zaragoza), cuyo objetivo es obtener los tiempos de ocurrencia de cada latido. Una vez conocidos dichos tiempo, el siguiente paso es calcular los intervalos RR (distancia entre latidos consecutivos) mediante diferenciación en el dominio discreto, tras lo cual resulta sencillo obtener los gráficos de Poincaré representando cada intervalo RR como función del anterior. Como se ha explicado previamente, este proceso se realizó solamente para los periodos correspondientes a la noche (entre las 22:30 y las 05:00). Además tanto los gráficos de Poincaré como todos los parámetros obtenidos (temporales, frecuenciales y dominio de los gráficos de Poinacaré) fueron calculados en intervalos de 5 minutos, con incrementos de 1 minuto. De este modo, se dispone de la evolución temporal de dichos parámetros minuto a minuto. Todos los parámetros obtenidos, así como una explicación más detallada de los procesos seguidos para ello puede consultarse en los apartados 3 y 5.4 de la memoria respectivamente. Una vez calculados todos los parámetros a analizar para cada uno de los pacientes, los pacientes son divididos en grupos atendiendo a su riesgo de padecer asma, y un test no paramétrico de Wilcoxon es aplicado para comprobar si los parámetros estudiados presentan diferencias significativas en cada uno de los grupos.

Como resultados del proyecto encontramos, en primer lugar, la interfaz gráfica de usuario empleada en el análisis de los gráficos de Poincaré. Todas las características así como un resumen de las principales ventanas de dicha interfaz pueden consultarse en el apartado 6 de la memoria.

En cuanto al análisis estadístico de los diferentes parámetros analizados, los resultados de los test de Wilcoxon aplicados muestran que, en muchos casos, ninguno de ellos muestra diferencias significativas entre los diferentes grupos. A pesar de que a lo largo de la noche sí que aparecen periodos en los que algunos de los índices son capaces de clasificar correctamente a los pacientes, se trata de casos aislados y, por lo tanto, no puede considerarse que dichos índices sean representativos del riesgo de padecer asma.

El problema principal que encontramos aquí es que los pacientes no están clasificados en función de si les ha sido diagnosticado asma o no, sino simplemente del riesgo que presentan de sufrir asma (atendiendo a la evaluación de un parámetro conocido como índice modificado de predicción de asma, que se deriva de la presencia de ciertos síntomas frecuentemente relacionados con el asma). De este modo, puede ocurrir que pacientes clasificados en los diferentes grupos presenten o no presenten asma, estando por lo tanto los pacientes asmáticos (en caso de haberlos) distribuidos entre los diferentes grupos. Por otro lado, tanto la evolución temporal de los parámetros analizados mostrados en la interfaz gráfica desarrollada como las tablas de resultados muestra la existencia de una alta variabilidad en los valores de los parámetros entre los diferentes sujetos, incluso entre aquellos pertenecientes a un mismo grupo. Esto causa que los valores medianos y las desviaciones típicas de los valores obtenidos en el análisis de los diferentes grupos de pacientes por separado muestren valores muy similares, lo que hace imposible distinguirlos. Además, como la hipótesis subyacente a los nuevos parámetros extraídos de los gráficos de Poincaré consistía en la posibilidad de observar diferencias entre los sujetos asmáticos y los no asmáticos, la validez de dichos índices no ha podido ser demostrada en la base de datos disponible, debido a que no es posible extraer una referencia de la información disponible para poder establecer comparaciones.

A partir de los resultados obtenidos, pueden establecerse varias líneas de trabajo futuras:

- Llevar a cabo una ampliación de las capacidades de la interfaz gráfica de usuario, incluyendo la posibilidad de analizar otros índices no lineales o la selección del intervalo temporal de análisis deseado (que hasta ahora es fijo y de 5 minutos).
- Comprobar la validez de los nuevos índices propuestos en una base de datos más sólida y que cuente con una referencia de pacientes asmáticos y no asmáticos, para poder estudiar si dichos parámetros aportan información adicional a aquella proporcionada por los índices clásicos.
- Implementar un método para corregir los gráficos de Poincaré en función del ángulo observado: si el ángulo de los gráficos no es de 45º, se está cometiendo un error en el cálculo de los parámetros típicamente derivados de ellos, que puede evitarse ajustando los gráficos en función de dicho ángulo.
- Desarrollar un método para conseguir una estimación de la forma de los gráficos más exacta: al trabajar sobre segmentos de 5 minutos de duración, se dispone de pocos puntos, lo que puede llevar a errores en la clasificación automática de la forma.
- Corregir el algoritmo EDBSCAN, que se muestra muy restrictivo en algunos casos, eliminando información útil junto con los ectópicos.

Todo el trabajo presentado a continuación ha sido desarrollado en colaboración con la Universidad Tecnológica de Tampere y con la Universidad de Zaragoza, y está además enmarcado en un proyecto de investigación doctoral titulado “Evaluación no invasiva del sistema nervioso autónomo a través de la variabilidad de bioseñales. Aplicación a situaciones clínicas relacionadas con el estrés.” (“Noninvasive evaluation of autonomic nervous system through the variability of biosignals. Application to stress-related clinical situations.”). El estudio desarrollado en este trabajo será continuado durante el desarrollo del proyecto.

Como todavía no existe un método clínico para la detección prematura de asma durante la infancia, el tema tratado aquí constituye un campo de investigación interesante en el que aún quedan muchos progresos por hacer. La hipótesis inicial que da sentido a este trabajo es que la actividad anómala del sistema nervioso autónomo está estrechamente relacionada con la patogénesis del asma, por lo que el análisis de la actividad del sistema nervioso autónomo a través de la variabilidad del ritmo cardíaco podría ser de gran utilidad para comprender los mecanismos subyacentes a esta patología.

En este trabajo se ha estudiado la capacidad de los diferentes índices usados en el análisis de la variabilidad del ritmo cardíaco así como de dos nuevos parámetros extraídos del gráfico de Poincaré para estratificar el riesgo de padecer asma. Sin embargo, los resultados obtenidos no han sido significativos, por lo que ninguno de los índices estudiados puede utilizarse para este propósito. De este modo, pueden plantearse futuros estudios para buscar un método robusto y efectivo que permita detectar el asma en niños de forma precisa, ya que el número de pacientes que presentan asma de forma prematura ha aumentado drásticamente en las últimas décadas. La aplicación de técnicas basadas en análisis de la variabilidad del ritmo cardíaco está justificada como una forma no invasiva de afrontar este problema.

Además del análisis de los diferentes índices, se ha desarrollado una interfaz gráfica de usuario, que ha demostrado ser de gran utilidad a la hora de interpretar la información

contenida en los gráficos de Poincaré, permitiendo también compararla de forma sencilla con la proporcionada por los parámetros temporales y frecuenciales clásicos.

Por último, la información proporcionada por los nuevos parámetros propuestos no ha podido ser analizada, debido a que ninguno de los índices estudiados es capaz de distinguir entre pacientes y, por lo tanto, no se dispone de una referencia. En este aspecto, análisis más detallados de los gráficos de Poincaré podrían suponer la definición de nuevos parámetros para su interpretación, debido a que la información disponible hasta ahora está altamente correlada con los parámetros clásicos y, por lo tanto, no explota las características no lineales de este método de análisis.

TAMPEREEN TEKNILLINEN YLIOPISTO
TAMPERE UNIVERSITY OF TECHNOLOGY

FRANCISCO JAVIER MILAGRO

POINCARÉ PLOT ANALYSIS AND GRAPHICAL USER INTERFACE DEVELOPMENT FOR THE STUDY OF HEART RATE VARIABILITY IN ASTHMATIC CHILDREN

Master of Science thesis

Examiner: Prof. Jari Viik
Examiner and topic approved by the
Faculty Council of the Faculty of
Computing and Electrical Engineering
on 4th May 2016

ABSTRACT

FRANCISCO JAVIER MILAGRO: Poincaré Plot analysis and Graphical User Interface development for the study of Heart Rate Variability in asthmatic children
Tampere University of Technology
Master of Science thesis, 66 pages, 15 Appendix pages
June 2016
Master's Degree Programme in Information Technology
Major: Biomedical Engineering
Examiner: Prof. Jari Viik
Keywords: HRV, Poincaré plot, asthma, non-linear analysis, GUI

Asthma is a chronic lung disease that inflames and narrows the airways, and although it affects people of all ages it most often starts during childhood. However, there is still not a clinical method for the premature diagnosis of asthma, what makes it dependent on the doctor criteria.

Some studies have shown that the pathophysiology of asthma is related with an abnormal ANS function that is responsible of bronchoconstriction. As ANS activity is reflected in HRV, the analysis of this HRV could lead to an interpretation of the physiologic processes underlying asthma, thus serving as a non-invasive way to diagnose it. It is nowadays agree that the several processes involved in HR control interact in a non-linear way and so non-linear analysis of HRV has received high research interest in the last years, so in this work the focus is on Poincaré plot analysis, which is one of the most representative non-linear HRV analysis techniques.

Poincaré plot is a quantitative-visual technique extracted from non-linear dynamics, although the indexes extracted from it have been proven to not provide additional information to that obtained with other methods. Due to this fact, in this work a research in the origins of Poincaré plot has been attempted, in order to define new parameters that can display the non-linear characteristics of the plot. The angle of the plot and the short-term analysis of its shape were proposed, being the objective to find an index that can be used to classify a set of patients aged 3-7 years attending to their risk of suffering from asthma. Furthermore, a GUI was developed so that the information provided by Poincaré plots can be easily compared and integrated with the information extracted from several other indexes.

Although the methods proposed for the extraction of the angle and the shape information were successful, the results obtained in this work showed that the use of both the classical HRV indexes and the new proposed parameters is not enough to stratify the risk of asthma in children. However, the GUI developed was shown to result useful when interpreting Poincaré plot information. Also a qualitative analysis of a Poincaré domain filtering technique proposed in the literature was performed, and several future work lines were established.

PREFACE

In first place, I would like to thank my supervisors Raquel Bailón (University of Zaragoza) and Jari Viik (Tampere University of Technology) for their advice and constant interest and availability. Their invaluable help and support have made this thesis possible.

I would also like to be grateful of my family, who has made my studies in Tampere University of Technology possible. Thank you for your help and affection.

Finally, I can not forget the wonderful people I have met here in Tampere, who have also encouraged me when I have needed it. To all of them, thank you.

Tampere, 24.5.2016

Francisco Javier Milagro

TABLE OF CONTENTS

LIST OF FIGURES

LIST OF TABLES

LIST OF ABBREVIATIONS AND SYMBOLS

ANS	Autonomic Nervous System
AR	Autoregressive
AV	Atrioventricular
CNS	Central Nervous System
DBSCAN	Density-Based Spatial Clustering of Applications with Noise
ECG	Electrocardiogram
EDBSCAN	Ensemble Density-Based Spatial Clustering of Applications with Noise
ENS	Enteric Nervous System
FFT	Fast Fourier Transform
GUI	Graphical User Interface
HF	High Frequency
HR	Heart Rate
HRV	Heart Rate Variability
IPFM	Integrated Pulse Frequency Modulation
LF	Low Frequency
NN	Normal-to-Normal
PNS	Parasympathetic Nervous System
PSD	Power Spectral Density
RMSSD	Root Mean Square of Successive Differences
RSA	Respiratory Sinus Arrhythmia
SA	Sinoatrial
SDANN	Standard Deviation of Averaged NN intervals
SDNN	Standard Deviation of NN intervals
SDSD	Standard Deviation of the Successive Differences
SNS	Sympathetic Nervous System
TINN	Triangular Interpolation of the NN interval
TP	Total Power
ULF	Ultra Low Frequency
VLF	Very Low Frequency
	Uniform Resource Locator

1. INTRODUCTION

Asthma is a chronic lung disease that inflames and narrows the airways, and although it affects people of all ages it most often starts during childhood. Actually, in the past three decades a dramatic increase of the incidence and the prevalence of asthma has been observed among children [1], and asthma is nowadays considered in the United States as the most common chronic disease of childhood [2]. In spite of this fact, there is still not a clinical method for the premature diagnosis of asthma, what makes it dependent on the doctor criteria.

One of the main symptoms of asthma is bronchial hyper-reactivity, which appears to be related with abnormal autonomic nervous system (ANS) function [3]. Moreover, some studies reveal that the pathogenesis of asthma might be closely related to an improper activity of the parasympathetic branch of the ANS [4] as it is involved in bronchoconstriction mechanisms [5][6].

Nowadays, the study of ANS function through heart rate variability (HRV) analysis has received a wide research interest, as it has been proved as a powerful tool for the non-invasive investigation of the ANS activity and the underlying physiological processes that are controlled by it. Due to the fact that both, the pathogenesis of asthma and the HRV are predominantly dependent on ANS activity, the altered parasympathetic function responsible of asthma symptoms may be reflected by changes in heart rate (HR) [4][7]. Hence, HRV analysis could be a reliable source of information of the intrinsic processes that produce asthma. In this way, diagnosis of asthma could be enhanced with the information provided by the study of HRV.

HRV has been often characterized by the use of time and frequency domain methods. While time domain methods are computationally simple, frequency domain methods provide information about the origin of the variations observed in HR (sympathetic or parasympathetic branch of the ANS). However, since some years ago it is commonly accepted that the cardiovascular system has a nonlinear behaviour [8][9], what implies that the classical indexes may not be the best approach to study them. In

this way, nonlinear techniques are thought to be able to provide a better description of the cardiovascular function [10].

Although several nonlinear approaches for the analysis of HRV have been proposed in the literature, in this work the focus is on Poincaré plot, which is a new visual and quantitative technique whereby different shapes can be classified into different functional classes, thus indicating the degree of heart failure in a subject [10][11][12]. Essentially, Poincaré plot consist in the representation of each RR interval (the period between consecutive heart beats) as a function of the previous RR interval. As it is a visual technique, in this work a Graphical User Interface (GUI) for the analysis of Poincaré plot and its relation with the classical time and frequency domain indexes is developed. It also allows to display more complicated versions of Poincaré plot (higher order and lagged plots), and to extract information about the shape of the plot in order to aid on its classification.

In spite of the fact that Poincaré plot is a method taken from nonlinear dynamics some authors have proved that the measures extracted from it are highly correlated with both time [13] and frequency [14] domain classical indexes, so the nonlinear features of the plot are not being exploited. Here, the analysis of two new parameters extracted from Poincaré plot is proposed. These new parameters and also the commonly used ones are studied in this work in order to see if they are capable of distinguishing between subjects with different risk of suffering from asthma.

This Master's Thesis is developed in collaboration with the University of Zaragoza, and is integrated within a Ph.D. project titled "Noninvasive evaluation of autonomic nervous system through the variability of biosignals. Application to stress-related clinical situations". This project is developed by the Biomedical Signal Interpretation and Computational Simulation (BSICoS) group.

2. ANATOMICAL AND PHYSIOLOGICAL BACKGROUND

2.1 Cardiovascular system

The cardiovascular system, also known as circulatory system, plays a vital role in the survival of the human body, as it is responsible for delivering oxygen and nutrients and removing wastes from organs. It is composed by the heart, the blood and the blood vessels.

The heart is a pyramidal-shaped organ which is enclosed within the inferior mediastinum, the middle cavity of the thorax, and flanked on each side by the lungs. It is essentially composed by muscular tissue, as well as connective and fibrous tissues [15] [16]. The heart has four chambers or cavities, two atria (in the upper side) and two ventricles (in the lower side), and left atria and ventricle are separated from their right homonyms by the interatrial and the interventricular septum respectively [16]. Figure 2.1 shows a more complete anatomical vision of the heart.

The mechanical functioning of the heart consists of two phases: diastole and systole. During diastole, atria do contract in order to fill the ventricles with the blood coming from either the cava vein or the pulmonary vein. Once the diastole has finished, systole starts, and ventricular contraction takes place for pumping the blood to the rest of the body. The conduction of the blood along the body is possible due to blood vessels and can be divided into two different circuits known as pulmonary and systemic circuits (Figure 2.2). The pulmonary circuit has its origin on the right atrium, when oxygen poor and CO_2 rich blood arrives from the superior and inferior venae cava. The right atrium pumps this blood into the right ventricle which further pumps it into the lungs through the pulmonary arteries. After the gas exchange that takes place in the lungs, the blood is returned to the left atrium through the pulmonary veins. The systemic circuit starts in the left atrium which pumps oxygen rich and CO_2 poor blood into the left ventricle that further pumps

this blood to the rest of the body though the aorta. After the exchange of gases, nutrients and wastes that takes place in the different organs of the body, the blood returns to the right atrium through the vena cava, thus starting the process again.

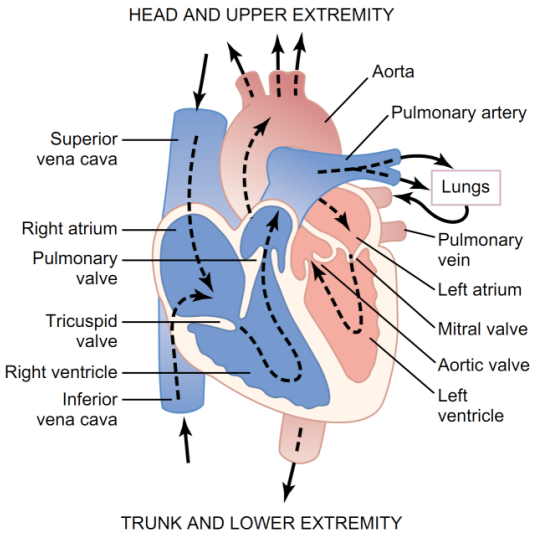

Figure 2.1 *Anatomy of the heart. The main cavities and blood vessels that connect them to the rest of the body are shown in the figure (adapted from [15]).*

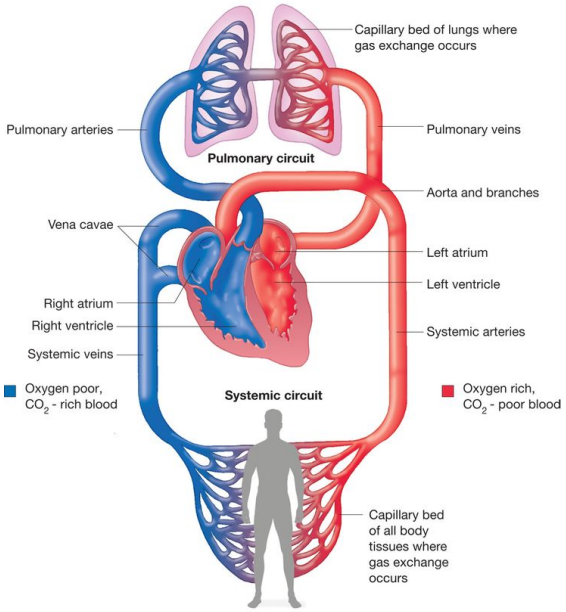

Figure 2.2 *The systemic and pulmonary circulations. Systemic circulation starts in the left atrium and the blood is pumped towards the organism from the left ventricle. Oxygen poor blood is then returned to right atrium, where pulmonary circulation starts. The oxygen poor blood is pumped towards the lungs by the right ventricle, and after the gas exchange the oxygen rich blood is returned to the left atrium, in order to repeat the cycle.*

2.2 Electrophysiology of the heart

The electrical functioning of the heart is a very complex mechanism that is the responsible of its mechanical activity. In Figure 2.3 the anatomical structures that are involved in this process are shown schematically.

The heart contains different kinds of cells, some of what are specialized in the conduction of electrical impulses known as action potentials: an action potential occurs as a response to the change in the ionic concentration outside and inside the cells, which produces a change in the cell membrane potential. Each action potential (see Figure 2.3 (b)) starts with a sudden change from the negative resting membrane potential to a positive membrane potential (depolarization), followed by a period when the potential remains practically constant ("plateau" phase) and ends with a smoother transition towards the resting potential (repolarization) [15]. These electrical impulses are generated in the sinoatrial (SA) node, which is the natural pace-maker of the heart and is located in the right atrium. These impulses spread through the atria walls depolarizing the cardiac cells present there.

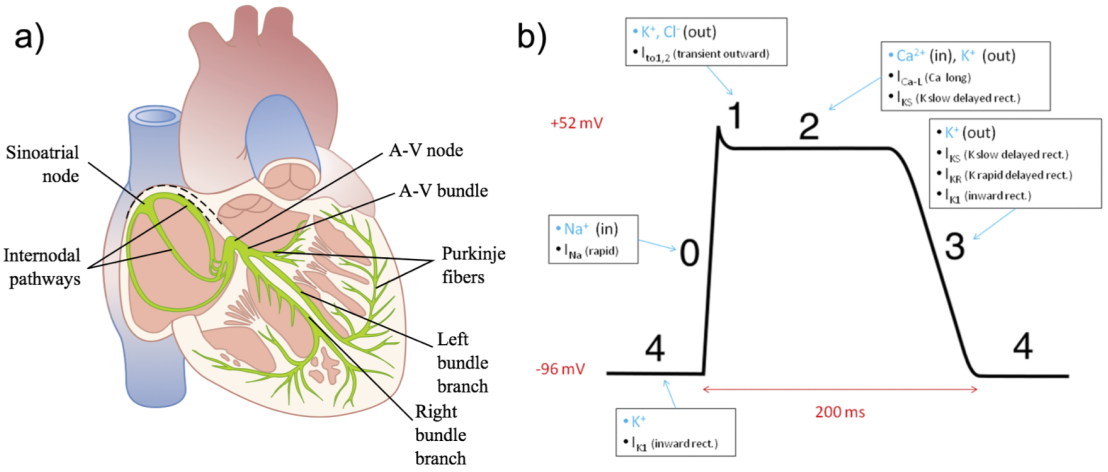

Figure 2.3 *a) Schematic of intrinsic conduction system of the heart. b) Action potential of the cardiac cells and the ionic exchange that generate it (adapted from [15]).*

Once all the cells in the atria are depolarized atria do contract, pumping blood into the ventricles, and afterwards a repolarization stage takes place in order to prepare the cardiac atrial cells to be able to drive a new electric impulse. The time between the depolarization of a cell and the moment when it is capable of being depolarized again is known as refractory period.

The electrical impulse produced by the SA node can not reach the ventricles, due to the fact that atria and ventricles are electrically isolated by a fibrous wall. However, the electrical impulse will reach the atrioventricular (AV) node, which is the responsible for driving it towards the ventricles. The impulse from the AV node is transmitted to the AV bundle (or bundle of His) and later to the Purkinje fibers, which are fast conduction channels that distribute the electrical impulse homogeneously to all the ventricular cells, thus causing the synchronous contraction of the ventricles and the further pumping of blood towards the body.

2.3 Autonomic Nervous System

The nervous system is composed of two main parts: the central nervous system (CNS), made up by the brain and the spinal cord, and the peripheral nervous system, formed by the nerves and the ganglia on the outside of the CNS. While the function of the CNS is to integrate all the information it receives from, and to coordinate and influence the activity of all parts of the body, the role of the peripheral nervous system is to connect the CNS to the organs and limbs, essentially serving as a communication channel between them. Looking forward into the peripheral nervous system, it can be further divided into two subsystems: the somatic nervous system, that is the voluntary motor system that overcomes the muscular control of the limbs, body and head, and the autonomic nervous system (ANS), that regulates the internal organs and so is referred to as the involuntary motor system [17].

The ANS has a fundamental role in maintaining homeostasis, and its efferent part is divided into three branches with two often opposing branches, the sympathetic nervous system (SNS) and the parasympathetic nervous system (PNS), that exert opposing effects on most organs. However, each of the motor neuron sets that integrates these divisions interact in a very complex way, so that the control over the organs activity can not be interpreted as a simple linear sum of two systems exerting opposing effects [17]. The connections of both branches with the various organs in the human body and the effect that they exert are shown in Figure 2.4. The third branch is the enteric nervous system (ENS) that innervates the digestive organs [17].

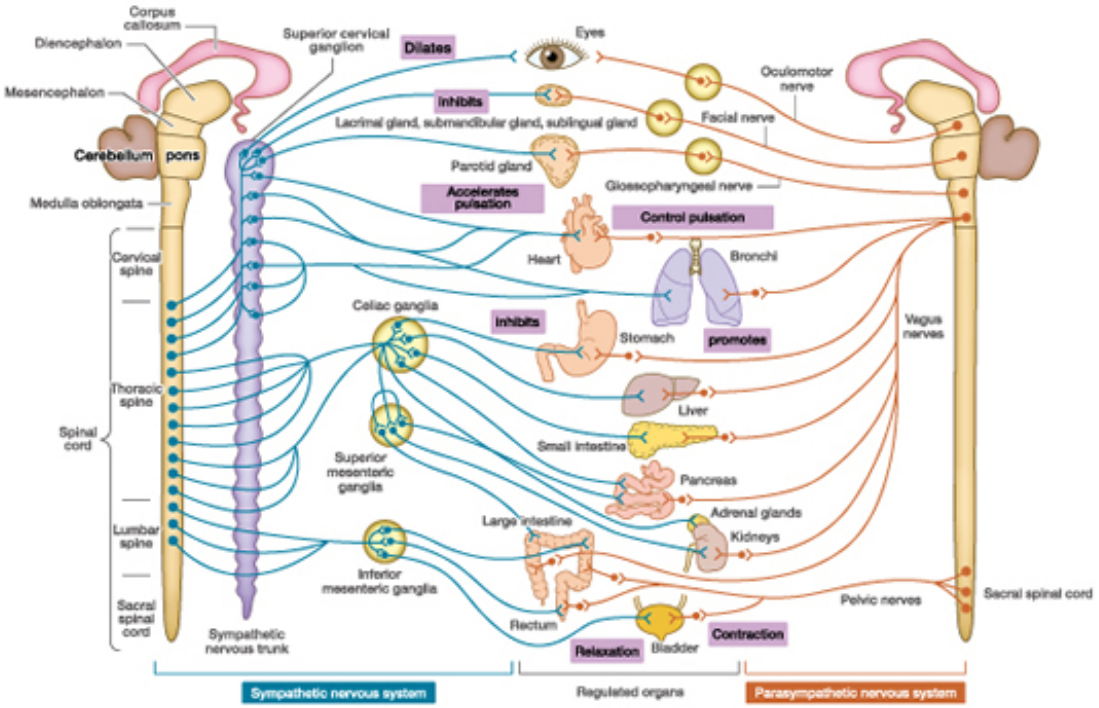

Figure 2.4 *Sympathetic and parasympathetic branches of the ANS and their connections to the different organs in the human body (adapted from [18]).*

2.3.1 Sympathetic Nervous System

The cells of the sympathetic nerves arise from the thoracic and lumbar areas of the spinal cord, some of them forming synapses in the sympathetic nerve trunk. Besides, some of these nerve cells do not synapse in the sympathetic nerve trunk, but are rather distributed to several organs that are innervated from the sympathetic ganglia situated near the abdominal visceral [18].

The sympathetic division is often referred to as the "fight-or-flight" system, due to the fact that it activates when the body is immersed in any kind of stressing or threatening situation, thus preparing the body to deal with it. Some examples of the effect of SNS are the increase of HR, blood pressure and blood glucose levels, vasodilation and the dilation of the bronchioles of the lungs, the release of adrenaline or the withdrawal of blood from the digestive organs [16]. Moreover, the release of various hormones is controlled by the SNS, what explains the fact that once the SNS has stopped its actuation, the effect produced by it still remains until the hormones release and effect have concluded.

2.3.2 Parasympathetic Nervous System

The cells of the parasympathetic nerves arise from the cranial nerve nuclei, and those nerve cells form synapses at the ganglia either within or adjacent to the functional organs [18].

The parasympathetic division is most active when the body is at rest and homeostasis is not threatened in any way. This branch of the ANS, often know as the "rest-and-digest" system, is concerned on what involves the digestion of the food and the elimination of wastes, and the conservation of body energy, particularly by decreasing demands of the cardiovascular system [16]. Some examples of the effect of PNS are the activation of the digestive track, the constriction of eye pupils or the regulation of heart and respiratory rates.

2.4 Heart Rate Variability

Heart rate variability (HRV) is defined as the variation between consecutive heartbeats over time and it is mainly dependent on the extrinsic HR regulation [10]. If we take a look to an electrocardiogram (ECG) recording, we can easily identify the QRS-complex (Figure 2.5), which is due to ventricular depolarization and is formed by the waves referred to as S-, R- and Q-waves. The interval between two consecutive R-waves in an ECG recording is known as RR-interval (see Figure 2.5) and this RR-interval represents the instant HR, so the series composed by successive RR-intervals are a representation of the temporal evolution of the HR. If the HR would be constant over studied time the RR intervals would be constant as well, but there are always fluctuations around mean HR due to continuous alteration in neural regulation and thus the beat-to-beat intervals vary over time [17]. This variability is, precisely, what is known as HRV. In Figure 1.6 an example of RR-interval evolution over time is shown.

As seen in the previous section, the heart activity is mainly regulated by the ANS and the complex interaction between the opposing branches of the ANS and the resulting effect they exert on cardiovascular system regulation and the autonomic tone is referred to as the sympathovagal balance [17] [19]. Increased SNS or diminished PNS activity leads to cardio-acceleration, while a reduced SNS activity or an increased PNS activity results in cardio-deceleration [10]. However, SNS and PNS act over different time scales: while the parasympathetic response is almost

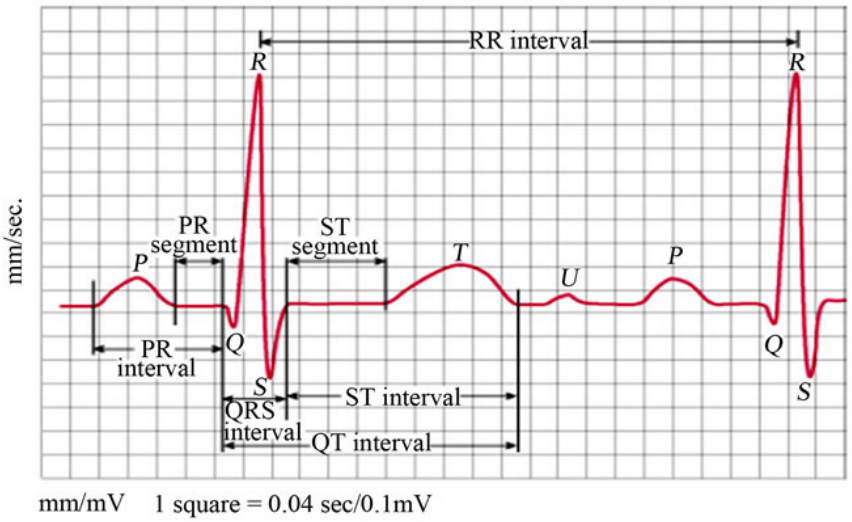

Figure 2.5 *ECG main waves and segments. The RR interval, described as the period between two consecutive R peaks, is shown in the figure (adapted from [20]).*

immediate (about 400 milliseconds latency period) the sympathetic response has a delay that can reach 5 seconds followed by a stable increase in the HR during the next 20 to 30 seconds [17], what makes the analysis of the relationship between the activity of both systems more complicated that the linear sum of opposing effects (as explained in previous section).

There are many different events that may produce variation in HR, e.g., an increase in the HR is not always due to a stress situation. For example, respiration have a direct effect in HR: the inspiration will generate a tachycardiac reflex that will increase the HR, while expiration will cause a bradychardiac effect, thus reducing the HR. This effect is referred to as respiratory sinus arrhythmia (RSA). Hence, the HR does not remain constant even if the body is at rest.

As there are several commercial devices that nowadays provide an automated measurement of HRV [21], HRV has received widespread research interest in recent years, due to the fact that ANS activity can be investigated non-invasively using relatively basic signal processing techniques [22]. Thus HRV has been proved as a powerful tool in the analysis of ANS activity in cardiological diseases such as arrhythmias [23] [24], myocardial infraction [21][25] or coronary artery disease [26], but also in non-cardiac diseases such as sleep apnea [27] or asthma [28].

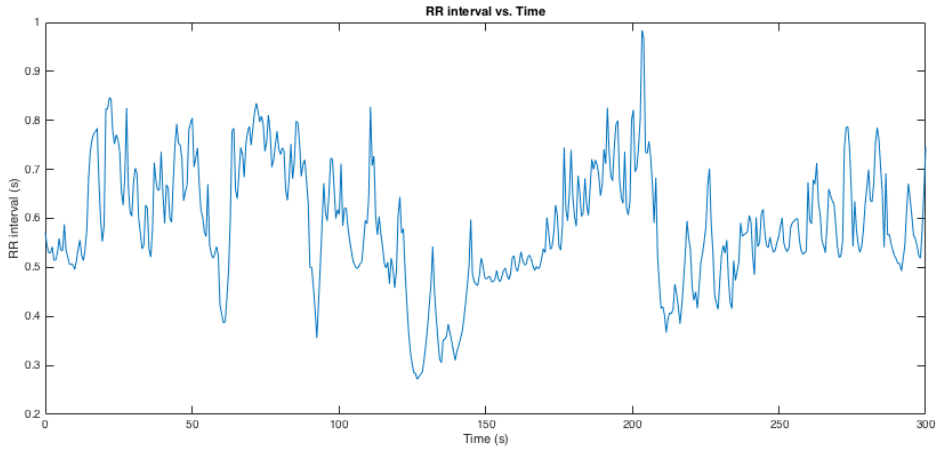

Figure 2.6 *Example of RR-interval evolution over 5-minute segment. HR has a continuous variation even at rest, which is regulated by ANS branches activity.*

2.5 Asthma

Asthma is a chronic (long-term) lung disease that produces inflammation and narrowing of the airways. It also causes recurrent periods of wheezing (a whistling sound during the breathing), coughing, shortness of breath and chest tightness. The coughing is more prone to occur during the night or at the early morning [29]. The occurrence of nocturnal asthma is mostly related with the reduced lung function and changes in hormonal levels related with circadian rhythms.

One of the main characteristics of asthma is the spasmodic contraction of the bronchioles, which usually makes breathing difficult [30]. It is usually triggered by bronchial hyperresponsiveness towards a variety of specific and non-specific stimuli [31].

Due to the effect of the irritants, the body tends to generate a high amount of antibodies, which attach to specific cells in the bronchioles and small bronchi of the respiratory tract. The reaction of these antibodies with the irritant leads to the release of some substances as histamine [31], thus allowing them to fight pathogens in the various infected tissues [32]. The combined effect of these factors will produce localized edema in the walls of the small bronchioles as well as an increase in the mucus segregation and spasm of the bronchiolar smooth muscle. These effects are also many times accompanied by a wheezing or whistling sound, which is very characteristic of asthma and is produced because of the narrow of the airways. The continued presence of these symptoms may lead to the remodelling of the airways,

which are often characterized by an increased thickness and an increase in muscle mass and mucous glands in asthmatic patients [33]. Usually, asthmatic subjects do not have difficulty for inspiring, but have complication to expire the air from the lungs [31]. Although symptoms are not always present, asthma has no cure, but it can be controlled by treatment [34].

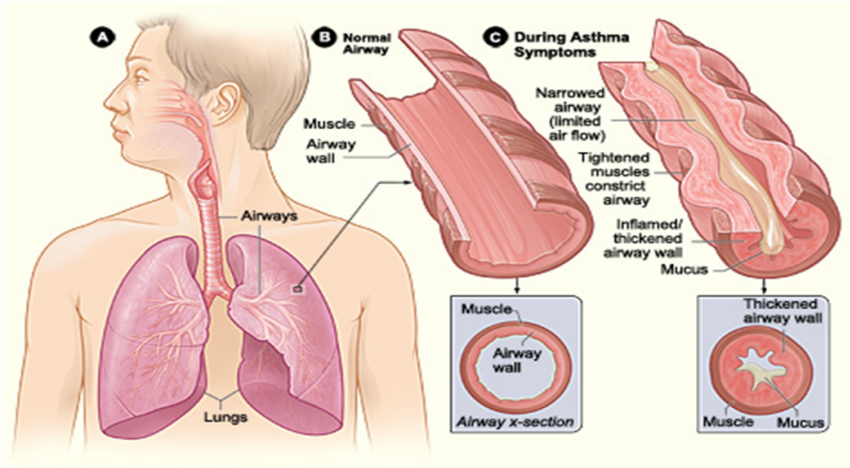

Figure 2.7 *Schematic showing the effects of asthma symptoms in the airways. Airways are narrowed, their walls are inflamed and the segregation of mucus increased (adapted from [29]).*

Yet asthma affects people of any age, it is prone to start during childhood. Actually, in the past three decades a dramatic increase of the incidence and the prevalence of asthma has been observed among children [1], and asthma is nowadays considered in the United States as the most common chronic disease of childhood [2].

Yet asthma has already been analyzed through HRV in adults [35], the group of study of this thesis is formed entirely by children aged between 3 and 7. The main problem in premature asthma diagnosis is that there is not a clinical method to detect it, so nowadays it mainly depends on the doctor criteria.

2.6 ANS control of HRV and respiratory system in asthma

As described in the previous section, one of the main symptoms of asthma is hyper-reactivity, and according to [3] this mechanism may be related with abnormal ANS control that occurs in asthmatic subjects. Moreover, the parasympathetic branch of ANS appears to be related with the pathogenesis of asthma [4], and several studies has shown that it is directly involved in bronchoconstriction both in asmathic and

non-asmathic subjects [5][6]. Furthermore, cardiac vagal activity appears to be increased in asthma as well according to the exaggerated bradychardiac response to some acetylcholine-blocker drugs in asthmatic subjects [4]. For that reason, in [7] it is suggested that cardiac and bronchial auntonomic control might be related, being this relationship altered in subjects suffering from asthma.

Following this assumptions, some studies suggest that the altered bronchial autonomic control in asthma may be reflected by changes in HR [4][7], most of them showing higher resting HR and a generalized increase of total HRV in asthmatic subjects [36][37]. Moreover, Morrison et al. [38] performed an investigation where effects of asthma were almost reversed during vagal blockade achieve with the administration of atropine, what implies that PNS plays an important role in asthma.

3. HRV ANALYSIS

As explained in the previous section, HRV analysis is a valuable tool both in clinical use and in physiological research [21][39] due to the fact that it may reflect the activity of the ANS. For this purpose, different techniques for HRV analysis have been developed in recent years and several indexes that can be obtained from it have been defined. The initial assumption is that these indexes reflects different aspects of the inherent variability of the HR in order to adapt to external and internal changes, and their values may differ from the normal range in various diseases and with age [14].

However, when analyzing HRV, there are some aspects that need to be take into account. First of all, the relation between the length of the RR intervals and the HR is non-linear, as shown in Figure 3.1. This non-linear relation may become a problem when comparing the value of certain parameters extracted from intervals with different mean HR [17]. Hence, the parameters that reflect the total power of variations are most affected by this non-linearity than most of the non-linear parameters, that usually do not reflect power of variations. The use of normalized parameters and some non-linear parameters may diminish the effect of non-linear relation between HR and the RR intervals length [17][40].

Another important fact when analyzing HRV is the presence of ectopic beats in the recordings. The ectopic beats are those that have not their origin in the SA node but in another part of the heart, due to the spontaneous depolarization of the cells present there, thus producing a premature heart beat. As the aim of analysing variations in HR is usually to obtain a representation of ANS activity, ectopic beats must be rejected as they are not related with ANS action. Ectopic beats are an important source of error, as they are present both in healthy patients and patients with heart disease, so there are plenty of algorithms and criteria that can be used to remove the ectopic beats from the recording [41][42][43].

Although time- and frequency-domain analysis have been the dominant procedures

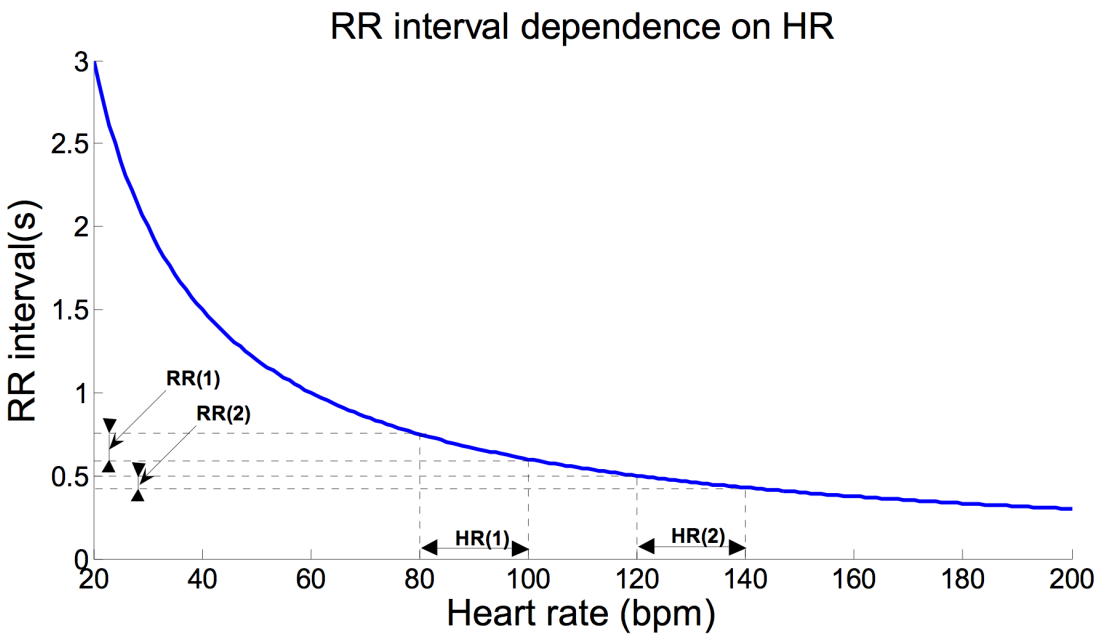

Figure 3.1 *RR interval as a function of HR. There is not a lineal dependence between the length of the RR intervals and the observed HR, so the same increase in HR will produce a different shortening of the RR intervals for different HR initial values (adapted from [17]).*

in the analysis of HRV in the last decades, in recent years it has become evident that the cardiac systems are non-linear in their function [44]. Moreover, the advances in the study of non-linear dynamics and deterministic chaos and the further acceptation of the heart activity as a biologic non-linear system [45] has lead to the development of a series of non-linear analysis methods, that are expected to represent the cardiac activity in a more accurate well. The basis of these techniques is that they depart from the assumption that the human body can not be considered as a linear system anymore.

3.1 Time Domain Analysis

Clinical studies of HRV have frequently been synonymous with the use of simple time domain measures [22]. The parameters obtained from the time domain analysis have the advantage that no complex calculations are needed. Furthermore, depending on the period considered for the analysis, it is possible to distinguish between short- and long-term HRV which allows to focus in different components acting in the variation of HR. On the other hand, the main problem with time domain parameters is that, as there is no frequency distinction, it is not possible to know if the cause of the

variations is due to the activity of rather SNS or PNS. In spite of that, temporal analysis is still wide used due to its simplicity and its capability of distinguish between healthy subjects and subjects suffering from certain diseases: many of the parameters obtained from time domain analysis have been shown to have higher values in patients suffering from diseases that cause tachycardiac effects (such as sick sinus syndrome or atrial fibrillation) and lower values in the case of diseases causing bradychardiac effects (such as complete heart block or left bundle branch block) [10][46][47].

In the time domain analysis of HRV, RR intervals are usually referred to as NN intervals, due to the fact that RR intervals are also called normal-to-normal intervals because only the intervals between consecutive QRS complexes resulting from normal sinus depolarizations are considered. When analyzing RR intervals in temporal domain, the time course of these RR intervals is denoted as RR_n, with $n = 1, 2, ..., N$. There are several indexes defined for the time domain analysis of HRV [21][22][48], being the most well-known the following:

- **SDNN:** standard deviation of all NN intervals of the analyzed period. It is defined as the square root of the variance of the NN intervals [13]. Since the variance is mathematically equal to the total spectral power, SDNN contains information about all the cyclic components responsible of the variability. As the length of the analyzed recording decreases, SDNN constitutes an estimate of shorter and shorter cycle lengths [21]. Mathematically, SDNN is described as:

$$SDNN = \sqrt{E[RR_n^2] - \overline{RR}^2} \tag{3.1}$$

- **SDSD:** standard deviation of the successive differences of the NN intervals. It is an important measure of short-term HRV [13] and can be described as:

$$SDSD = \sqrt{E[\Delta RR_n^2] - \overline{\Delta RR}^2} \tag{3.2}$$

- **SDANN:** standard deviation of the averages of all NN intervals in all 5-minute segments of the entire ECG recording [22]. It represents an estimate of the changes in the HR due to cycles longer than 5-minutes [21].

- **RMSSD:** root mean-square of successive differences of adjacent NN intervals

[13]. RMSSD is an estimate of the short-term variability of the HR [14], and it is defined as:

$$RMSSD = \sqrt{\frac{1}{N-1}\sum_{n=1}^{N-1}(RR_{n+1} - RR_n)^2} \tag{3.3}$$

- **pNN50:** is the number of successive differences of intervals which differ by more than 50 milliseconds expressed as a percentage of the total number of ECG cycles analyzed [10]. As RMSSD, pNN50 is an estimate of the high-frequency variation in heart-rate, and thus both parameters are highly correlated [21]. In [49] it has been proved that although RMSSD provides a more detailed description of the short-term variability, pNN50 is much less vulnerable to the presence of artifacts in the recording [22]. Mathematically, it is expressed as:

$$pNN50 = \frac{|\Delta RR|_{>50ms}}{N} \tag{3.4}$$

, where $|\Delta RR|_{>50ms}$ is the total number of adjacent RR intervals which values are higher than 50 ms.

- **Triangular index and TINN:** both the triangular index of HRV and the triangular interpolation of the NN histogram (TINN) are well known geometrical-based analysis methods for HRV. Essentially, triangular index is the integral of the density distribution (the density distribution must be discrete, and the length of the bins is usually set as 8 ms) divided by the maximum of the distribution, whereas TINN is the baseline with of the density distribution measured as a base of a triangle [21]. Taking a look to Figure 3.2, the triangular index of HRV can be mathematically expressed as:

$$Tr.index = \frac{\int_N^M D(t)dt}{Y} \tag{3.5}$$

$$TINN = M - N \tag{3.6}$$

, where $D(t)$ is the density distribution of the RR intervals and the values of Y, M and N are described in Figure 3.2.

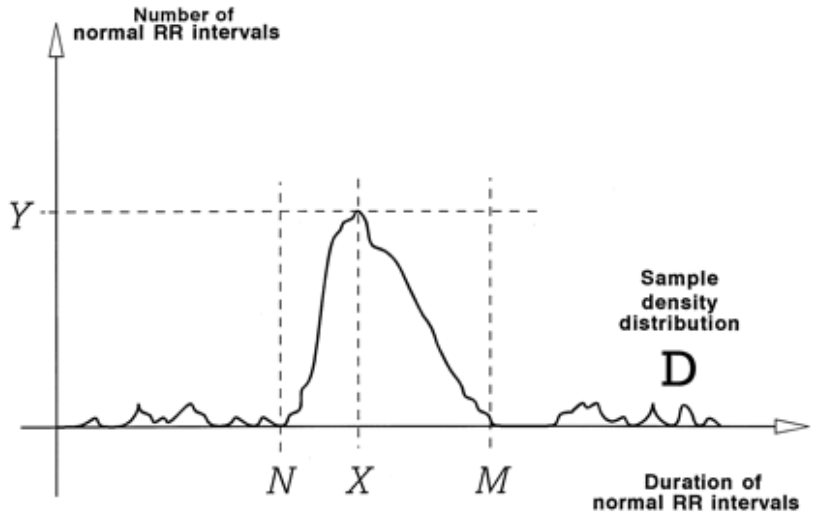

Figure 3.2 *Example of density distribution of the duration of normal RR intervals. Triangular index is calculated as the ratio between the integral of the PDF between N and M and its maximum value, Y. On the other hand, TINN is calculated as the difference between M and N (adapted from [21]).*

3.2 Frequency Domain Analysis

As described in the previous section, the main problem with time domain analysis is the lack of information of which branch of the ANS, SNS or PNS, is producing the variation in the HR. To solve this problem, various spectral methods for the analysis of HRV have been developed in last decades [21] and either Fourier Transform or autoregressive (AR) models can be used for the calculation of the power spectral density (PSD). It is well known that the spectral analysis of a signal through its PSD provides information about how the power (i.e., the variance) is distributed through the different frequencies present in the signal [21].

Traditionally, frequency domain analysis has been performed in short-term 5-minute intervals [39], although also long-term analysis is considered (typically 24-h segments) [21]. A typical spectrum of a 5-minute segment RR interval evolution is shown in Figure 3.3. When performing a short-term frequency analysis, three main spectral components can be distinguished [21]:

- **Very low frequency (VLF):** frequency components belonging to the range 0.003 - 0.04 Hz. According to [21] there is not a clear physiological explanation for it and it has not coherent properties, so VLF should be avoided from the

studies of the PSD. However, there are also studies that present VLF as a more powerful risk predictor in cardiovascular diseases than LF or HF [50].

- **Low frequency (LF):** frequency components belonging to the range 0.04 - 0.15 Hz. LF is thought to mainly represent the SNS activity, although with some parasympathetic contribution.
- **High frequency (HF):** frequency components belonging to the range 0.15 - 0.4 Hz. LF is thought to represent the PNS activity.

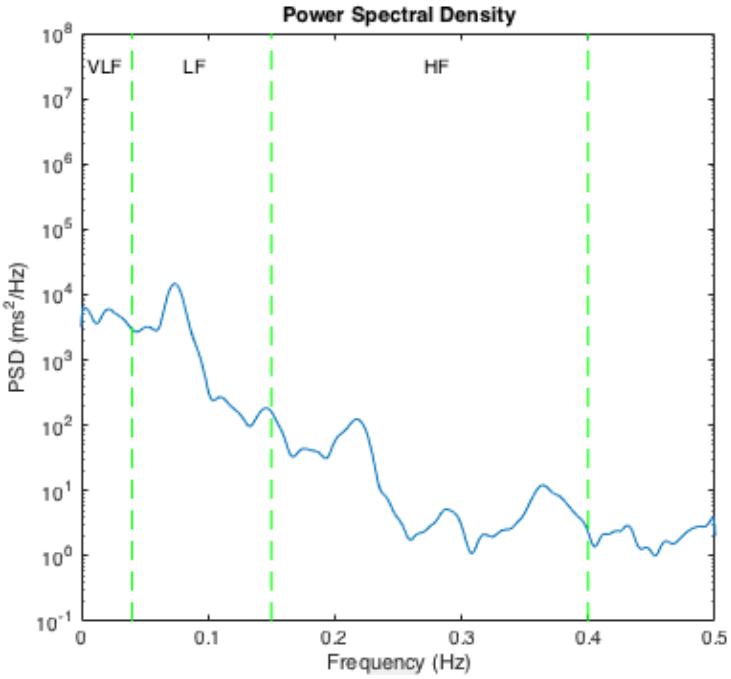

Figure 3.3 *Typical non-parametric PSD estimation for a 5-minute segment. The different frequency bands described in the text (VLF, LF and HF) are displayed in the image.*

In long-term analysis, a fourth frequency component known as ultra low frequency component (ULF) is measurable in the frequency range <= 0.003 Hz. However, and as for the VLF component, it physiological interpretation is still not clear [21]. Another important issue to take into account when performing long-term analysis is that the assumption of stationarity is no longer true for further analysis.

The main studied indexes when performing a frequency domain analysis are the following:

- **TP:** total power (TP) is the power of the segment analyzed, obtained by

integrating the PSD. Sometimes VLF is considered inside TP, but in many cases it is not.

- **LF:** is the power corresponding to the LF segment of the PSD. It is measured rather in ms^2/Hz or with respect to the TP, i.e., as a percentage. As described above, it is a measurement of SNS activity, with PNS components.
- **HF:** is the power corresponding to the HF segment of the PSD. It is measured rather in ms^2/Hz or with respect to the TP, i.e., as a percentage. As described above, it is a measurement of PNS activity.
- **LF/HF ratio:** it is the ratio between LF and HF, and it represent the relationship between the activity of SNS and PNS.

Usually, PSD estimation is composed by two main steps: first, the parameters of the method used for the PSD calculation are estimated and then PSD estimation is computed. Furthermore, the methods for PSD estimation are usually classified in non-parametric and parametric methods. Non-parametric methods are really extended due to its simplicity and most of them are based in the calculation of the Fast-Fourier Transform (FFT) in one or another way, although windowing used in these methods produces spectral leaking, thus leading to only moderate estimations. On the other hand, parametric methods are usually based in AR models, so as data can be modelled as the output of a causal, all pole discrete filter whose input is white noise [10]. The AR estimation of order p is expressed as:

$$x(n) = -\sum_{k=1}^{p} a(k)x(n-k) + w(n) \tag{3.7}$$

, where $a(k)$ are the AR coefficients and $w(n)$ is white noise with variance equal to σ^2.

One of the most important issues when using AR methods is the selection of p, and in [20] it is shown that $p = 16$ can be taken.

Another important aspect in the estimation of PSD for HRV analysis is the use of evenly sampled signals, what is not typical in the case of RR interval recordings, so a 4 Hz resampling rate is recommended [21]. However, also methods for PSD estimation from unevenly sampled signals has been proposed in the literature [22][52]

providing even a better performance that the use of evenly spaced samples in some situations [52]. It is also recommended that the sampling frequency of the recording instruments used should be higher than 250 Hz [21], as the resolution could be not enough for spectral analysis of HRV otherwise.

Finally, and although frequency analysis methods have the advantage of discriminate between different ranges of frequencies and so to determine which branch of the ANS is the main responsible for the variation in the HR [10]. On the other hand, some studies have shown that the diagnostic performance of the spectral components are not better than when using time domain parameters [21][53].

3.3 Non-linear Analysis

Although time and frequency domain indexes have been widely used in HRV analysis for many years, nowadays it is commonly accepted that the cardiovascular system has a nonlinear behaviour [8][9], what implies that the classical indexes may not be the best approach to study them. Hence, the use of nonlinear techniques may describe cardiovascular behaviour in a more accurate way [10]. However, this idea is not only applied to the cardiovascular system: most of the biological systems can be characterized by underlying nonlinear behaviour, including the respiratory system [54]. As ANS control of cardiovascular and respiratory systems is thought to be related [4], it is reasonable to think that nonlinear analysis of both systems may lead to a deeper understanding of the physiological processes taking place into the ANS [54].

In recent years, many research studies have proposed several parameters taken from nonlinear dynamics for the study of HRV, most of which are based in measuring the entropy of the RR interval series or describing its fractal behaviour. Some examples of the most used methods are correlation dimension analysis [55], detrended fluctuation analysis [56], largest Lyapunov exponent [57], approximate and sample entropy [58] and parameters obtained from Poincaré plots [13]. In this study, the focus is on Poincaré plot analysis, which is introduced in the next section.

Although the already mentioned nonlinear methods have been widely studied in the field of nonlinear dynamics, they have to be modified when applied to biological systems, as biological signals have a series of specifics that must be taken into account [10]. First of all, biological data is usually contaminated by high level of random

noise with inter- or intra-system origin and that is not always easy to remove by filtering, so the methods applied must be robust to the noise influence. On the other hand, long recordings are needed, due to the slow variations caused by the low frequencies of the biological signals. However, it is not possible to assume stationarity of these long recordings: biological data is non-stationary, so the nonlinear methods developed for its analysis must consider that fact [10].

Finally, from the analysis of the nonlinear dynamics methods used for the study of HRV, some important conclusions can be drawn. According to [9], several of those methods have proven to be powerful risk stratifiers, and are really useful in the diagnosis and characterization of some cardiovascular diseases, while some of them are still being tested but are already showing promising capabilities. Moreover, nonlinear dynamics methods also provide additional information about the underlying physiological processes that is not available with the use of classical time and frequency domain indexes.

3.4 Poincaré Plot

Poincaré plot is a visual technique consisting in the representation of each RR interval as a function of the previous RR interval. It is a new visual and quantitative technique whereby different shapes can be classified into different functional classes, thus indicating the degree of heart failure in a subject [10][11][12]. Poincaré plots provide beat-to-beat information, that can reveal patterns of the nonlinear underlying processes [59], thus portraying the nature of the RR intervals. Hence, Poincaré plots are thought to hide further information than that provided by the classical time and frequency indexes, although they are still being studied. Poincaré plots may be constructed either from short intervals (e.g., 5-minute intervals) or long intervals (e.g., 24 hours recording), in order to display short- or long-term information of the HRV [21]. An example of a typical 5-minutes recording Poincaré plot is shown in Figure 3.4. Poincaré plots are also referred as Lorentz plots or first return maps in the literature.

Taking a look to Figure 3.4, three different regions can be distinguished within Poincaré plot. First of all, the line of identity (dashed green line in the figure) contains the points for what the RR interval at the time i is exactly equal to the RR interval at the time $i + 1$, thus implying no variation in consecutive RR intervals. This line of identity divides the plot into two symmetric regions. The upper-left

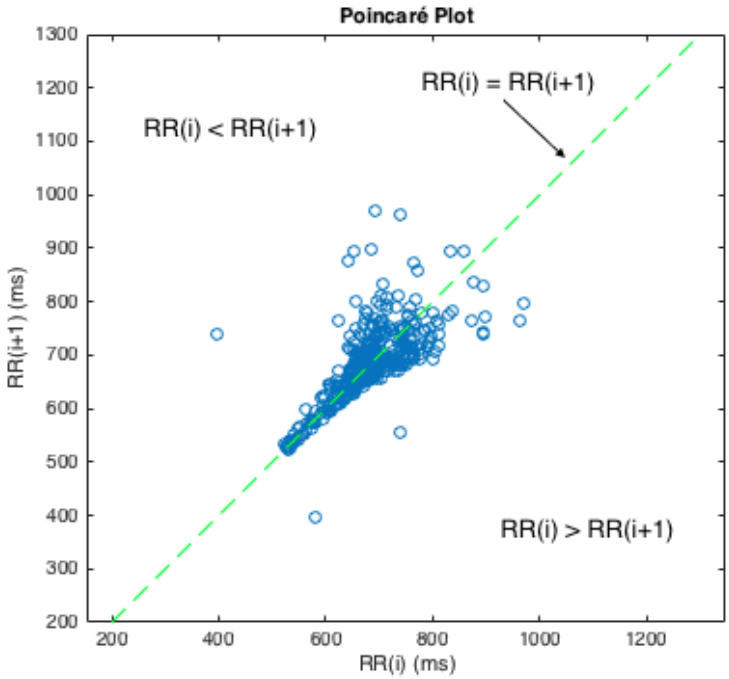

Figure 3.4 *Typical Poincaré plot representation for a 5-minute segment. There are three different regions shown in the image: the line of identity and the upper-left and lower-right regions, which are divided by the mentioned line. While the line of identity contains the points for what consecutive RR intervals have an equal length, the upper-left and lower-right regions hold the points for what the actual RR interval is longer or shorter than the previous one respectively.*

region contains all the points that satisfy the condition $RR_{i+1} > RR_i$, thus corresponding to prolongations in the RR lengths, while the lower-right region contains the points satisfying $RR_{i+1} < RR_i$, which implies a shortening of the RR intervals. A maintained prolongation or shortening of the RR intervals represents a tachycardiac or bradycardiac response respectively, and this kind of response are easy to identify by paying attention to the generation of a Poincaré plot.

3.4.1 Poincaré plot and nonlinear dynamics

In order to understand the nature of the Poincaré plot and its capability for representing the underlying nonlinear behaviour of the cardiovascular system, it is first important to go through some basic concepts of nonlinear dynamics. First of all, any system that evolves in time is called a dynamical system. A dynamical system is linear if the equation 3.8 is satisfied:

$$\frac{\mathrm{d}\overrightarrow{x}(t)}{\mathrm{d}t} = \overrightarrow{F}(\overrightarrow{x}(t), \overrightarrow{\mu}) \tag{3.8}$$

, where $\overrightarrow{x}(t)$ and $\overrightarrow{\mu}$ are the dynamical variables and the parameters of the system respectively.

Otherwise, the system is considered as nonlinear. However, as there exist an equation describing the behaviour of a nonlinear system, its state in any time is just determined for the state of the system in previous times, so given a set of initial conditions the response of the system is deterministic. Notwithstanding, one of the surprising mathematical discoveries of the last decades is that the solutions of this kind of deterministic nonlinear dynamical systems may be completely random. This behaviour is known as deterministic chaos [60]. What makes this discovery really important is that most dynamical systems are nonlinear, and most nonlinear system have random solutions [60]. As biological systems in general and cardiovascular system in particular have been proven to have a nonlinear behaviour [8][9], the deeper understanding of this deterministic chaos processes may lead to a better approach to the physiological processes governing biological signals.

Nevertheless, this processes are not easy to analyze and, in order to represent the temporal evolution of the system's state, phase space representations are often used. As described by nonlinear dynamics, a phase space is an abstract mathematical spaced that can be constructed from the dynamical variables of a given system. The state of that system at a given fixed time would be so represented by a point P in the phase space. Of course, if the system is described by n dynamical variables then P will be a point in the Euclidean space $\mathbb{R}^n$ [60]. Usually, the phase space representations contain stable structures that represent the behaviour of the dynamical system. These structures, which can have different topologies, are limited to a bounded region of the phase space and are commonly known as attractors [61]. However, in most cases we only dispose of the temporal evolution of a subset of the parameters describing the linear system but, since 1981 when Floris Takens first proposed his embedding theorem [62] some studies have shown that the knowledge of the temporal evolution of a single coordinate of a higher dimensional system is enough to reconstruct a phase space that will preserve the topology of the system [63].

Hence, according to nonlinear dynamics, Poincaré plot is considered as the 2-dimensional

reconstructed RR phase space, which is actually a projection of the reconstructed attractor that describes the dynamics of the cardiovascular system [13]. Essentially, it means that the Poincaré plot is capable of displaying heartbeat dynamics based on a simplified phase-space embedding [9].

3.4.2 Poincaré plot in the analysis of HRV

As previously introduced, Poincaré plot is a newer visual method that has been introduced in the analysis of HRV due to its capability to represent beat-to-beat behaviour. From Poincaré plots, some parameters have been defined has a method to provide quantitative measurements of the information enclosed by the plots. These parameters are the following:

- **SD1:** it is the standard deviation of the short-term RR interval variability [9]. In the plot, it can be identified with the minor axis of the cloud and it constitute a good marker of PNS activity, although some contribution of SNS is also measured by this parameter [14].
- **SD2:** it is the standard deviation of the long-term RR interval variability [9]. In the plot, it can be identified with the major axis of the cloud and, although it is related with the overall variability, it is more strongly driven by sympathetic than by parasympathetic activity [14].
- **SD1/SD2 ratio:** this is the ratio between the two previous parameters, and it represent the relation existing between short- and long-term variability.
- **S:** in order to have a mathematical measurement of the shape of the plot, the most extended technique consists on fitting an ellipse to the plot, where the values of SD1 and SD2 constitute the minor and major axes of the ellipse respectively [13]. With this technique, the parameter S is simply defined as the area of that ellipse:

$$S = \pi \times SD1 \times SD2 \tag{3.9}$$

Hence, S is a descriptor of the total HRV.

From the parameters described above, the SD1/SD2 ratio seems to be the most powerful predictor in the case of diseases such as atrial or ventricular fibrillation, where the parameter presents higher values, or ischemic cardiomyophaty and complete heart block, where the ratio value falls below normal [10][9][64].

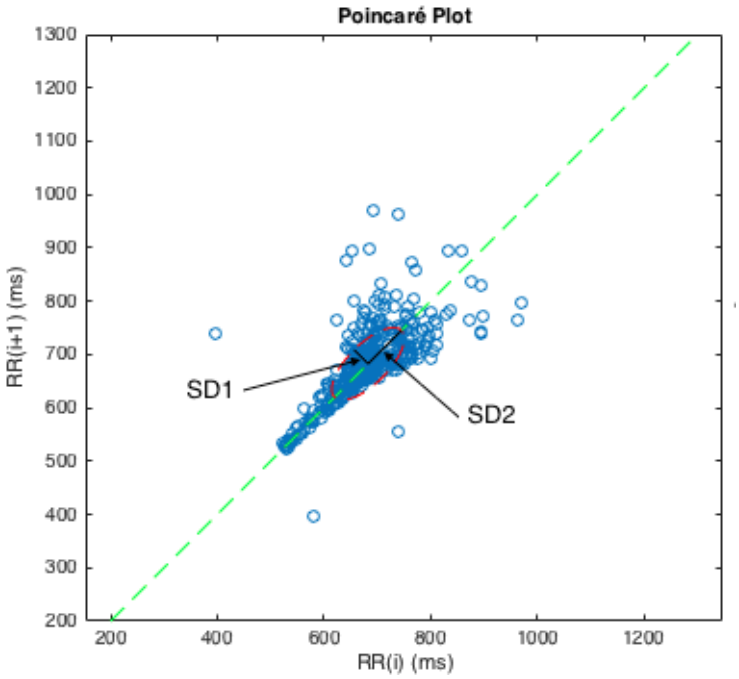

Figure 3.5 *The ellipse fitting technique is shown in the figure. The minor and major axes of the ellipse are SD1 and SD2 respectively.*

Although most typical parameters are SD1, SD2 and SD1/SD2 ratio, some studies propose the length and width of the Poincaré plot as measurements of the information displayed in the plots, but their use is definitively much less extended than the previously mentioned parameters.

In spite of the fact that most of the emphasis in the study of Poincaré plot focuses in the representation of consecutive RR intervals, one as a function of the previous, there are also some researchers that have generalized this technique, studying Poincaré plots that display the RR interval $n+m$ as a function of the RR interval n, being m an integer that may vary from 1 to some small positive value. Such kinds of representation are known as lagged Poincaré plots, and this practise is known as plotting the two-dimensional phase space with the time series embedded with lag m in nonlinear dynamics.

Lagged Poincaré plots are closely related with the power spectrum of the analyzed

RR intervals. In [13], an interesting relation between Poincaré plot parameters and the covariance function of the RR intervals is demonstrated. There, it is stated that we can express SD1 and SD2 as:

$$SD1^2 = \phi_{RR}(0) - \phi_{RR}(1) \tag{3.10}$$

$$SD2^2 = \phi_{RR}(0) + \phi_{RR}(1) \tag{3.11}$$

If we consider the Poincaré plot with lag m, the new expressions for SD1 and SD2 are:

$$SD1_m^2 = \phi_{RR}(0) - \phi_{RR}(m) \tag{3.12}$$

$$SD2_m^2 = \phi_{RR}(0) + \phi_{RR}(m) \tag{3.13}$$

And from the equations 3.12 and 3.13, covariance function at lag m can be expressed as a simple linear combination of SD1 and SD2 squared:

$$\phi_{RR}(m) = \frac{1}{2}(SD2_m^2 - SD1_m^2) \tag{3.14}$$

The result obtained in Equation 3.14 states that the whole set of lagged Poincaré plots is a complete description of the autocovariance function, thus equivalent to a complete description of the power spectrum of the RR intervals [13].

Another generalization of the Poincaré plot is the modification of the order of the plot, extending it to a three-dimensional phase space representation. Essentially 3^{rd} order Poincaré plots are scatter plots of the triples $\{RR_n, RR_{n+1}, RR_{n+2}\}$ in the three-dimensional Euclidean space. The projections of the 3^{rd} order plot in the different planes are either the regular Poincaré plot or the lag-2 Poincaré plot. This idea has been also extended to further dimensions, with the new projections being lagged versions of the Poincaré plot. Hence, the m^{th} order Poincaré plot is just described by the set of the first m-lagged Poincaré plots.

The shape of Poincaré plots have been also widely studied and different patterns have been associated with the degree of heart failure of a subject. However, this studies have been performed by visual inspection of the shapes found in long-term

recordings [11][59]. Although several patterns have been identified in those long-term recordings (e.g., comet, torpedo or fan shaped plots) the shape of Poincaré plots is variable over time in short-term recordings as they represent HRV of short RR interval segments, and the temporal evolution of the shape has still not been analyzed. In Figure 3.6 two different Poincaré plot patterns are shown.

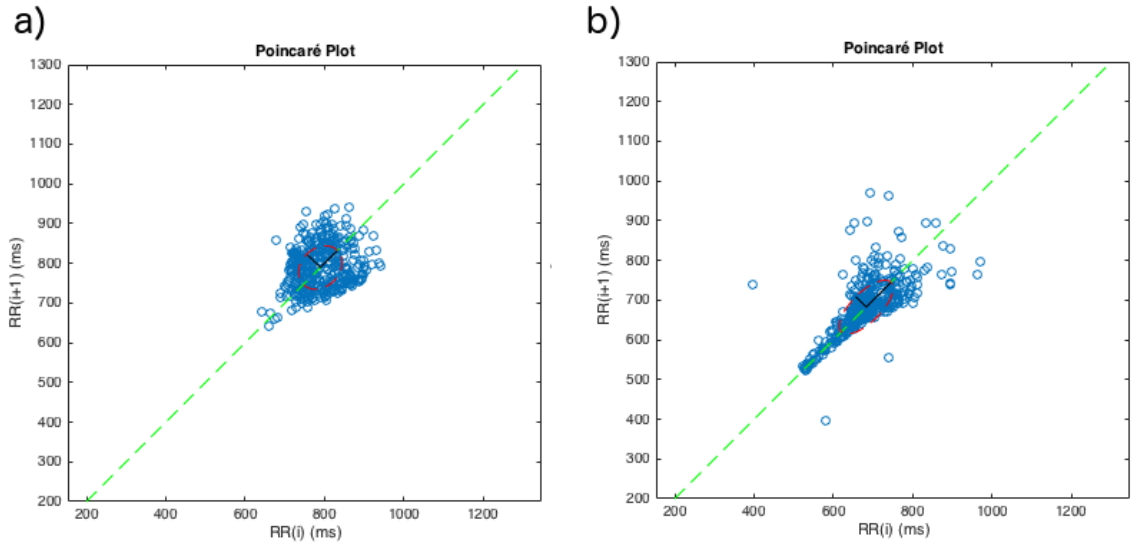

Figure 3.6 *The short-term Poincaré plot can present several shapes attending to the activity of the ANS: while the shape is almost circular in the case of image a), a comet-shaped plot is observable in image b). In the case of long recordings the shape can be used as a stratifier of heart disease.*

3.4.3 Relationship with classical indexes

Although Poincaré plot is a method taken from nonlinear dynamics as already explained, *Brennan et al.* showed in [13] that the indexes extracted from the plot, i.e., SD1 and SD2, are strongly correlated with the classical time-domain parameters, so they do not provide further information than the classical indexes. In the case of SD1, it is related with SDSD in the following manner:

$$SD1^2 = Var\left(\frac{1}{\sqrt{2}}RR_n - \frac{1}{\sqrt{2}}RR_{n+1}\right) = \frac{1}{\sqrt{2}}Var(RR_n - RR_{n+1}) = \frac{1}{2}SDSD^2 \quad (3.15)$$

, as stated in [13]. In the case of SD2, we can use the results of equations 3.10 and 3.11 to find that:

$$SD1^2 + SD2^2 = \phi_{RR}(0) + \phi_{RR}(0) = 2SDNN^2 \tag{3.16}$$

And using the results from equations 3.15 and 3.16:

$$SD2^2 = 2SDNN^2 - \frac{1}{2}SDSD^2 \tag{3.17}$$

So SD2 can be also expressed as a combination of some of the classical temporal indexes. Hence, as stated in [13], the ellipse fitting technique do not provide any information independent from that provided by the standard time domain indexes. On the other hand, the results of equations 3.15 and 3.17 allows to relate SD1 and SD2 with short- and long-term variability respectively, thus confirming the definitions of both parameters provided in the previous section.

The fact that standard Poincaré plot parameters are correlated with temporal indexes is the reason why in several studies Poincaré plot is classified as a geometrical method included in time domain analysis, as the indexes extracted from it do not portray information about the underlying nonlinear processes.

Furthermore, *Guzik et al.* also provide in [14] a comparison between SD1 and SD2 with the frequency domain parameters. According to this study, SD1 is highly correlated with HF also it is also significantly correlated with LF, thus confirming that SD1 contains information of both, PNS and SNS activity, although PNS information predominates here. On the other hand, SD2 was best correlated with measures of total HRV, which seems to be a consequence of the relation of total HRV with long-term HRV in short recordings. However, the correlation between SD2 and LF was twice as large as with HF in [14], what supports the idea that SD2 is more strongly related with SNS than PNS activity. Finally, S was highly correlated with most of the parameters analyzed, so S can be considered as the best descriptor of the total HRV extracted from Poincaré plot.

In conclusion, the main Problem with the analysis of HRV based on Poincaré plot is the lack of quantitative measures independent from the existing one, what suggests that nonlinear features of this method are not being exploited [13].

4. PURPOSE OF THE PRESENT STUDY

The Purpose of the present work is to study Poincaré plot analysis of HRV in detail in order to propose new parameters than may reflect additional features of HRV. The aim is to apply the defined parameters for the classification of a series of patients that have been classified in various groups attending to their asthma risk level. All the patients are children, aged between 3 and 7 years. The hypothesis underlying this study is that different changes in the parasympathetic activity of the patients belonging to the distinct risk groups might be observed, as abnormal parasympathetic activity is closely related to the pathogenesis of asthma. As parasympathetic activity is increased during sleep, the analysis is performed by using the ECG recordings acquired during the night period. This kind of nonlinear analysis for evaluating the risk of suffering from asthma in children has been never performed before, so the present work aims to provide a first approach to this problem. Although the main tool used here is Poincaré plot, also classical indexes are obtained and evaluated so that they can be used as a reference for Poincaré plot analysis.

In the previous section, Poincaré plot analysis has been treated in detail to understand its origins and the parameters that can be extracted from it, as well as the relationship between these parameters and the classical indexes used for HRV analysis. As shown there, although Poincaré plot analysis has its origin in non-linear dynamics, the studied parameters do not provide further information than the classical indexes, so it is not reflecting the non-linear behavior of HRV. Hence, in this work two new parameters are proposed: the angle formed by the line of identity and a numerical parameter that aims to provide a quantification of the plot's shape.

Furthermore, due to the fact that Poincaré plot is always referred in the literature as a visual tool for HRV interpretation, in this work the development of a GUI for aiding in the comparison between Poincaré plot and the classical parameters is also proposed. The mentioned GUI must be able to select a patient and a 5-minute interval to analyze, displaying the Poincaré plot obtained in this period as well as

the values of the several parameters, the PSD and the temporal evolution of every index along the whole duration of the ECG recording.

5. MATERIALS AND METHODS

Poincaré plot analysis is a method derived from nonlinear dynamics [10], although it has been proven that the parameters extracted from it do not provide additional information to that supplied by the classical temporal and frequencial indexes [14][13]. Hence, nonlinear features of Poincaré plot are not being exploited, so additional information may be hidden. In this section two additional parameters for the analysis of Poincaré plot are proposed. In addition, the data base used in this work is presented. Finally, the methods used for the analysis of the data base are described.

5.1 Patient material

The data base analyzed in this study is formed by ECG recordings of 34 children with ages between 3 to 7 years who were transferred to the Pediatric Allergy Unit of Helsinki University Hospital due to recurrent or persistent lower respiratory tract symptoms. Patients were classified in three different groups. They were divided into high risk (HR) and low risk (LR) groups according to their risk of asthma (which is decided from their modified asthma predictive index [65]), and the third group was composed with children with a history of wheeze and who were treated with inhaled corticosteroids (ICS). It is important to highlight that this classification is not based in the diagnosis of asthma or not, but just in the risk of having asthma as an statistical prediction.

Recordings duration are variable from 9 to about 19 hours each and in Figure 5.1 a 18 hours length signal from one of the patients is displayed. However, in this work the whole recording is not used due to the fact that the coughing associated with asthma usually occurs during the night or in the early morning [29]. Furthermore, it is known that vagal activity controlling the HR is increased at night and the lung function is worst around 4:00 a.m. [66]. For these reasons, in this thesis the focus is on the night periods, so just the segment of the recordings corresponding to the night is used (in Section 5.4 the definition of the night period is discussed).

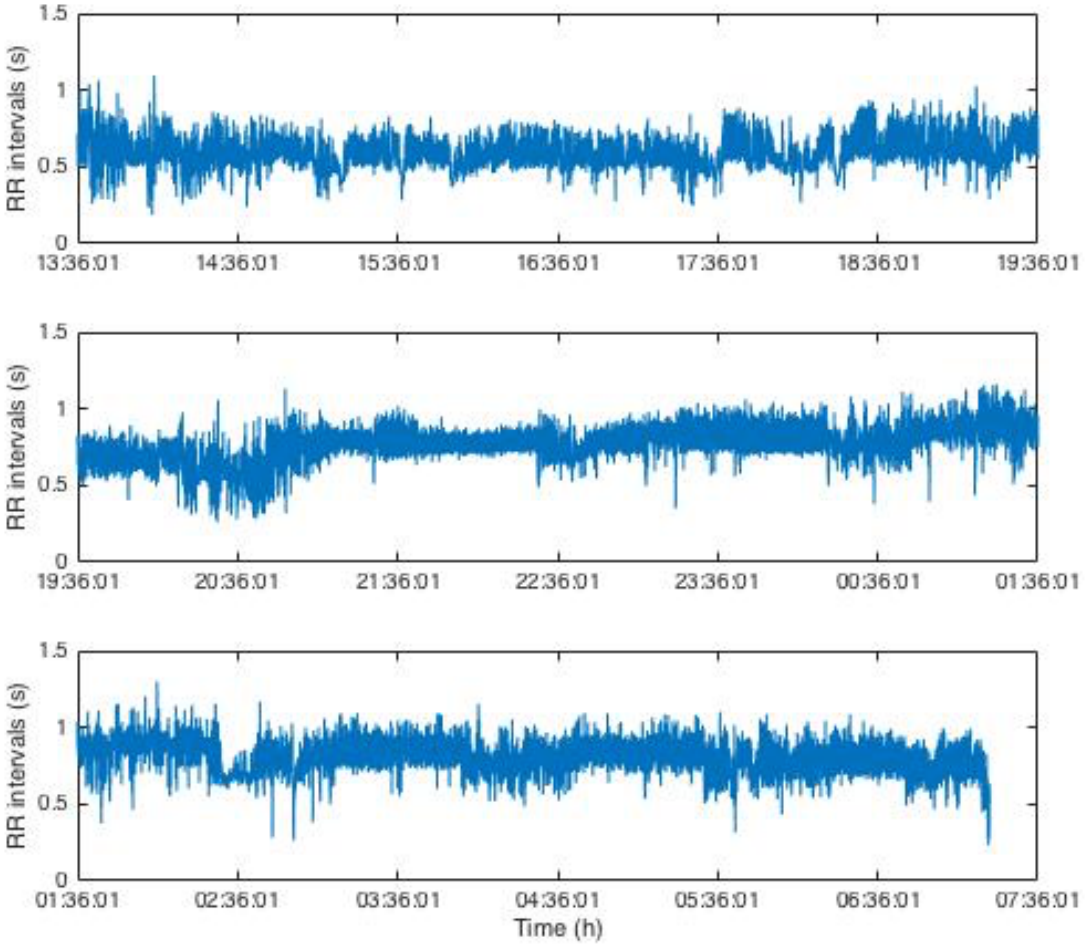

Figure 5.1 *The whole RR signal recording from one of the patients in the data base. As shown in the figure, HR values are continuously changing, and the average HR is different depending on the period of the day.*

The recordings were acquired by using a custom recording devices designed by Tampere University of Technology (Finland). These devices dispose of four skin electrodes that were symmetrically placed on the arms (close to the axilla) and thorax. The sampling frequency of the recording devices was 256 Hz.

Table 5.1 contains a summary of the information of the data base used in this work.

5.2 Poincaré domain proposed parameters

As introduced at the beginning of this section several studies have been proven that the parameters extracted from Poincaré plot do not provide additional information

Label	Quantity	Mean length (hh:mm:ss)
HR	13	13:02:34 (± 03:38:01)
LR	14	14:45:41 (± 03:43:33)
ICS	7	13:02:36 (± 02:54:33)
Total	34	13:45:02 (± 03:32:22)

Table 5.1 *Summary of the data base used in this work.*

than classical temporal and frequencial indexes [14][13]. In this work two new parameters are proposed, with the purpose of trying to reflect some features that may be useful in the understanding of the underlying processes represented through the plots. The first proposed parameter is the angle (or direction) in which the points are mainly oriented, and the second one is the shape of the plot. Although the shape has already been studied as an stratifier of heart disease [11][59], it has been always analyzed in a visual manner and in long-term recordings. Here, some possible features extracted from the shape are presented, in order to try to make this classification automatically so as the temporal evolution of short-term Poincaré plot shape can be studied.

5.2.1 Angle

The first proposed parameter is the angle of the Poincaré plot, from now referred to as θ, that can be calculated from the main direction along which the points forming the plot are spread. As described in Section 3.4, the line of identity divides the plot in two regions: the upper left region, where the condition $RR_{i+1} > RR_i$ is satisfied, and the lower right region, where the points satisfy $RR_{i+1} < RR_i$.

Due to the opposing effect of ANS branches the Poincaré plot is often symmetric, so the points are usually oriented along the line of identity, thus meaning that $\theta = 45^o$. A variation in the value of θ is only possible if one of the two following conditions is satisfied:

$$\theta > 45^o \iff \sum(RR_i < RR_{i+1}) > \sum(RR_i > RR_{i+1}) \tag{5.1}$$

$$\theta < 45^o \iff \sum(RR_i < RR_{i+1}) < \sum(RR_i > RR_{i+1}) \tag{5.2}$$

, where $\sum(RR_i < RR_{i+1})$ is the number of points above the line of identity and $\sum(RR_i > RR_{i+1})$ is the number of points below the line of identity.

The hypothesis that lead to the use of θ is that $\theta > 45^o$ is related with cardio-deceleration in the studied interval, as most of the RR intervals are longer than the previous. On the other hand, $\theta < 45^o$ is related with cardio-acceleration. The idea underlying this concept is to evaluate if sudden changes in the value of θ can be observed in the evaluated signals, as this could be an indicator of an asthma episode. However, this is not the only possible cause of a change in θ, as movement of the patient or awakeness periods could also be responsible of it.

An important condition for observing any change in θ is that the length of the interval analyzed is long enough to capture the event producing it, but short enough to avoid the way back to $\theta = 45^o$. In first instance, 5-minute periods will be considered, as recommended for the analysis of short-term Poincaré plot analysis [21], although this period can be modified if needed.

For the calculation of θ, Singular Value Decomposition (SVD) method is used [67].

5.2.2 Shape

Poincaré plot shape has already been analyzed in long-term recordings and it has been proven to be an stratifier of heart disease [11][59]. However, the temporal evolution of the shape in short-term recordings has still not being analyzed, and that is what is proposed in this work.

In the literature, several labels have been defined in order to classify the different shapes observed: comet, fan, torpedo, ... [11][59]. As it has been already discussed, the SD1 and SD2 parameters are closely related to the activity of the ANS, and so the shape is also related with it, due to the fact that these values have a direct influence on it. But the shape do not only depend of SD1 and SD2, as two the same values of these parameters can be observed in completely different shapes, so there must be some other hidden information involved in the generation of one or another pattern. As SD1 and SD2 are the only parameters used for describing the ellipse used in the ellipse fitting technique method, this is not the best way to describe the shape of a Poincaré plot what is clearly shown if we take another look to Figure 3.6 where the ellipse fitted to the plots do not describe the shape at all. By the

moment, most of the deeper studies concerning the shape have focused on the visual analysis and classification by experts, and so it would be interesting to dispose of a method that can label different patterns automatically.

In this work, a method to extract the shape is proposed. Essentially, the plot is first rotated an angle $-\theta$, being θ the angle described in the previous section. After that a scan is performed in order to extract the border of the shape. The way to do that is based in a sliding window that is displaced along the rotated plot. The standard deviation along the perpendicular direction of all the points covered by the sliding windows is calculated. By plotting all the standards deviations obtained, the result is the edge of the plot, so it constitute a quite reliable description of the shape. This process is shown in Figure 5.2.

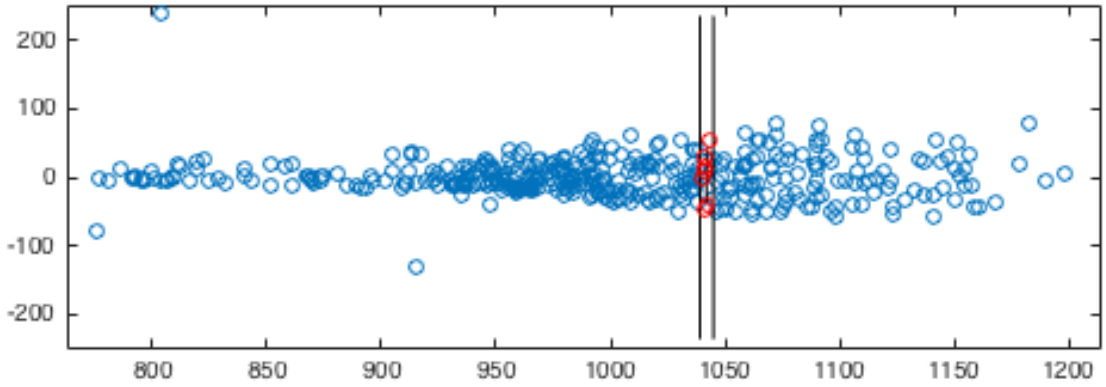

Figure 5.2 *The rotated Poincaré plot is scanned by a sliding window (represented with the two black lines in the image) which is displaced along the line of identity. The standard deviation of the points enclosed in the window (shown in red) is calculated for every position of the window, and the result is an approximation of the edge of the plot, and hence an approximation of its shape.*

Although this method aims to make the decision of the shape observed easier, it is still not able to automatically classify it. For this purpose, two new indexes that can be extracted from the Poincaré plot are proposed: $SD1^+$ and $SD1^-$. These parameters are calculated as the standard deviation of the plot along the perpendicular direction to the line of identity at the 70% and 30% of the length of the scanned shape respectively. The idea that underlays these new parameters is based on the observation that comet-shaped Poincaré plots have a maximum around 70% of their length [59]. The standard deviation of the plot at this point is what has been defined as $SD1^+$ here. On the other hand, $SD1^-$ is measured at the 30% of the length as by comparing both parameters the symmetry of the plot can be measured. Combining

the ratio between these parameters and the $\frac{SD1}{SD2}$ ratio, a numeric measurement of the shape an be obtained:

$$Sh = \frac{SD1}{SD2} + \frac{SD1^{-}}{SD1^{+}} \tag{5.3}$$

Taking a look to Equation 5.3, two components can be distinguished: $\frac{SD1}{SD2}$ is a kind of eccentricity measurement, being equal to 1 for the case of a circle and less if the plot is elongated along the line of identity ($SD2 > SD1$), while $\frac{SD1^{-}}{SD1^{+}}$ is a measurement of symmetry, being equal to 1 when the plot is exactly symmetric and less if the plot is wider for high values of the RR intervals (as in the case of a comet-shaped plot).

Using the value of Sh and considering noiseless plots, three different shape categories are tried to be distinguished:

- **Circular shape:** the values of SD1 and SD2 are similar, and the plot is symmetric, so $Sh \to 2$.
- **Elliptic shape:** in this case $SD2 > SD1$, but the plot is still symmetric, so $Sh \in (1, 2)$, as $\frac{SD1^{-}}{SD1^{+}} \to 1$.
- **Elongated non-elliptic shape:** this refers to either comet- or elongated triangular-shaped plots, where the points are spread along the line of identity and the plots are not symmetric. In this case, $SD2 > SD1$ and $SD1^{+} > SD1^{-}$, although it is difficult to determine a range for the value of Sh as it could take values higher than 1. However, it is expectable that $Sh \leq 1$ in this situation.

In this way, Sh constitute a numerical measure for classifying the shape of the Poincaré plot, although it is necessary to analyze if this value is enough to automatically classify it. This topic is covered and discussed in Section 6.

5.3 Poincaré domain filtering

Due to the fact that Poincaré plot is often presented as a visual technique, it is reasonable to think that the spatial distribution of the points could be used in order

to eliminate the ectopic beats. Several filters have been proposed in the literature in order to take advantage of the intrinsic characteristics of Poincaré plots [68][69] and in this work a combination of two of them is applied:

- **Square filter:** it is a simple filter, proposed in [68], that eliminates every single point produced by a RR interval shorter than 0.3 seconds or larger than 2 seconds. The selection of these thresholds is based in the physiological limits of the cardiovascular system [68].
- **Ensemble Density-Based Spatial Clustering of Applications with Noise (EDBSCAN) filter:** it is a cluster-based filtering method that was first proposed in [70]. Its performance it's a bit different from a k-means algorithm, and it has two main advantages: there is no need to select the number of clusters a priori and it is very robust against noise. Essentially, it consists on recursively apply the DBSCAN (Density-Based Spatial Clustering of Applications with Noise) algorithm [71], which basically operates as follows:

  1. Algorithm parameters are first defined. These parameters are a threshold ϵ and the minimum number of points that are considered to form a cluster, $MinPts$. The function of ϵ is to determine the maximum distance between two points in order to be considered into the same cluster.
  2. An initial point is selected, and all its neighbours are located. A point is considered as a neighbour of another if the Euclidean distance between them is less than ϵ.
  3. For each neighbour of the initial point, all its neighbours are located, and this process is iteratively repeated until there is no point whose distance to some of the analyzed points is less than ϵ. All the points analyzed until now are grouped in the same cluster.
  4. Steps 2 and 3 are repeated with the next point that has been still not selected.
  5. When there are no points left to select, the filtering process is ended. The clusters with a number of points that is less than $MinPts$ are automatically classified as outliers.

  The main problem with DBSCAN algorithm is to determine an appropriate value for ϵ. EDBSCAN consist on applying DBSCAN recursively to the same

data, using different values for ϵ in each iteration (the selection of the range of values used is shown in [70]). The results of each iteration is stored in a matrix A, called co-association matrix. Once the iterations have finished, the results of A are evaluated in order to decide which point is associated with which cluster. The evaluation of A is further discussed in [69] and [71].

The performance of the combination of both proposed filters is analyzed and discussed in Section 6.

5.4 Signal analysis and statistical methods

The signal analysis performed in this work consist on three main phases, that are the pre-processing stage, the extraction of time, frequency and Poincaré domain parameters, and the further analysis of these parameters in order to evaluate if they are able to distinguish between the different asthma risk groups. These stages are described in detail below.

The pre-processing stage is mainly performed with the aid of Biosigbrowser software [72], which is a software for HRV analysis developed by the Biomedical Signal Interpretation and Computational Simulation (BSICoS) group from the University of Zaragoza. However, Biosigbrowser impose that the ECG recording must be sampled at 1000 Hz. As the recorder signals are sampled at 256 Hz they must be resampled, so an interpolation with cubic splines is performed, thus conditioning the signals for its processing with the software.

First of all, the resampled ECG recording correspondent to each patient is loaded into the software, and a filtering is performed in order to remove the baseline (200^th order high-pass filter with 0.3 Hz cutoff frequency) and the power-line interference (nonlinear 50 Hz filter). After that, QRS complex detection is performed. The QRS complex detector integrated in Biosigbrowser is a wavelet-based detector described in [73]. These steps are very important, as a correct detection of the QRS complexes and the further removal of the beats that have not their origin in the sinusal node is critical for the derivation of the RR interval series used for HRV analysis. An overall view of Biosigbrowser interface is displayed in Figure 5.3.

The result provided by Biosigbrowser is an ensemble of annotation files for each patient: one annotation file including the QRS complexes position for each hour of

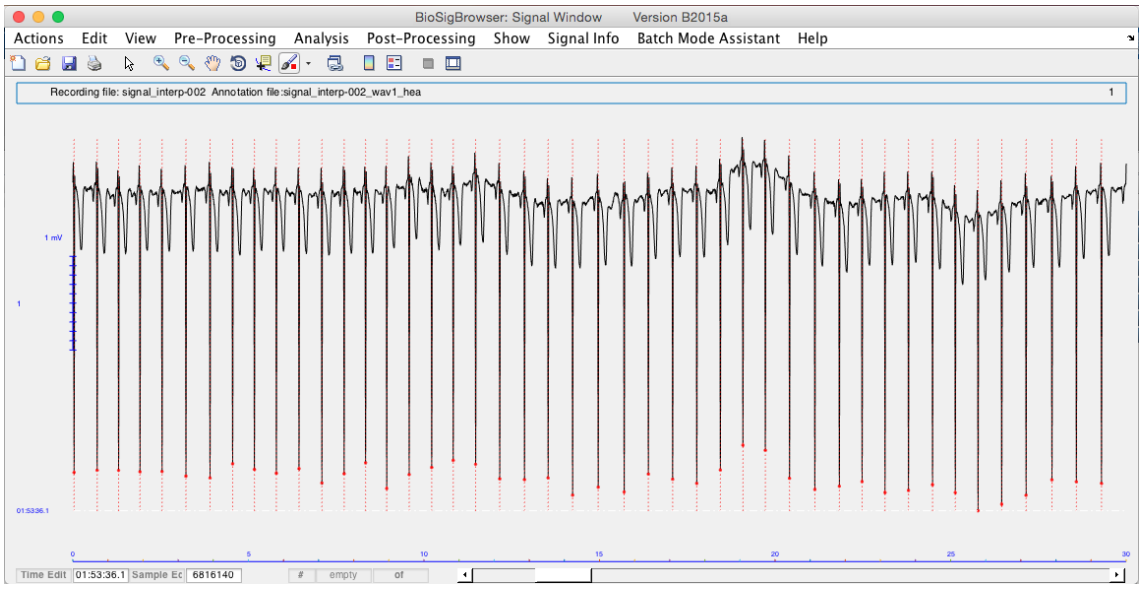

Figure 5.3 *The interface of Biosigbrowser is displayed. 30 seconds of the ECG recording from one of the patients is shown here, and the annotations corresponding to the QRS complexes position are marked with red dashed lines, while the fiducial points are indicated with a red circle.*

the analyzed ECG recording. These several annotation files are merged into one single file per patient, in order to facilitate the further analysis.

The next step is to obtain time, frequency and Poincaré domain parameters. As for this work only the interval of the recording corresponding to the night period is going to be analyzed the signals must be first segmented. The ECG recordings of the different patients have different starting times and duration, so the night period is defined between 22:30:00 and 05:00:00 in order to dispose of the same signal length for every patient. Hence, just the QRS complexes detected in this period are considered, and the RR interval series are obtained by just differentiating the QRS complexes epochs registered in the annotation files. For the later analysis only these RR interval series are taken into account and from this point the whole analysis is performed using MatLab software.

From the RR interval series time domain parameters described previously are obtained. These parameters are obtained from 5-minute intervals using a sliding window for this purpose: the length of the window is 5 minutes and it is displaced in 1 minute steps, so the parameters are obtained each minute taking the previous and next 2 minutes of the recording into account. The result from this stage is a struct containing the value of each parameter for each analyzed time interval and the mean

value and standard deviation of the parameters along all the intervals evaluated.

After the time domain parameters, frequency domain parameters are calculated. As in the previous case, parameters are are obtained for each 5-minute segment with 1-minute step. However, the RR interval series are not evenly sampled due to the fact that HR is not constant and the estimation of the PSD for each segment can be performed either by using methods that directly work over the unevenly sampled series, as the Lomb's periodogram [52], or resampling the RR interval series in order to obtain an evenly sampled series from which PSD can be computed by mean of the classical spectral analysis techniques (parametric or non-parametric estimation). In this work evenly sampled series were used, so the original series were resampled at 4 Hz sampling frequency as recommended in [21] and linear interpolation was employed. After that, PSD estimation was computed with Welch's periodogram method [74], which is the most classical non-parametric method for PSD estimation. It essentially consists on spliting the analyzed interval into overlapping segments, and calculating the modified periodogram of each segment. The obtained periodograms are later averaged. The parameters that must be selected when using this method are the window used and its length, and the percentage of overlapping between segments. In the present study 30 seconds Hamming window and 50% overlapping were selected.

All the frequency parameters described in Section 3.2 were derived from the estimated PSD of each segment. As in the case of time domain parameters, the mean and standard deviation of each parameter along the whole set of intervals were also calculated and all the values of the various parameters were stored in a struct.

Finally, Poincaré plot was constructed for each 5-minutes interval (using the same sliding window than in the time and frequency analysis). All the classical parameters derived from Poincaré plot and also the two proposed ones, angle and shape, were calculated from each interval. As already explained, the angles was computed with the SVD method, while the shape parameter was derived as shown in Equation 5.3. These parameters were obtained in two different situations: first from the Poincaré plot generated with the RR interval series already described and then from the filtered version of the Poincaré plot, where the filtering was performed directly in the Poincaré domain with the filters introduced in the section above. In the second case, new RR interval series are generated because the previous ones were obtained after ectopic beats correction, so applying the new filtering over these already cor-

rected series would no allow to evaluate the filter behavior in a proper manner. The new series are obtained from the annotations generated by Biosigbrowser but without performing the ectopic beat correction step. After that, Poincaré plots were generated and the parameters derived. The output of this analysis are two different structs, one with the information extracted from non-filtered Poincaré plot and another from the filtered plots.

Once all the parameters in the three studied domains were calculated a statistical analysis for evaluating the ability of each index for distinguishing between the three proposed groups was performed. The statistical analysis was based in a non-parametric Wilcoxon test performed with a confidence interval of 0.05. This test was performed considering the whole night period, but also hour per hour, in order to identify if there is a specific time period during the night were the differences between groups are better defined. For both cases, four different tests were performed, using different values as the input of the Wilcoxon test. The four proposed inputs are the median, inter-quartile range (iqr), minimum and maximum of the values of the parameters for each patient in the defined analysis interval.

6. RESULTS AND DISCUSSION

The main interface of the GUI developed is shown in Figure 6.1. The interface is divided into sections in order to make its use as easy as possible and there are three main sections. The first one contains the different menus and is located in the left side. These menus allow to select the information we want to analyze and the methods used, as well as some other functions that will be later described. The second section is formed by the three panels located in the center of the interface, each of which present different information: the upper panel shows the selected 5-minutes RR interval signal segment being analyzed, the lower left panel shows the Poincaré plot of the signal (although some other representations derived from Poincaré plot are also shown here: lagged or 3^{rd} order Poincaré plots) and the lower right one shows either the spectrum of the signal or the temporal evolution of the selected parameter. Finally, the third section contain the values of all the parameters calculated from the signal, both in the 5-minute segment analyzed and in the whole recording. In this section all the elements of the GUI and their features are described.

First of all the patient to analyze must be selected. In Figure 6.2 the Patient & time selection menu is shown. By selecting the number of the patient from the patient dropdown menu all the information of the selected patient is loaded into the GUI. Just below this dropdown menu the classification label of the patient is displayed. As described in Section 5.1, the possible labels are HR (high-risk), LR (low-risk) and ICS (inhaled corticosteroids). The other parameter controllable from this menu is the current time of analysis. The eligible time periods cover the whole night recording, in 5-minute intervals that can be selected from minute to minute. The time interval to analyze can be selected either from the time dropdown menu or by introducing it manually, checking the Manual Selection box. Moreover, it is possible to go to the next or the previous segment rapidly by using the buttons Next and Prev.

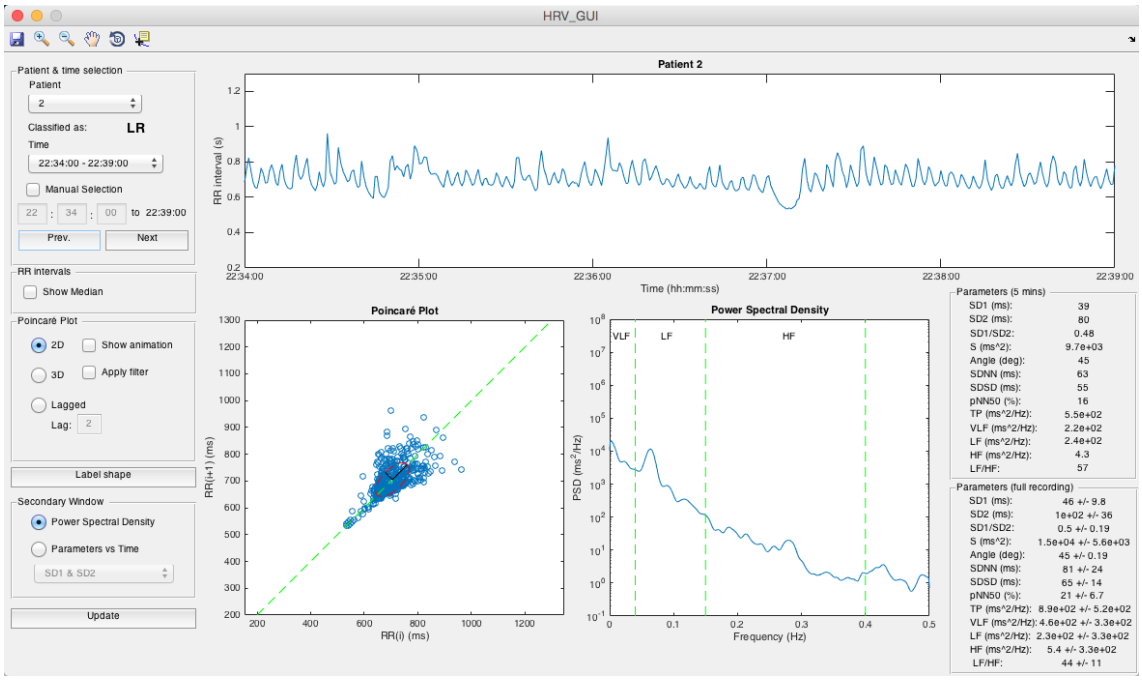

Figure 6.1 *Main window of the GUI. The menus controlling the characteristics of each domain analysis are located in the left of the image. In the center, three panels shows different visual information: the upper one shows the RR interval series of the 5-minute selected segment, the lower-left displays the Poincaré plot of that segments and the fitted ellipse, and the lower right displays either the PSD of the analyzed segment or the temporal evolution of a selected parameter (this option is later described in the text).*

The next menu is the RR intervals menu, and it only consist of a box that allows to show or hide the median of the RR intervals signal, calculated with a 25^{th} order median filter, in the upper panel. When selected, the median of the signal is plotted with a dashed-red line, as shown in Figure 6.3.

Just below the RR intervals menu the Poincaré plot menu is found, and here it is possible to select the information displayed in the lower left panel of the GUI. This menu contains several different representation options:

- **2D:** plots the 2D Poincaré plot of the selected segment, including the line of identity, the SD1 and SD2 values and the fitted ellipse.
- **3D:** plots the 3D Poincaré plot by including RR_{n+2} as a new dimension in the original Poincaré plot. It is also possible to select any of the 2D projections of the 3D view.
- **Lagged:** plots the m-lagged Poincaré plot, where m can be selected in the

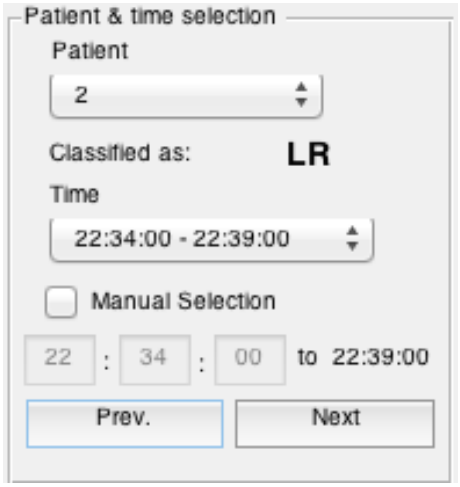

Figure 6.2 *Patient and time selection menu. Both the patient and the interval to analyze can be selected here, and also movement to next and previous 5-minute interval is possible.*

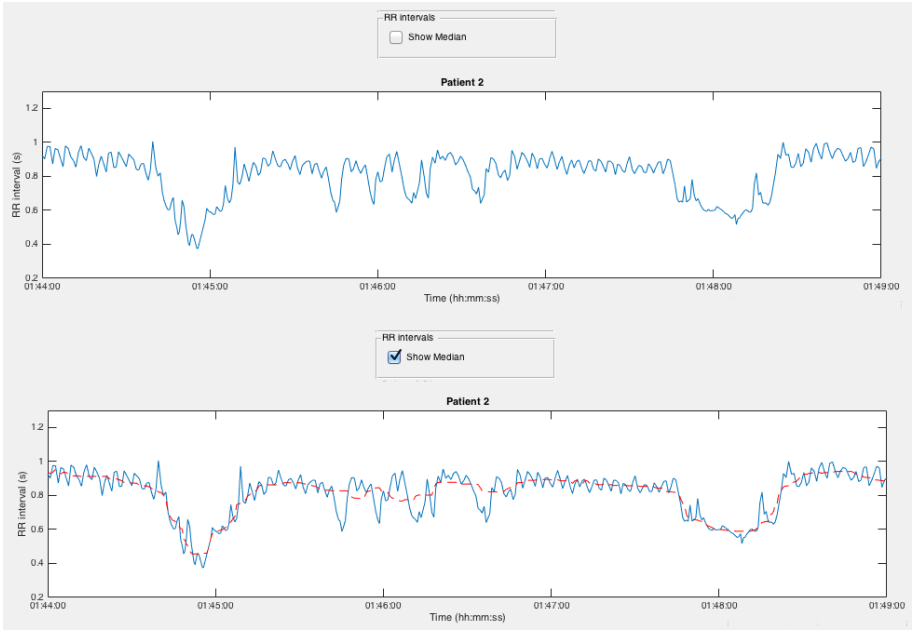

Figure 6.3 *The median of the current segment (red dashed line) can be shown in the upper panel just by checking the Show median box in the RR intervals menu.*

window Lag with values from 2 to 10.

- **Show animation:** by checking the Show animation box, the Poincaré plot is plotted point by point, so it is possible to analyze how it has been generated and to check where the origin of any point is, as a black vertical line indicating the current point is displayed in the RR interval (upper) panel.

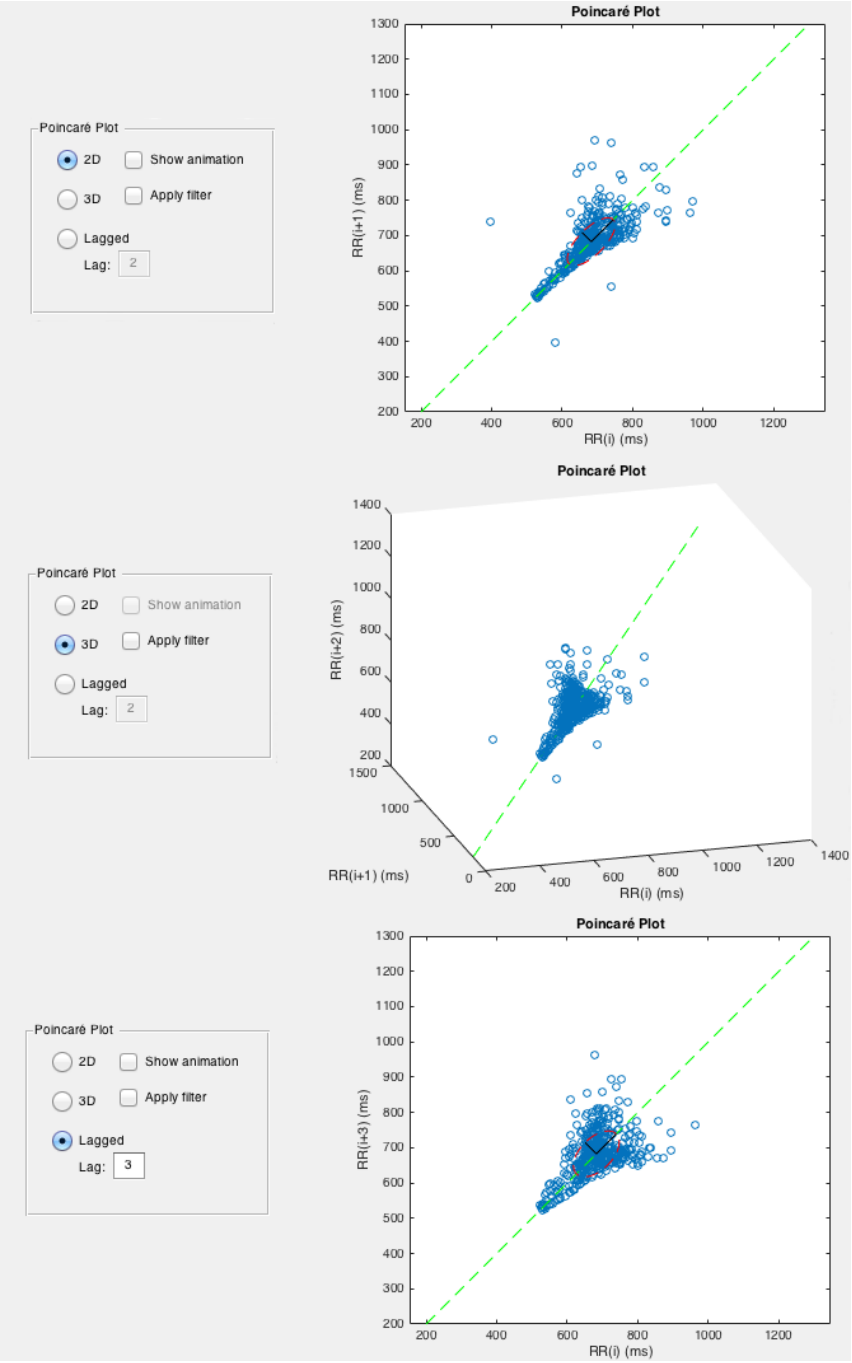

Figure 6.4 *From the Poincaré plot menu several representations can be chosen: traditional 2D Poincaré plot (upper panel), 3D plot by including the lag-2 information (middle panel) and lag-m plot, with m varying from 2 to 10 (lower panel). In the case of 3D representation also the projections in the planes X, Y and Z can be shown.*

- **Apply filter:** by checking the Apply filter box, the filtered version of the Poincaré plot is displayed. The filtering process consist on applying the filters

described in the previous section, both square and EDBSCAN filters. When this option is selected, all the parameters concerning the Poincaré plot are calculated from the filtered version.

- **Label shape:** the button label shape opens a new window, shown in Figure 6.5. In this window the scan of the shape described in Section 5.2.2 is shown in the right panel, while in the left panel an augmented view of the Poincaré plot is displayed in order to aid in the decision of the shape observed. Several different shapes can be selected, and the selected label is saved in a file together with the information of the temporal interval when the current shape was observed. Additionally, the midpoint of the shape and the points corresponding to the 30% and 70% of the plot length are labeled, with a red and two black circles respectively. The aim of this labels is to provide a reference in order to visually evaluate the symmetry of the plot, and also to rapidly detect if there is a maximum at about the 70% of the length, as usually occur in the case of comet-shaped plots [59]. Furthermore, the black circles allow to visually compare the values of $SD1^-$ and $SD1^+$ in a rapid way.

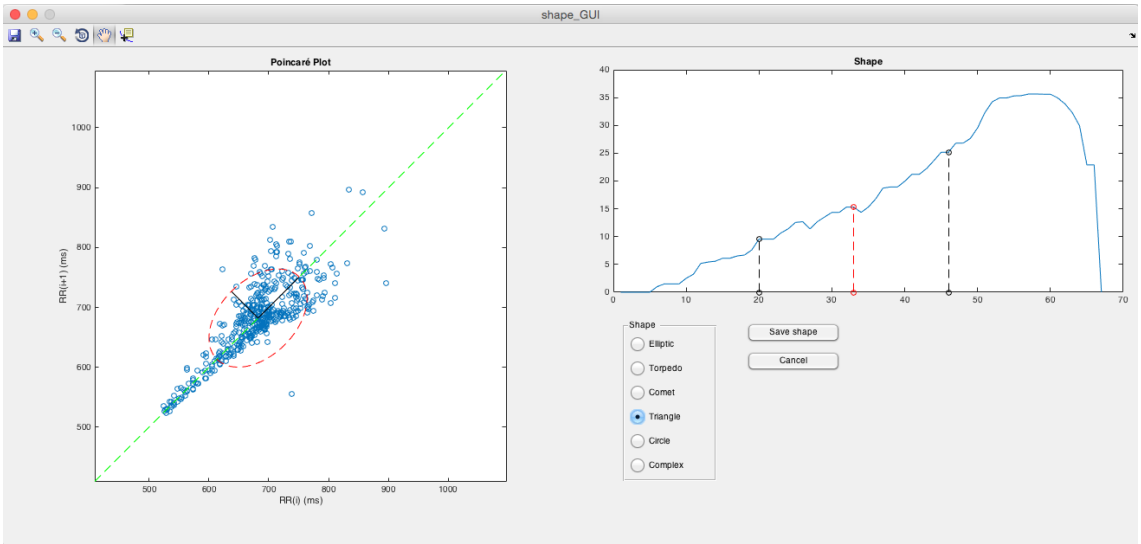

Figure 6.5 *Several options can be selected to label the shape of the Poincaré plot. The red circle in the scanned shape indicates the midpoint, while the black circles indicate the 30% and 70% of the scanned shape length, it is, the values of $SD1^-$ and $SD1^+$ respectively.*

The last available menu is the Secondary Window menu, which controls the parameters displayed in the lower right panel. It is possible to select between Power Spectral Density, which displays the PSD of the analyzed segment in the lower right

panel, and Paramters vs Time. If the last option is selected, the dropdown menu situated just below it becomes available, allowing to choose between several HRV parameters. Once one is selected, its evolution against time is plotted in the lower right panel. The different options are:

- Poincaré domain parameters: SD1 & SD2, SD1/SD2 ratio, S and angle.
- Time domain parameters: SDNN, SDSD and pNN50.
- Frequency domain parameters: TP, VLF, LF, HF and LF/HF ratio.

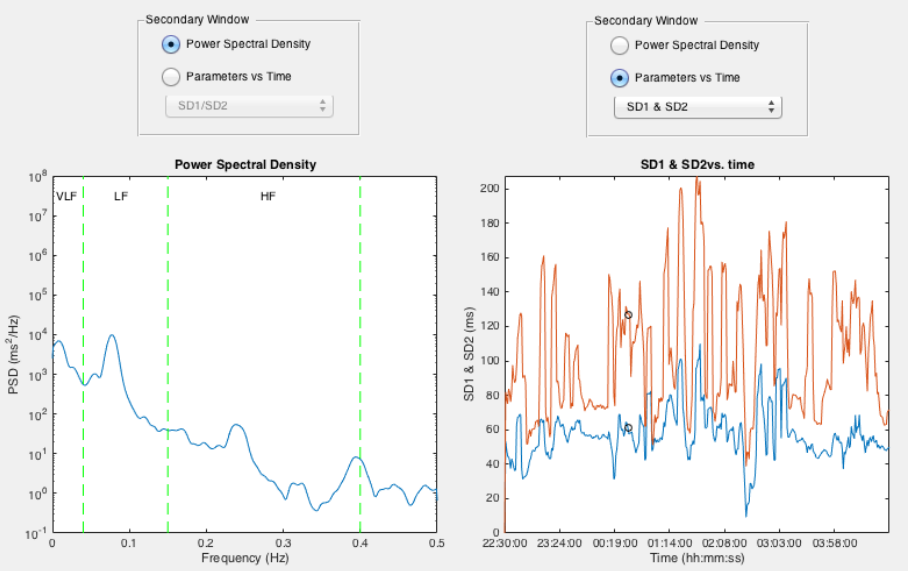

Figure 6.6 *In the secondary window menu it is possible to select if we prefer to plot the PSD or the temporal evolution of any parameter in the lower right panel. In the image an example of both PSD and temporal evolution of SD1 and SD2 is displayed. In the case of having selected to plot the temporal evolution of any parameter, the initial time of the 5-minute interval from where the parameter is calculated is marked with a black circle over the parameter value.*

Finally, the value of all the parameters described above is numerically displayed in the right section of the GUI. As shown in Figure 6.7, each parameter has two different values: one extracted from the selected 5-minute interval and the other corresponding to the whole recording. It is important to remember that if the Apply filter box in the Poincaré menu is checked, the values of the parameters concerning the Poincaré plot will be calculated from the filtered version instead of the original one.

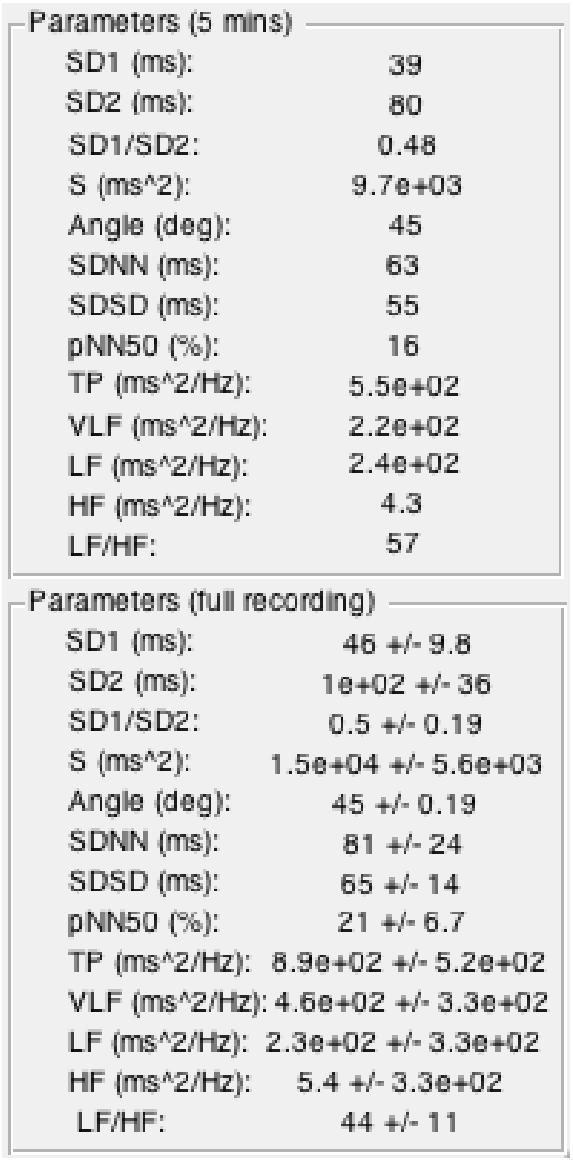

Figure 6.7 *Examples of the parameters values for one patient. These parameters are displayed in the right side of the GUI, and each parameter is calculated from the current 5-minute interval and from the whole recording.*

The GUI developed here results very useful for the visual inspection of what is going on in a defined analysis interval, as the different indexes extracted from distinct domains can be rapidly visualized and compared. However, the comparison is not only visual since numerical values are also displayed in the interface (as shown in Figure 6.7). In this way, given a certain time interval, it is easy to compare it with other intervals and search for any event of interest, as a sudden increase or decrease in HR that may be related, e.g., with an asthmatic episode. The several options included in the GUI provides the possibility of evaluate those events from

various different perspectives: for example, given a sudden change in the shape of the Poincaré plot we can take a look to the PSD of the same interval to identify which branch of the ANS is more likely to have produced it, or evaluate how the time domain indexes have been modified.

Together with the reduction in time consuming tasks like selecting the interval to display, extract all the indexes and plot the different results we want to compare, an important advantage of the developed GUI is that it is menu-based, and each menu is independent on the others. This is a valuable feature in the sense that the capabilities of the GUI can be constantly updated without need to modify the previous code. In this way, one of the future work lines of this work is to introduce the possibility to display more nonlinear indexes apart from those extracted from Poincaré plot, thus increasing the information displayed in the GUI and making the analysis features more complete.

Once the interface development was completed, the next step was the analysis of the signals corresponding to each group of patients, in order to study the capability of the different proposed indexes to distinguish between them. As already explained in Section 5.4 the analysis was performed just during the night period, and the several indexes were calculated both for the whole night and in one hour duration intervals. After the extraction of the parameters for these proposed intervals, four different measures were proposed: median, iqr, minimum and maximum of all the indexes in the analysis interval. The patients were divided in groups according to their label and the results obtained for the patients in different groups were analyzed through a non-parametric Wilcoxon test, in order to investigate the capability of the studied indexes to distinguish between them.

As a summary of the results of the analysis, the mean and standard deviation for each studied index and for each analysis interval obtained for the three different risk groups are displayed in a series of tables. Some examples containing the data related with the median and the iqr for three different intervals of analysis are shown below, but the full set of results is included in the Appendix.

Table 6.1 *Median (mean value and standard deviation) of the different parameters between 23:00 and 00:00. Significative differences between groups ($p < 0.05$) are marked with $*$ in the case of LR vs. HR, † in the case of LR vs. ICS and ‡ for HR vs. ICS).*

	23:00-00:00		
	LR	**HR**	**ICS**
SDNN (ms)	70.56 ± 22.12	80.25 ± 37.30	81.08 ± 26.62
SDSD (ms)	68.75 ± 24.72	75.08 ± 52.77	78.10 ± 32.44
pNN50 (%)	40.13 ± 17.69	34.30 ± 23.37	42.00 ± 16.53
TP (ms^2/Hz)	712.87 ± 460.42	1091.41 ± 825.78	1073.96 ± 575.91
VLF (ms^2/Hz)	347.15 ± 267.85	564.61 ± 463.41	506.20 ± 300.54
LF (ms^2/Hz)	259.85 ± 163.70	370.26 ± 401.31	402.51 ± 288.24
HF (ms^2/Hz)	9.79 ± 5.27	12.98 ± 16.37	11.58 ± 8.92
LF/HF (n.u.)	28.97 ± 12.89	36.34 ± 16.46	35.81 ± 17.77
SD1 (ms)	72.61 ± 22.97	75.49 ± 42.81	76.13 ± 23.52
SD2 (ms)	99.81 ± 27.91	104.71 ± 40.59	107.61 ± 35.02
SD1/SD2 (n.u.)	0.73 ± 0.11	0.68 ± 0.20	0.71 ± 0.11
S (ms^2)	26018.03 ± 15467.86	32207.26 ± 24297.47	29708.12 ± 17764.69
θ (^{o})	64.76 ± 39.42	65.77 ± 50.84	58.11 ± 35.09
Sh (n.u.)	1.47 ± 0.32	1.45 ± 0.69	1.40 ± 0.25

Table 6.2 *Median (mean value and standard deviation) of the different parameters between 01:00 and 02:00. Significative differences between groups ($p < 0.05$) are marked with $*$ in the case of LR vs. HR, † in the case of LR vs. ICS and ‡ for HR vs. ICS).*

	01:00-02:00		
	LR	**HR**	**ICS**
SDNN (ms)	77.90 ± 37.39	86.11 ± 48.21	95.24 ± 40.06
SDSD (ms)	67.75 ± 27.98	75.91 ± 48.45	99.65 ± 44.77
pNN50 (%)	35.64 ± 17.51	34.34 ± 20.14	49.34 ± 13.20
TP (ms^2/Hz)	978.04 ± 934.11	1296.93 ± 1363.07	1644.53 ± 1893.39
VLF (ms^2/Hz)	524.62 ± 532.70	709.12 ± 826.53	755.73 ± 951.08
LF (ms^2/Hz) †	258.27 ± 184.41	350.55 ± 349.43	602.05 ± 501.20
HF (ms^2/Hz)	10.08 ± 5.82	13.00 ± 15.54	15.31 ± 9.51
LF/HF (n.u.)	25.41 ± 7.95	33.49 ± 11.05	35.90 ± 14.91
SD1 (ms)	68.36 ± 30.94	90.46 ± 51.06	56.04 ± 22.73
SD2 (ms)	104.86 ± 51.60	121.50 ± 60.61	80.35 ± 23.99
SD1/SD2 (n.u.)	0.68 ± 0.19	0.70 ± 0.15	0.69 ± 0.12
S (ms^2)	26641.70 ± 20552.96	46385.89 ± 41557.12	16893.66 ± 12960.73
θ (^{o})	64.01 ± 48.85	61.52 ± 41.82	63.73 ± 50.61
Sh (n.u.)	1.34 ± 0.48	1.35 ± 0.32	±

Table 6.3 *Median (mean value and standard deviation) of the different parameters between 03:00 and 04:00. Significative differences between groups ($p < 0.05$) are marked with $*$ in the case of LR vs. HR, † in the case of LR vs. ICS and ‡ for HR vs. ICS).*

	03:00-04:00		
	LR	**HR**	**ICS**
SDNN (ms)	86.07 ± 24.92	89.98 ± 43.15	92.78 ± 29.32
SDSD (ms)	71.00 ± 25.27	83.2 ± 54.36	89.85 ± 39.30
pNN50 (%)	38.07 ± 16.07	37.36 ± 20.51	46.06 ± 16.17
TP (ms^2/Hz)	1445.31 ± 1733.68	1348.28 ± 1112.40	1268.31 ± 834.47
VLF (ms^2/Hz)	818.63 ± 1109.07	663.43 ± 565.99	584.64 ± 310.27
LF (ms^2/Hz)	269.61 ± 161.91	411.53 ± 442.61	506.76 ± 445.42
HF (ms^2/Hz)	9.88 ± 4.84	15.1 ± 15.63 ± 13.66	8.96
LF/HF (n.u.)	30.28 ± 13.82	32.98 ± 12.95	33.20 ± 14.75
SD1 (ms)	91.45 ± 50.09	91.44 ± 43.17	96.65 ± 62.74
SD2 (ms)	135.96 ± 68.57	124.99 ± 53.49	148.75 ± 91.1
SD1/SD2 (n.u.)	0.67 ± 0.12	0.72 ± 0.13	0.64 ± 0.13
S (ms^2)	62364.71 ± 96988.26	45734.65 ± 32530.40	82593 ± 135473.99
θ (^{o})	45.08 ± 0.27	65.86 ± 50.75	45.05 ± 0.16
Sh (n.u.)	3.25 ± 7.35	1.38 ± 0.55	1.19 ± 0.23

Table 6.4 *Iqr (mean value and standard deviation) of the different parameters between 23:00 and 00:00. Significative differences between groups ($p < 0.05$) are marked with $*$ in the case of LR vs. HR, † in the case of LR vs. ICS and ‡ for HR vs. ICS).*

	23:00-00:00		
	LR	**HR**	**ICS**
SDNN (ms)	14.59 ± 13.62	29.7 ± 27.43	32.81 ± 25.74
SDSD (ms)	14.77 ± 7.49	16.83 ± 12.5	23.24 ± 27.97
pNN50 (%)	8.94 ± 6.27	10.94 ± 10.51	17.73 ± 13.21
TP (ms^2/Hz)	368.05 ± 323.06	741.23 ± 727.31	903.01 ± 707.68
VLF (ms^2/Hz) †	223.51 ± 176.83	545.79 ± 523.78	563.56 ± 475.61
LF (ms^2/Hz)	107.99 ± 82.48	110.77 ± 98.81	182.52 ± 205.18
HF (ms^2/Hz)	5.41 ± 5.61	5.39 ± 4.74	5.22 ± 4.64
LF/HF (n.u.)	10.41 ± 7.64	8.83 ± 6.84	14.95 ± 13.97
SD1 (ms)	34.87 ± 37.89	30.56 ± 43.34	44.41 ± 38
SD2 (ms)	42.04 ± 33.23	57.24 ± 52.47	46.1 ± 34.88
SD1/SD2 (n.u.)	0.19 ± 0.13	0.17 ± 0.15	0.17 ± 0.15
S (ms^2)	21907.26 ± 23880.99	25345.3 ± 27807.26	27265.61 ± 25262.29
θ (^{o})	39.98 ± 78.59	41.72 ± 101.66	26.99 ± 69.94
Sh (n.u.)	0.46 ± 0.49	0.45 ± 0.39	0.52 ± 0.7

Table 6.5 *Iqr (mean value and standard deviation) of the different parameters between 01:00 and 02:00. Significative differences between groups ($p < 0.05$) are marked with $*$ in the case of LR vs. HR, † in the case of LR vs. ICS and ‡ for HR vs. ICS).*

	01:00-02:00		
	LR	**HR**	**ICS**
SDNN (ms)	23.35 ± 19.82	22.68 ± 15.23	42.51 ± 33.08
SDSD (ms) ‡	22.4 ± 24.03	14.22 ± 12.17	47.6 ± 30.96
pNN50 (%)	14.42 ± 14.4	9.70 ± 6.87	18.96 ± 15.88
TP (ms^2/Hz)	486.82 ± 563.76	589.62 ± 546.78	1638.64 ± 2750.02
VLF (ms^2/Hz)	296.75 ± 362.54	455.46 ± 504.94	794.56 ± 1514.08
LF (ms^2/Hz) †‡	147.57 ± 157.06	136.57 ± 162.6	512.6 ± 385.55
HF (ms^2/Hz)	5.52 ± 5.4	5.02 ± 6.34	11.48 ± 9.01
LF/HF (n.u.)	5.95 ± 3.72	9.05 ± 8.9	12.22 ± 8.74
SD1 (ms)	30.24 ± 30.23	47.78 ± 49.59	23.97 ± 29.68
SD2 (ms)	35.75 ± 35.12	53.9 ± 39.18	39.25 ± 39.28
SD1/SD2 (n.u.)	0.21 ± 0.23	0.16 ± 0.11	0.16 ± 0.15
S (ms^2)	15184.11 ± 19479.99	37630.40 ± 46132.76	15242.69 ± 21974.14
θ (^{o})	38.68 ± 97.37	36.73 ± 90.25	38.73 ± 100.65
Sh (n.u.)	0.59 ± 0.56	0.52 ± 0.61	0.65 ± 0.59

Table 6.6 *Iqr (mean value and standard deviation) of the different parameters between 03:00 and 04:00. Significative differences between groups ($p < 0.05$) are marked with $*$ in the case of LR vs. HR, † in the case of LR vs. ICS and ‡ for HR vs. ICS).*

	03:00-04:00		
	LR	**HR**	**ICS**
SDNN (ms)	39.13 ± 30.05	29.04 ± 24.13	34.23 ± 28.49
SDSD (ms)	22.32 ± 17.56	16.69 ± 10.14	32.53 ± 30.21
pNN50 (%)	12.79 ± 10.27	11.39 ± 5.82	20.76 ± 19.82
TP (ms^2/Hz)	1681.25 ± 3235.68	872.28 ± 882.4	749.52 ± 541.76
VLF (ms^2/Hz)	1057.96 ± 2032.22	530.6 ± 600.06	516.23 ± 423.47
LF (ms^2/Hz)	139.51 ± 125.7	146.24 ± 113.14	280.39 ± 256.75
HF (ms^2/Hz)	5.2 ± 4.02	5.87 ± 4.35	6.63 ± 7.18
LF/HF (n.u.)	10.9 ± 16.48	11.9 ± 16.64	11.33 ± 4.98
SD1 (ms)	74.05 ± 96.97	41.97 ± 54.89	86.44 ± 119.37
SD2 (ms)	102.49 ± 131.61	62.93 ± 53.5	129.91 ± 175.12
SD1/SD2 (n.u.)	0.19 ± 0.13	0.16 ± 0.14	0.11 ± 0.07
S (ms^2)	93429.73 ± 193469.67	38729.11 ± 48919.12	134007.77 ± 268527.89
θ (^{o})	0.33 ± 0.42	41.67 ± 101.26	0.19 ± 0.26
Sh (n.u.)	4.45 ± 14.73	0.47 ± 0.6	0.34 ± 0.2

Taking a look to Tables 6.1- 6.6, it is possible to see that none of all the analyzed indexes is capable of distinguishing between the given study groups. Although there are some of them that are able to distinguish between two of the three groups in certain periods (e.g., see Table 6.5) it can not be considered that they can be used to classify the patients in the group they belong to, as only isolated classifications take place, i.e., these indexes are not always able to classify the patients and hence they are neither good markers of asthma risk.

The main problem here is that the patients are not classified attending to the existence of asthma or not, but just to their asthma risk (obtained through the evaluation of their modified asthma predictive index [65]) which is actually derived from the presence of certain symptoms that are usually related with asthma, e.g. wheezing or markers of atopy. Due to this fact, it is possible that patients classified as low risk or high risk do suffer from asthma, but this information is not reflected in the data base, as there is not a method to ensure which of the patients have developed the disease, and the different HRV analysis methods have been shown to not serve as risk stratifiers in this case. This results could reflect that the abnormal ANS activity related with asthma do not manifest in advance to an asthmatic episode, and as we are unknown of the information related to if a patient has gone through an episode during the recording time, the information extracted here can not be used as a marker for deciding the risk of suffering from asthma in a given patient

Both in the tables and in the temporal evolution of the indexes displayed in the GUI it can be noticed that there is a wide intersubject variability of all the parameters in the three groups despite the fact that the data base is well balanced, i.e., the same parameter can take several different values for the several patients even if they belong to the same group (it can be seen in the high standard deviation over the mean value of all the parameters). Due to this fact, when the medians, iqrs, minimums and maximums of the analyzed time intervals are studied, the intersubject variability can be translated in a compound of highly different values inside every group that cause the mean and standard deviation of these values to be very similar for all of them. Furthermore, as the initial hypothesis was that a modification in the parasympathetic activity of the patients classified in the HR group could be observed but this fact can not be derived from the performed analysis, the ability of the new proposed Poincaré plot parameters to provide new information can not be checked, as it has not been possible to extract a gold standard from the data in order to perform a comparison. However, it is possible to study the typical values

of these new parameters in order to understand the information that they provide.

First of all, regarding at the values obtained for the angles in the hour-per-hour analysis, it is possible to see that the angle is not always 45^o as it is typically considered when deriving SD1 and SD2 from a Poincaré plot. Although it tends to this value when we consider longer periods of time (as seen in the results for whole night evaluation), when performing short-term analysis of the plots it is important to notice that the angle is changing. Even if the changes observed are not very strong, it is true that a modification in the principal direction of the plot will directly affect the values of SD1 and SD2, that are usually calculated taking the 45^o direction as a reference. In this way, when performing short-term analysis via Poincaré plots, the angle should be first corrected in order to obtain an accurate calculation of SD1 and SD2.

On the other hand, the study of the evolution of the shape over time has not been proven to serve as an indicator of asthma risk. This is an expected result if we consider that the shape is regulated by sympathovagal balance and as none of the SNS or PNS activity descriptor are capable of stratifying the risk of suffering from asthma, neither the shape analysis is. By observing the values obtained both in the hour-per-hour and in the whole night analysis it is noticeable that the shape of the plots is predominantly elongated, what agrees with the results of previous studies guided by visual analysis [11][59], although maximum values over the studied intervals reveal that there are some cases in which strong changes in the shape can be observed. This effect is clearly observable in the LR group, and in the periods corresponding to the early morning, but the high variability between patients does not allow this shape parameter to be used as a marker. Nevertheless, it would be interesting to perform a deeper study of this effect so as to identify if it is produced by a physiological process or it is just an outlier.

Another fact concerning the study of the evolution of the shape over time is that the visual inspection of the results obtained when considering just 5-minute segments reveals that the description of the shape via the method proposed here is not always as robust as desired, due to the lack of points in the plot. In other words, although it is possible to decide what is the concrete shape observed in a 5-minute short-term Poincaré plot, the decision do not always agree with that obtained by the automatic analysis proposed here. Retaking the method proposed to extract the shape, that consisted on a scan performed along the line of identity where the

standard deviation of the points covered by the scanning window was annotated for each possible position of the window, the lack of points in some cases led up to abrupt shapes that made the calculation of $SD1^+$ and $SD1^-$ unreliable, thus conducing to a wrong classification of the observed shape. An example of bad classification due to the lack of points is shown in Figure 6.8 However, the use of longer periods of analysis, as in the case of several hours segments analyzed when considering the whole night, the definition of the shape was much more accurate attending to the high number of points composing the plots.

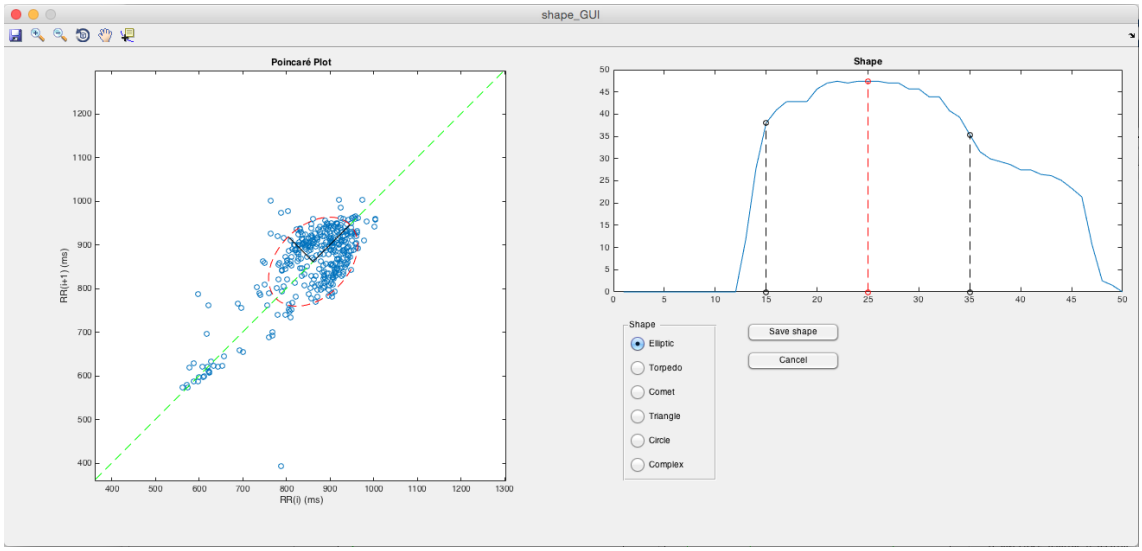

Figure 6.8 *Although the plot displayed in the image would be visually classified as comet-shaped due to the elongated tail and the greater dispersion of points for higher RR intervals, attending to its shape parameter it would be classified as elliptical ($SD1^+$ and $SD1^-$ are similar). This is due to the lack of points that creates an empty zone along the line of identity. The presence of points in this empty space would modify the mean value of the plot and the difference $SD1^+$ and $SD1^-$ would be enhanced.*

Finally, a qualitative study of the Poincaré domain filtering introduced in Section 5.3 was tackled. Although in [69] (where the EDBSCAN filtering technique was first applied to Poincaré plot) the filter was tested with long-term plots, in this case much shorter periods are analyzed (5-minute intervals). The sense of applying the proposed filter to short recordings is that in this way we can take advantage of the spatial distribution of the points in the plot for the elimination of ectopic beats, what is impossible with classical filtering techniques. The parameters of the EDBSCAN algorithm selected in this work were $MinPts = 5$ and 5 iterations.

In order to evaluate the advantages or disadvantages of applying the Poincaré domain filtering instead of the ectopic beat detection and correction, both filters were

applied to the signals and the results were visually analyzed. An example of the application of the ectopic beat removal and correction supplied by Biosigbrowser and the Poincaré domain filtering algorithm is shown in Figure 6.9. As the performance of the ectopic detection and correction of Biosigbrowser has been widely tested, the results provided by it were used as a golden standard for evaluating the results of the new filtering method.

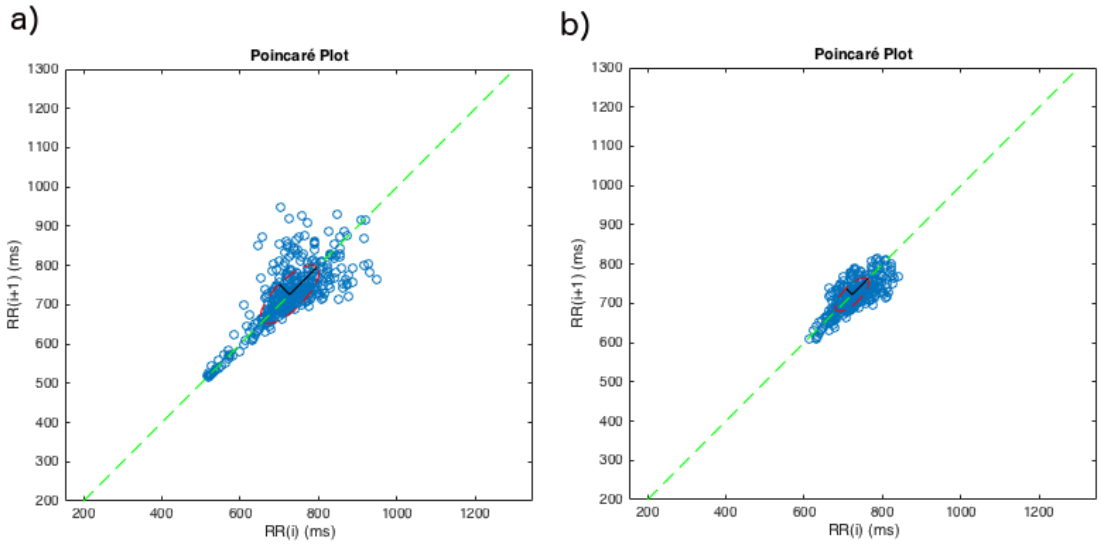

Figure 6.9 *In a) the Poincaré plot obtained after ectopic beat detection and correction with the algorithm provided by Biosigbrowser. In b) the same 5-minute RR interval series has been filtered in the Poincaré domain.*

The main problem with the proposed filter is that it is very restrictive, as shown in Figure 6.9, and hence it eliminates some non-ectopic beats. The elimination of non-ectopic beats leads to a loose of information related with sinusal regular activations, which are directly mediated by ANS activity, so the filtering stage is eliminating useful information. Although in [69] it is presented as a method robust against noise, in short recordings it has been shown to be excessively restrictive. A possible explanation for understanding why the performance of the filter is decreased in shorter intervals is again the lack of enough points to properly define the shape of the plot. As it is a cluster-based approach, zones of the plot where the density of points is not high enough or where the points are spread due to the reduced number of them will be eliminated by the filter, as they will be considered as outliers. Another disadvantage of this filtering technique is that ectopic beats are eliminated but not corrected, i.e., once a a beat has been considered as ectopic it is removed from the plot, but not corrected. A possible enhancement of the filter could be

related with transferring the information of the removed beats to the RR interval series, and then applying a correction algorithm there. On the other hand, the problem of over-filtering will still remain when working with short recordings, so this technique does not seem to be appropriate in that kind of analysis.

From the results obtained in this work, several future work lines can be established. On one hand and as already discussed, the GUI is based on several independent menus, so the enhancement of the features provided by the GUI will be attempted. The intention is to add the capability to obtain some non-linear indexes, e.g. Dentrended Fluctuation Analysis or complexity measurements, that can provide further HRV analysis capabilities. Moreover, it would be interesting to add the possibility of manually select the length of the time interval used, as by the moment only 5-minute segments are allowed.

On the other hand, the analysis performed here could be improved in several ways. The first working line would be the test of the new parameters proposed in this work, i.e., angle and short-term shape analysis of Poincaré plots. As no significative results have been obtained here, it has been not possible to evaluate if these new parameters provide additional information to that obtained from the classical parameters extracted from the plots. In this way, these measurements will be further studied in other data bases where the classical indexes show significant results that can be used as a reference. Furthermore, the modification in the results obtained by the use of SD1 and SD2 after correcting the angle of the plot has not been tested here, so an in deep study should be performed.

Another line of work is the development of a method for short-term Poincaré plot shape correction. As discussed above, the scanning method proposed here can lead to wrong classification due to the lack of points in the plot and hence an algorithm to enhance this process by performing certain correction of the scanned shape would be useful.

Finally, it has been proposed that one of the main problems with Poincaré domain filtering is that the ectopic beats removed are not then corrected, so a correction method to allow an interpolation of these removed beats would helpful to conserve as much information as possible, thus aiding in the further analysis of the plots.

7. CONCLUSIONS

This work was performed in collaboration with the University of Zaragoza, and is integrated within a Ph.D. project titled "Noninvasive evaluation of autonomic nervous system through the variability of biosignals. Application to stress-related clinical situations". In this way, the study performed here will be continued during the development of the project.

As there is not still a method for the premature detection of asthma in children, this topic constitute an interesting research field where many progress can be still done. The initial hypothesis that gives sense to this thesis is that abnormal ANS activity is closely related with the pathogenesis of asthma, so the analysis of this ANS activity means HRV could be useful in order to understand the involved physiological underlying processes.

In this work the ability of the different indexes used for HRV analysis and two new proposed parameters to stratify the risk of asthma in different risk groups has been tested. However, the results obtained were not statistically significant, so it was shown that none of the studied indexes can be used for this purpose. In this way, further studies must be realized to find an effective method for the accurate detection of asthma in children due to the fact that the number of individuals suffering from this chronic disease has increased dramatically in lasts decades. The sense of attempting this problem with HRV analysis is to provide a method as non-invasive as possible.

On the other hand, a GUI for aiding in the visual analysis of Poincaré plots was developed. The mentioned GUI was proven to be very useful when interpreting the information of the plots, as they can be easily compared with the most well-known HRV parameters thus merging the information displayed by several different methods.

Finally, the information provided by the new proposed Poincaré plot features could

not be analyzed, as the results for the rest of used parameters were not significant. Hence, more detailed studies will be designed in the future, as the non-linear characteristics of Poincaré plot are not being exploited with SD1 and SD2, so further information related with the non-linear processes controlling HRV might be hidden.

BIBLIOGRAPHY

[1] DM Mannino, DM Homa, CA Pertrowski, et al., "Surveillance for asthma – United States, 1960-1995," MMWR CDC Surveill Summ, pp. 1-11, 1998.

[2] M. M. Adams PF, "Current estimates from the National Health Interview Survey 1994. Viral and health statistics," 1995.

[3] Kaliner M, Shelhamer JH, Davis PB, Smith LJ, Venter JC. Autonomic nervous system abnormalities and allergy. Ann Intern Med 1982;96:349-57.

[4] Lewis, M. J.; Short, A. L.; Lewis, K. E. Autonomic nervous system control of the cardiovascular and respiratory systems in asthma. Respiratory medicine, 2006, vol. 100, no 10, p. 1688-1705.

[5] Warren JB, Jennings SJ, Clark TJ. Effect of adrenergic and vagal blockade on the normal human airway response to exercise. Clin Sci (London) 1984;66(1):79-85.

[6] McFadden Jr ER, Lenner KAM, Strohl KP. Postexertional airway rewarming and thermally induced asthma. New insights into pathophysiology and possible pathogenesis. J Clin Invest 1986;78:18-25.

[7] Kallenbach JM, Webster T, Dowdeswell R, Reinach SG, Scott Milar RN, Zwi S. Reflex heart rate control in asthma: evidence of parasympathetic overactivity. Chest 1985; 87(5):644-8.

[8] Michaels, D. C., et al. Chaotic activity in a mathematical model of the vagally driven sinoatrial node. Circulation research, 1989, vol. 65, no 5, p. 1350-1360.

[9] Voss, Andreas, et al. Methods derived from nonlinear dynamics for analysing heart rate variability. Philosophical Transactions of the Royal Society of London A: Mathematical, Physical and Engineering Sciences, 2009, vol. 367, no 1887, p. 277-296.

[10] Acharya, U. Rajendra, et al. Heart rate variability: a review. Medical and biological engineering and computing, 2006, vol. 44, no 12, p. 1031-1051.

[11] Woo MA, Stevenson WG, Moser DK, Trelease RB, Harper RH (1992) Patterns of beat-to-beat heart rate variability in advanced heart failure. Am Heart J 123:704-707

[12] Brennan, Michael; Palaniswami, Marimuthu; Kamen, Peter. Poincaré plot interpretation using a physiological model of HRV based on a network of oscillators. American Journal of Physiology-Heart and Circulatory Physiology, 2002, vol. 283, no 5, p. H1873-H1886.

[13] Brennan, Michael; Palaniswami, Marimuthu; Kamen, Peter. Do existing measures of Poincaré plot geometry reflect nonlinear features of heart rate variability?. Biomedical Engineering, IEEE Transactions on, 2001, vol. 48, no 11, p. 1342-1347.

[14] Guzik, Przemyslaw, et al. Correlations between the Poincaré plot and conventional heart rate variability parameters assessed during paced breathing. The Journal of Physiological Sciences, 2007, vol. 57, no 1, p. 63-71.

[15] Guyton, A. C.; Hall, J. E. Textbook of medicine physiology. Philadelphia, PA: WB Saunders, 1996, p. 592.

[16] Marieb, Elaine Nicpon. Essentials of human anatomy & physiology. 10th edition. Benjamin Cummings, 2000.

[17] Virtanen, M. Heart rate variability parameters in diagnosis of coronary artery disease from exercise ECG. Master's Thesis, Tampere University of Technology, 2006.

[18] A comprehensive approach to life science, 2nd Ed. CSLS/The University of Tokyo, 2011

[19] Ravits, J.M., AAEM minimonograph #48: autonomic nervous system testing. Muscle Nerve, 1997. 20(8): p. 919-37.

[20] Chandramouleeswaran, Sridhathan; Haidar, Ahmed MA; Samsuri, Fahmi. Wavelet diagnosis of ECG signals with kaiser based noise diminution. 2012.

[21] TASK FORCE OF THE EUROPEAN SOCIETY OF CARDIOLOGY, et al. Heart rate variability standards of measurement, physiological interpretation, and clinical use. Eur Heart J, 1996, vol. 17, p. 354-381.

[22] Sörnmo, Leif; Laguna, Pablo. Bioelectrical signal processing in cardiac and neurological applications. Academic Press, 2005.

[23] Farrell, Thomas G., et al. Risk stratification for arrhythmic events in postinfarction patients based on heart rate variability, ambulatory electrocardiographic variables and the signal-averaged electrocardiogram. Journal of the American College of Cardiology, 1991, vol. 18, no 3, p. 687-697.

[24] Owis, Mohamed I., et al. Study of features based on nonlinear dynamical modeling in ECG arrhythmia detection and classification. Biomedical Engineering, IEEE Transactions on, 2002, vol. 49, no 7, p. 733-736.

[25] Vanoli, Emilio, et al. Heart rate variability during specific sleep stages a comparison of healthy subjects with patients after myocardial infarction. Circulation, 1995, vol. 91, no 7, p. 1918-1922.

[26] Bailon, R., et al. Coronary artery disease diagnosis based on exercise electrocardiogram indexes from repolarisation, depolarisation and heart rate variability. Medical and Biological Engineering and Computing, 2003, vol. 41, no 5, p. 561-571.

[27] Stein, Phyllis K.; Pu, Yachuan. Heart rate variability, sleep and sleep disorders. Sleep medicine reviews, 2012, vol. 16, no 1, p. 47-66.

[28] Morrison, J. F. J.; Pearson, S. B.; Dean, H. G. Parasympathetic nervous system in nocturnal asthma. British medical journal (Clinical research ed.), 1988, vol. 296, no 6634, p. 1427.

[29] "What Is Asthma?," 10 2015. [Online]. Available: http://www.nhlbi.nih.gov/health/health-topics/topics/asthma.

[30] Busse W, Lemanske R (2001) Asthma New Engl J Med 344(5):350-362

[31] Ionescu, Clara Mihaela. The human respiratory system: an analysis of the interplay between anatomy, structure, breathing and fractal dynamics. Springer Science & Business Media, 2013.

[32] Di Giuseppe, M.; et al. (2003). Nelson Biology 12. Toronto: Thomson Canada. p. 473.

[33] Bousquet, Jean, et al. Asthma: from bronchoconstriction to airways inflammation and remodeling. American journal of respiratory and critical care medicine, 2000, vol. 161, no 5, p. 1720-1745.

[34] T. S. Valerie C. Scanlon, "Essentials of Anatomy and Physiology, 5th Edition," in Essentials of Anatomy and Physiology, 5th Edition, Philadelphia, F.A. DAVIS COMPANY, 2007, p. 349.

[35] JR Gong, Henry, et al., "Altered heart-rate variability in asthmatic and healthy volunteers exposed to concentrated ambient coarse particles," Inhalation Toxicology, vol. 16, no. 6-7, pp. 335-343, 2004.

[36] Garrard CS, Seidler A, McKibben A, McAlpine LE, Gordon D. Spectral analysis of heart rate variability in bronchial asthma. Clin Autonom Research 1992;2:105-11.

[37] Tokuyama K, Morikawa A, Mitsuhashi M, Mochizuki H, Tajima K, Kuroume T. Beat-to-beat variation of the heart rate in children with allergic asthma. J Asthma 1985; 22(6):285-8.

[38] Inman MD, Watson RM, Killian KJ, O'Byrne PM. Methacho- line airway responsiveness decreases during exercise in asthmatic subjects. Am Rev Respir Dis 1990;141:1414-7.

[39] Kleiger, Robert E.; Stein, Phyllis K.; Bigger, J. Thomas. Heart rate variability: measurement and clinical utility. Annals of Noninvasive Electrocardiology, 2005, vol. 10, no 1, p. 88-101.

[40] Sacha, Jerzy; Pluta, Wladyslaw. Different methods of heart rate variability analysis reveal different correlations of heart rate variability spectrum with average heart rate. Journal of electrocardiology, 2005, vol. 38, no 1, p. 47-53.

[41] Berntson, Gary G., et al. An approach to artifact identification: Application to heart period data. Psychophysiology, 1990, vol. 27, no 5, p. 586-598.

[42] Malik, M., et al. Prognostic value of heart rate variability after myocardial infarction. A comparison of different data-processing methods. Medical and Biological Engineering and Computing, 1989, vol. 27, no 6, p. 603-611.

[43] Storck, N., et al. Automatic computerized analysis of heart rate variability with digital filtering of ectopic beats. Clinical Physiology, 2001, vol. 21, no 1, p. 15-24.

[44] Lewis Jr, William M. Phase locking, period-doubling bifurcations, and irregular dynamics in periodically stimulated cardiac cells. Oecologia (Berlin), 1975, vol. 19, p. 75.

[45] Akay, Metin. Nonlinear Biomedical Signal Processing Vol. II: Dynamic Analysis and Modeling. Wiley-IEEE press, 2000.

[46] Rajendra, A.; Lim, C.; Paul, J. HRV analysis using correlation dimension and DFA. Innovations and Technology in Biology and Medicine, France, 2002, p. 333-339.

[47] Acharya, R.; Kannathal, N.; Krishnan, S. M. Comprehensive analysis of cardiac health using heart rate signals. Physiological measurement, 2004, vol. 25, no 5, p. 1139.

[48] Kleiger, R. E., et al. Time domain measurements of heart rate variability. Cardiology clinics, 1992, vol. 10, no 3, p. 487-498.

[49] Garcia Gonzalez, Miguel Angel; PallÃ s Areny, Ramon. A novel robust index to assess beat-to-beat variability in heart rate time-series analysis. 2001.

[50] Bigger, J. Thomas, et al. Frequency domain measures of heart period variability and mortality after myocardial infarction. Circulation, 1992, vol. 85, no 1, p. 164-171.

[51] Boardman, Anita; Schlindwein, Fernando Soares; Rocha, Ana Paula. A study on the optimum order of autoregressive models for heart rate variability. Physiological measurement, 2002, vol. 23, no 2, p. 325.

[52] Laguna, Pablo; Moody, George B.; Mark, Roger G. Power spectral density of unevenly sampled data by least-square analysis: performance and application to heart rate signals. Biomedical Engineering, IEEE Transactions on, 1998, vol. 45, no 6, p. 698-715.

[53] Makikallio, Timo H., et al. Clinical applicability of heart rate variability analysis by methods based on nonlinear dynamics. Cardiac electrophysiology review, 2002, vol. 6, no 3, p. 250-255.

[54] Hoyer, D., et al. Nonlinear analysis of heart rate and respiratory dynamics. Engineering in Medicine and Biology Magazine, IEEE, 1997, vol. 16, no 1, p. 31-39.

[55] Carvajal, RaÃºl, et al. Correlation dimension analysis of heart rate variability in patients with dilated cardiomyopathy. Computer Methods and Programs in Biomedicine, 2005, vol. 78, no 2, p. 133-140.

[56] Peng, C.K., et al. Quantification of scaling exponents and crossover phenomena in nonstationary heartbeat time series. Chaos: An Interdisciplinary Journal of Nonlinear Science, 1995, vol. 5, no 1, p. 82-87.

[57] Wolf A, Swift JB, Swinney HL, Vastano JA (1985) Determining Lyapunov exponents from a time series. Physica D 16:285-317

[58] Richman JS, Moorman JR (2000) Physiological time-series analysis using approximate entropy and sample entropy. Am J Physiol Heart Circ Physiol 278:H2039-H2049

[59] Marciano, F., et al. Quantification of Poincaré'maps for the evaluation of heart rate variability. En Computers in Cardiology 1994. IEEE, 1994. p. 577-580.

[60] Akay, Metin. Nonlinear Biomedical Signal Processing Volumen II. Dynamical analysis and modeling, 2001.

[61] Thompson, John Michael Tutill; Stewart, H. Bruce. Nonlinear dynamics and chaos. John Wiley & Sons, 2002.

[62] Takens, Floris. Detecting strange attractors in turbulence. Springer Berlin Heidelberg, 1981.

[63] Packard, Norman H., et al. Geometry from a time series. Physical Review Letters, 1980, vol. 45, no 9, p. 712.

[64] Laitio, Timo T., et al. Relation of heart rate dynamics to the occurrence of myocardial ischemia after coronary artery bypass grafting. The American journal of cardiology, 2002, vol. 89, no 10, p. 1176-1181.

[65] Castro-Rodriguez, Jose A., et al. A clinical index to define risk of asthma in young children with recurrent wheezing. American journal of respiratory and critical care medicine, 2000, vol. 162, no 4, p. 1403-1406.

[66] Turki, Jamal, et al. Genetic polymorphisms of the beta 2-adrenergic receptor in nocturnal and nonnocturnal asthma. Evidence that Gly16 correlates with the nocturnal phenotype. Journal of Clinical Investigation, 1995, vol. 95, no 4, p. 1635.

[67] Golub, Gene H.; Reinsch, Christian. Singular value decomposition and least squares solutions. Numerische mathematik, 1970, vol. 14, no 5, p. 403-420.

[68] Piskorski, Jaroslaw; Guzik, Przemyslaw. Filtering poincare plots. Computational methods in science and technology, 2005, vol. 11, no 1, p. 39-48.

[69] Matthias Hortenhuber et al., Comparison of Two Filtering Methods for Heart Rate Variability Analysis. Simulation Notes Europe SNE 24(3-4), 2014, 137-142.

[70] Xia, Luning; Jing, Jiwu. An Ensemble Density-based Clustering Method. En International Conference on Intelligent Systems and Knowledge Engineering 2007. Atlantis Press, 2007.

[71] Ester, Martin, et al. A density-based algorithm for discovering clusters in large spatial databases with noise. En Kdd. 1996. p. 226-231.

[72] Bolea, J., et al. Biosigbrowser, biosignal processing interface. Information Technology and Applications in Biomedicine, 2009, p. 1-4.

[73] Martínez, Juan Pablo, et al. A wavelet-based ECG delineator: evaluation on standard databases. Biomedical Engineering, IEEE Transactions on, 2004, vol. 51, no 4, p. 570-581.

[74] Welch, Peter D. The use of fast Fourier transform for the estimation of power spectra: A method based on time averaging over short, modified periodograms. IEEE Transactions on audio and electroacoustics, 1967, vol. 15, no 2, p. 70-73.

APPENDIX. COMPLETE RESULT TABLES

Here, all the tables containing the numerical results obtained in this work are displayed. The caption of each table contains information about the measurements shown on it and the analysis period when the measurements were obtained.

Table 1 *Median (mean value and standard deviation) of the different parameters between 23:00 and 00:00. Significative differences between groups ($p < 0.05$) are marked with $*$ in the case of LR vs. HR, † in the case of LR vs. ICS and ‡ for HR vs. ICS).*

	23:00-00:00		
	LR	**HR**	**ICS**
SDNN (ms)	70.56 ± 22.12	80.25 ± 37.30	81.08 ± 26.62
SDSD (ms)	68.75 ± 24.72	75.08 ± 52.77	78.10 ± 32.44
pNN50 (%)	40.13 ± 17.69	34.30 ± 23.37	42.00 ± 16.53
TP (ms^2/Hz)	712.87 ± 460.42	1091.41 ± 825.78	1073.96 ± 575.91
VLF (ms^2/Hz)	347.15 ± 267.85	564.61 ± 463.41	506.20 ± 300.54
LF (ms^2/Hz)	259.85 ± 163.70	370.26 ± 401.31	402.51 ± 288.24
HF (ms^2/Hz)	9.79 ± 5.27	12.98 ± 16.37	11.58 ± 8.92
LF/HF (n.u.)	28.97 ± 12.89	36.34 ± 16.46	35.81 ± 17.77
SD1 (ms)	72.61 ± 22.97	75.49 ± 42.81	76.13 ± 23.52
SD2 (ms)	99.81 ± 27.91	104.71 ± 40.59	107.61 ± 35.02
SD1/SD2 (n.u.)	0.73 ± 0.11	0.68 ± 0.20	0.71 ± 0.11
S (ms^2)	26018.03 ± 15467.86	32207.26 ± 24297.47	29708.12 ± 17764.69
θ (^{o})	64.76 ± 39.42	65.77 ± 50.84	58.11 ± 35.09
Sh (n.u.)	1.47 ± 0.32	1.45 ± 0.69	1.40 ± 0.25

Table 2 *Median (mean value and standard deviation) of the different parameters between 00:00 and 01:00. Significative differences between groups ($p < 0.05$) are marked with $*$ in the case of LR vs. HR, † in the case of LR vs. ICS and ‡ for HR vs. ICS).*

	00:00-01:00		
	LR	**HR**	**ICS**
SDNN (ms)	74.28 ± 24.24	87.25 ± 44.08	85.69 ± 26.09
SDSD (ms)	70.41 ± 28.58	76.35 ± 48.54	88.63 ± 32.09
pNN50 (%)	38.60 ± 19.86	33.25 ± 20.20	46.74 ± 13.35
TP (ms^2/Hz)	830.98 ± 473.21	1312.63 ± 1138.03	1096.55 ± 578.27
VLF (ms^2/Hz)	425.21 ± 273.20	705.41 ± 606.93	470.37 ± 232.99
LF (ms^2/Hz)	270.33 ± 164.90	383.26 ± 381.37	486.51 ± 326.52
HF (ms^2/Hz)	10.67 ± 6.47	12.49 ± 14.02	14.48 ± 8.19
LF/HF (n.u.)	27.04 ± 10.56	34.58 ± 13.08	34.00 ± 17.65
SD1 (ms)	73.79 ± 22.88	83.84 ± 49.67	62.88 ± 20.40
SD2 (ms)	101.60 ± 25.80	119.41 ± 55.95	93.31 ± 25.25
SD1/SD2 (n.u.)	0.74 ± 0.16	0.66 ± 0.14	0.69 ± 0.17
S (ms^2)	27351.29 ± 13117.86	42152.01 ± 37996.90	21182.99 ± 12430.05
θ (^{o})	83.88 ± 70.89	51.97 ± 25.26	77.11 ± 85.60
Sh (n.u.)	1.43 ± 0.41	1.29 ± 0.32	1.35 ± 0.45

Table 3 *Median (mean value and standard deviation) of the different parameters between 01:00 and 02:00. Significative differences between groups ($p < 0.05$) are marked with $*$ in the case of LR vs. HR, † in the case of LR vs. ICS and ‡ for HR vs. ICS).*

	01:00-02:00		
	LR	**HR**	**ICS**
SDNN (ms)	77.90 ± 37.39	86.11 ± 48.21	95.24 ± 40.06
SDSD (ms)	67.75 ± 27.98	75.91 ± 48.45	99.65 ± 44.77
pNN50 (%)	35.64 ± 17.51	34.34 ± 20.14	49.34 ± 13.20
TP (ms^2/Hz)	978.04 ± 934.11	1296.93 ± 1363.07	1644.53 ± 1893.39
VLF (ms^2/Hz)	524.62 ± 532.70	709.12 ± 826.53	755.73 ± 951.08
LF (ms^2/Hz) †	258.27 ± 184.41	350.55 ± 349.43	602.05 ± 501.20
HF (ms^2/Hz)	10.08 ± 5.82	13.00 ± 15.54	15.31 ± 9.51
LF/HF (n.u.)	25.41 ± 7.95	33.49 ± 11.05	35.90 ± 14.91
SD1 (ms)	68.36 ± 30.94	90.46 ± 51.06	56.04 ± 22.73
SD2 (ms)	104.86 ± 51.60	121.50 ± 60.61	80.35 ± 23.99
SD1/SD2 (n.u.)	0.68 ± 0.19	0.70 ± 0.15	0.69 ± 0.12
S (ms^2)	26641.70 ± 20552.96	46385.89 ± 41557.12	16893.66 ± 12960.73
θ (^{o})	64.01 ± 48.85	61.52 ± 41.82	63.73 ± 50.61
Sh (n.u.)	1.34 ± 0.48	1.35 ± 0.32	1.40 ± 0.25

Table 4 *Median (mean value and standard deviation) of the different parameters between 02:00 and 03:00. Significative differences between groups ($p < 0.05$) are marked with $*$ in the case of LR vs. HR, † in the case of LR vs. ICS and ‡ for HR vs. ICS).*

	02:00-03:00		
	LR	**HR**	**ICS**
SDNN (ms)	79.00 ± 32.67	91.24 ± 46.36	91.97 ± 49.34
SDSD (ms)	67.02 ± 26.94	76.85 ± 45.77	93.50 ± 55.89
pNN50 (%)	35.56 ± 14.59	35.02 ± 18.14	45.63 ± 21.21
TP (ms^2/Hz)	967.84 ± 828.07	1434.28 ± 1279.73	1640.08 ± 2014.17
VLF (ms^2/Hz)	511.16 ± 462.16	772.74 ± 769.06	756.37 ± 926.06
LF (ms^2/Hz)	250.65 ± 180.42	347.91 ± 322.79	583.43 ± 646.74
HF (ms^2/Hz)	9.35 ± 5.64	13.27 ± 14.25	12.82 ± 11.39
LF/HF (n.u.)	28.93 ± 11.34	33.38 ± 11.57	38.12 ± 16.96
SD1 (ms)	69.48 ± 35.53	98.33 ± 43.33	57.34 ± 20.31
SD2 (ms)	110.62 ± 51.11	133.33 ± 58.60	84.28 ± 24.83
SD1/SD2 (n.u.)	0.63 ± 0.13	0.71 ± 0.11	0.67 ± 0.06
S (ms^2)	29603.16 ± 29909.27	52974.11 ± 34150.13	16852.24 ± 10683.25
θ ()	45.02 ± 0.32	54.54 ± 37.82	44.97 ± 0.26
Sh (n.u.)	3.23 ± 7.35	1.34 ± 0.31	1.37 ± 0.33

Table 5 *Median (mean value and standard deviation) of the different parameters between 03:00 and 04:00. Significative differences between groups ($p < 0.05$) are marked with $*$ in the case of LR vs. HR, † in the case of LR vs. ICS and ‡ for HR vs. ICS).*

	03:00-04:00		
	LR	**HR**	**ICS**
SDNN (ms)	86.07 ± 24.92	89.98 ± 43.15	92.78 ± 29.32
SDSD (ms)	71.00 ± 25.27	83.2 ± 54.36	89.85 ± 39.30
pNN50 (%)	38.07 ± 16.07	37.36 ± 20.51	46.06 ± 16.17
TP (ms^2/Hz)	1445.31 ± 1733.68	1348.28 ± 1112.40	1268.31 ± 834.47
VLF (ms^2/Hz)	818.63 ± 1109.07	663.43 ± 565.99	584.64 ± 310.27
LF (ms^2/Hz)	269.61 ± 161.91	411.53 ± 442.61	506.76 ± 445.42
HF (ms^2/Hz)	9.88 ± 4.84	15.1 ± 15.63 ± 13.66	8.96
LF/HF (n.u.)	30.28 ± 13.82	32.98 ± 12.95	33.20 ± 14.75
SD1 (ms)	91.45 ± 50.09	91.44 ± 43.17	96.65 ± 62.74
SD2 (ms)	135.96 ± 68.57	124.99 ± 53.49	148.75 ± 91.1
SD1/SD2 (n.u.)	0.67 ± 0.12	0.72 ± 0.13	0.64 ± 0.13
S (ms^2)	62364.71 ± 96988.26	45734.65 ± 32530.40	82593 ± 135473.99
θ (^{o})	45.08 ± 0.27	65.86 ± 50.75	45.05 ± 0.16
Sh (n.u.)	3.25 ± 7.35	1.38 ± 0.55	1.19 ± 0.23

Table 6 *Median (mean value and standard deviation) of the different parameters between 04:00 and 05:00. Significative differences between groups ($p < 0.05$) are marked with $*$ in the case of LR vs. HR, † in the case of LR vs. ICS and ‡ for HR vs. ICS).*

	04:00-05:00		
	LR	**HR**	**ICS**
SDNN (ms)	80.98 ± 23.21	86.01 ± 41.21	93.99 ± 35.51
{SDSD (ms)}	70.69 ± 26.06	78.85 ± 52.74	99.77 ± 46.12
pNN50 (%)	39.57 ± 17.69	35.86 ± 21.05	49.62 ± 19.54
TP (ms^2/Hz)	922.75 ± 407.56	1165.89 ± 973.29	1301.36 ± 792.25
VLF (ms^2/Hz)	478.49 ± 239.92	596.89 ± 493.83	498.32 ± 293.97
LF (ms^2/Hz)	267.69 ± 143.02	368.30 ± 384.93	606.24 ± 474.30
HF (ms^2/Hz)	9.00 ± 4.2	13.95 ± 17.43	16.03 ± 10.54
LF/HF (n.u.)	31.02 ± 12.40	32.32 ± 11.27	34.17 ± 14.95
SD1 (ms)	71.79 ± 23.39	79.06 ± 52.02	71.19 ± 26.79
SD2 (ms)	109.47 ± 31.46	119.15 ± 57.42	111.59 ± 37.54
SD1/SD2 (n.u.)	0.66 ± 0.11	0.68 ± 0.16	0.65 ± 0.10
S (ms^2)	26335.66 ± 12983.05	37915.38 ± 42509.40	27070.57 ± 15615.88
θ (^{o})	45.00 ± 0.00	65.35 ± 73.37	44.99 ± 0.00
Sh (n.u.)	1.27 ± 0.23	1.31 ± 0.32	1.17 ± 0.19

Table 7 *Iqr (mean value and standard deviation) of the different parameters between 23:00 and 00:00. Significative differences between groups ($p < 0.05$) are marked with $*$ in the case of LR vs. HR, † in the case of LR vs. ICS and ‡ for HR vs. ICS).*

	23:00-00:00		
	LR	**HR**	**ICS**
SDNN (ms)	14.59 ± 13.62	29.7 ± 27.43	32.81 ± 25.74
SDSD (ms)	14.77 ± 7.49	16.83 ± 12.5	23.24 ± 27.97
pNN50 (%)	8.94 ± 6.27	10.94 ± 10.51	17.73 ± 13.21
TP (ms^2/Hz)	368.05 ± 323.06	741.23 ± 727.31	903.01 ± 707.68
VLF (ms^2/Hz) †	223.51 ± 176.83	545.79 ± 523.78	563.56 ± 475.61
LF (ms^2/Hz)	107.99 ± 82.48	110.77 ± 98.81	182.52 ± 205.18
HF (ms^2/Hz)	5.41 ± 5.61	5.39 ± 4.74	5.22 ± 4.64
LF/HF (n.u.)	10.41 ± 7.64	8.83 ± 6.84	14.95 ± 13.97
SD1 (ms)	34.87 ± 37.89	30.56 ± 43.34	44.41 ± 38
SD2 (ms)	42.04 ± 33.23	57.24 ± 52.47	46.1 ± 34.88
SD1/SD2 (n.u.)	0.19 ± 0.13	0.17 ± 0.15	0.17 ± 0.15
S (ms^2)	21907.26 ± 23880.99	25345.3 ± 27807.26	27265.61 ± 25262.29
θ (^{o})	39.98 ± 78.59	41.72 ± 101.66	26.99 ± 69.94
Sh (n.u.)	0.46 ± 0.49	0.45 ± 0.39	0.52 ± 0.7

Table 8 *Iqr (mean value and standard deviation) of the different parameters between 00:00 and 01:00. Significative differences between groups ($p < 0.05$) are marked with $*$ in the case of LR vs. HR, † in the case of LR vs. ICS and ‡ for HR vs. ICS).*

	00:00-01:00		
	LR	**HR**	**ICS**
SDNN (ms)	32.42 ± 26.51	29.99 ± 24.51	28.92 ± 29.80
SDSD (ms)	20.63 ± 18.13	24.32 ± 21.52	37.13 ± 30.86
pNN50 (%)	11.89 ± 8.97	15.65 ± 10.80	19.21 ± 17.07
TP (ms^2/Hz)	697.89 ± 752.13	822.17 ± 921.49	642.19 ± 645.46
VLF (ms^2/Hz)	467.4 ± 464.31	585.04 ± 673.74	389.40 ± 282.62
LF (ms^2/Hz)	160.28 ± 130.11	191.18 ± 232.55	260.35 ± 223.51
HF (ms^2/Hz)	5.34 ± 5.35	5.29 ± 7.01	9.19 ± 9.73
LF/HF (n.u.)	10.58 ± 8.95	8.37 ± 7.02	12.03 ± 11.52
SD1 (ms)	45.50 ± 41.79	41.81 ± 41.08	28.94 ± 28.27
SD2 (ms)	60.22 ± 56.71	56.34 ± 51.14	48.33 ± 46.48
SD1/SD2 (n.u.)	0.24 ± 0.30	0.18 ± 0.15	0.11 ± 0.13
S (ms^2)	28284.43 ± 26397.81	35314.95 ± 44906.60	17281.63 ± 22378.59
θ (^{o})	51.87 ± 92.05	14.20 ± 50.63	12.27 ± 30.53
Sh (n.u.)	0.63 ± 0.64	0.67 ± 0.64	0.45 ± 0.35

Table 9 *Iqr (mean value and standard deviation) of the different parameters between 01:00 and 02:00. Significative differences between groups ($p < 0.05$) are marked with $*$ in the case of LR vs. HR, † in the case of LR vs. ICS and ‡ for HR vs. ICS).*

	01:00-02:00		
	LR	**HR**	**ICS**
SDNN (ms)	23.35 ± 19.82	22.68 ± 15.23	42.51 ± 33.08
SDSD (ms) ‡	22.4 ± 24.03	14.22 ± 12.17	47.6 ± 30.96
pNN50 (%)	14.42 ± 14.4	9.70 ± 6.87	18.96 ± 15.88
TP (ms^2/Hz)	486.82 ± 563.76	589.62 ± 546.78	1638.64 ± 2750.02
VLF (ms^2/Hz)	296.75 ± 362.54	455.46 ± 504.94	794.56 ± 1514.08
LF (ms^2/Hz) †‡	147.57 ± 157.06	136.57 ± 162.6	512.6 ± 385.55
HF (ms^2/Hz)	5.52 ± 5.4	5.02 ± 6.34	11.48 ± 9.01
LF/HF (n.u.)	5.95 ± 3.72	9.05 ± 8.9	12.22 ± 8.74
SD1 (ms)	30.24 ± 30.23	47.78 ± 49.59	23.97 ± 29.68
SD2 (ms)	35.75 ± 35.12	53.9 ± 39.18	39.25 ± 39.28
SD1/SD2 (n.u.)	0.21 ± 0.23	0.16 ± 0.11	0.16 ± 0.15
S (ms^2)	15184.11 ± 19479.99	37630.40 ± 46132.76	15242.69 ± 21974.14
θ (^{o})	38.68 ± 97.37	36.73 ± 90.25	38.73 ± 100.65
Sh (n.u.)	0.59 ± 0.56	0.52 ± 0.61	0.65 ± 0.59

Table 10 *Iqr (mean value and standard deviation) of the different parameters between 02:00 and 03:00. Significative differences between groups ($p < 0.05$) are marked with $*$ in the case of LR vs. HR, † in the case of LR vs. ICS and ‡ for HR vs. ICS).*

	02:00-03:00		
	LR	**HR**	**ICS**
SDNN (ms)	22.34 ± 21.17	30.95 ± 21.52	38.81 ± 25.45
SDSD (ms)	24.15 ± 22.46	26.31 ± 31.42	24.35 ± 15.21
pNN50 (%)	16.04 ± 11.84	13.93 ± 9.05	11.58 ± 8.47
TP (ms^2/Hz)	522.77 ± 623.74	854.90 ± 724.64	1626.57 ± 2577.63
VLF (ms^2/Hz)	315.50 ± 339.45	579.89 ± 602.15	936.75 ± 1531.82
LF (ms^2/Hz)	156.93 ± 149.08	236.49 ± 311.18	240.38 ± 204.31
HF (ms^2/Hz)	4.22 ± 5.65	8.21 ± 8.86	4.62 ± 3.96
LF/HF (n.u.)	11.23 ± 13.87	13.59 ± 13.01	7.11 ± 7.45
SD1 (ms)	33.50 ± 38.17	59.01 ± 63.55	22.63 ± 15.35
SD2 (ms) †	35.41 ± 35.23	65.98 ± 51.21	21.25 ± 16.37
SD1/SD2 (n.u.)	0.16 ± 0.13	0.21 ± 0.13	0.15 ± 0.13
S (ms^2)	22261.68 ± 40700.79	45041.33 ± 51623.83	10104.96 ± 9493.78
θ (^{o})	0.42 ± 0.45	22.69 ± 74.61	0.31 ± 0.36
Sh (n.u.)	4.28 ± 14.79	0.43 ± 0.51	0.38 ± 0.34

Table 11 *Iqr (mean value and standard deviation) of the different parameters between 03:00 and 04:00. Significative differences between groups ($p < 0.05$) are marked with $*$ in the case of LR vs. HR, † in the case of LR vs. ICS and ‡ for HR vs. ICS).*

	03:00-04:00		
	LR	**HR**	**ICS**
SDNN (ms)	39.13 ± 30.05	29.04 ± 24.13	34.23 ± 28.49
SDSD (ms)	22.32 ± 17.56	16.69 ± 10.14	32.53 ± 30.21
pNN50 (%)	12.79 ± 10.27	11.39 ± 5.82	20.76 ± 19.82
TP (ms^2/Hz)	1681.25 ± 3235.68	872.28 ± 882.4	749.52 ± 541.76
VLF (ms^2/Hz)	1057.96 ± 2032.22	530.6 ± 600.06	516.23 ± 423.47
LF (ms^2/Hz)	139.51 ± 125.7	146.24 ± 113.14	280.39 ± 256.75
HF (ms^2/Hz)	5.2 ± 4.02	5.87 ± 4.35	6.63 ± 7.18
LF/HF (n.u.)	10.9 ± 16.48	11.9 ± 16.64	11.33 ± 4.98
SD1 (ms)	74.05 ± 96.97	41.97 ± 54.89	86.44 ± 119.37
SD2 (ms)	102.49 ± 131.61	62.93 ± 53.5	129.91 ± 175.12
SD1/SD2 (n.u.)	0.19 ± 0.13	0.16 ± 0.14	0.11 ± 0.07
S (ms^2)	93429.73 ± 193469.67	38729.11 ± 48919.12	134007.77 ± 268527.89
θ (^{o})	0.33 ± 0.42	41.67 ± 101.26	0.19 ± 0.26
Sh (n.u.)	4.45 ± 14.73	0.47 ± 0.6	0.34 ± 0.2

Table 12 *Iqr (mean value and standard deviation) of the different parameters between 04:00 and 05:00. Significative differences between groups ($p < 0.05$) are marked with $*$ in the case of LR vs. HR, † in the case of LR vs. ICS and ‡ for HR vs. ICS).*

	04:00-05:00		
	LR	**HR**	**ICS**
SDNN (ms)	35.85 ± 27.49	35.27 ± 23.14	21.35 ± 13.46
SDSD (ms)	16.78 ± 10.88	21.91 ± 11.98	24.47 ± 14.16
pNN50 (%)	12.67 ± 5.59	14.47 ± 6.03	15.11 ± 3.91
TP (ms^2/Hz)	916.05 ± 925.95	938.59 ± 794.87	566.24 ± 434.58
VLF (ms^2/Hz)	587.69 ± 511.92	602.30 ± 531.23	392.40 ± 222.83
LF (ms^2/Hz)	117.62 ± 62.61	175.93 ± 155.63	235.71 ± 171.54
HF (ms^2/Hz)	4.99 ± 2.92	5.99 ± 5.22	5.37 ± 2.89
LF/HF (n.u.)	11.68 ± 13.51	8.52 ± 5.76	9.65 ± 7.61
SD1 (ms)	33.85 ± 37.14	99.51 ± 204.75	32.66 ± 25.20
SD2 (ms)	65.66 ± 49.16	117.09 ± 209.70	48.76 ± 24.55
SD1/SD2 (n.u.)	0.19 ± 0.12	0.21 ± 0.14	0.12 ± 0.05
S (ms^2)	29893.39 ± 28826.35	231687.25 ± 728968.71	22897.04 ± 18428.18
θ (^{o})	0.14 ± 0.11	20.92 ± 74.81	0.11 ± 0.04
Sh (n.u.)	0.47 ± 0.40	0.46 ± 0.35	0.28 ± 0.10

Table 13 *Minimum (mean value and standard deviation) of the different parameters between 23:00 and 00:00. Significative differences between groups ($p < 0.05$) are marked with $*$ in the case of LR vs. HR, † in the case of LR vs. ICS and ‡ for HR vs. ICS).*

	23:00-00:00		
	LR	**HR**	**ICS**
SDNN (ms)	63.26 ± 23.77	65.39 ± 39.95	64.67 ± 28.43
SDSD (ms)	61.36 ± 23.65	66.66 ± 54.50	66.47 ± 37.39
pNN50 (%)	35.66 ± 18.75	28.82 ± 24.59	33.13 ± 21.45
TP (ms^2/Hz)	528.84 ± 386.10	720.79 ± 768.93	622.39 ± 508.35
VLF (ms^2/Hz)	235.39 ± 259.47	291.71 ± 384.64	224.41 ± 198.00
LF (ms^2/Hz)	205.85 ± 149.12	314.87 ± 382.037	311.24 ± 291.59
HF (ms^2/Hz)	7.08 ± 4.79	10.28 ± 14.31	8.96 ± 9.59
LF/HF (n.u.)	23.76 ± 12.91	31.92 ± 16.09	28.33 ± 12.85
SD1 (ms)	55.18 ± 18.17	60.21 ± 47.27	53.92 ± 16.80
SD2 (ms)	78.78 ± 28.96	76.08 ± 39.50	84.55 ± 37.52
SD1/SD2 (n.u.)	0.63 ± 0.13	0.59 ± 0.19	0.62 ± 0.11
S (ms^2)	15064.40 ± 9333.32	19534.60 ± 21187.12	16075.31 ± 10446.88
θ (^{o})	44.76 ± 0.46	44.90 ± 0.16	44.61 ± 0.61
Sh (n.u.)	1.24 ± 0.36	1.22 ± 0.53	1.13 ± 0.32

Table 14 *Minimum (mean value and standard deviation) of the different parameters between 00:00 and 01:00. Significative differences between groups ($p < 0.05$) are marked with $*$ in the case of LR vs. HR, † in the case of LR vs. ICS and ‡ for HR vs. ICS).*

	00:00-01:00		
	LR	**HR**	**ICS**
SDNN (ms)	58.07 ± 23.02	72.25 ± 45.11	71.23 ± 35.14
SDSD (ms)	60.09 ± 27.60	64.19 ± 49.67	70.06 ± 35.38
pNN50 (%)	32.65 ± 21.41	25.42 ± 20.71	37.14 ± 18.81
TP (ms^2/Hz)	482.03 ± 335.27	901.55 ± 962.80	775.45 ± 700.26
VLF (ms^2/Hz)	191.51 ± 146.73	412.89 ± 495.88	275.67 ± 264.37
LF (ms^2/Hz)	190.19 ± 131.71	287.66 ± 340.70	356.34 ± 347.49
HF (ms^2/Hz)	8.00 ± 5.15	9.85 ± 13.66	9.88 ± 8.40
LF/HF (n.u.)	21.74 ± 8.43	30.40 ± 11.47	27.99 ± 12.92
SD1 (ms)	51.04 ± 19.52	62.94 ± 44.16	48.41 ± 20.53
SD2 (ms)	71.49 ± 23.17	91.23 ± 56.82	69.14 ± 23.02
SD1/SD2 (n.u.)	0.62 ± 0.16	0.57 ± 0.18	0.63 ± 0.19
S (ms^2)	13209.07 ± 8108.98	24494.54 ± 25808.95	12542.17 ± 8842.16
θ (^{o})	57.94 ± 49.66	44.87 ± 0.13	70.97 ± 70.34
Sh (n.u.)	1.11 ± 0.37	0.95 ± 0.21	1.12 ± 0.39

Table 15 *Minimum (mean value and standard deviation) of the different parameters between 01:00 and 02:00. Significative differences between groups ($p < 0.05$) are marked with $*$ in the case of LR vs. HR, † in the case of LR vs. ICS and ‡ for HR vs. ICS).*

	01:00-02:00		
	LR	**HR**	**ICS**
{SDNN (ms)}	66.22 ± 38.03	74.76 ± 47.31	73.98 ± 28.36
SDSD (ms)	56.55 ± 27.15	68.80 ± 45.71	75.85 ± 36.88
pNN50 (%)	28.42 ± 19.26	29.48 ± 21.65	39.86 ± 14.68
TP (ms^2/Hz)	734.63 ± 829.86	1002.12 ± 1132.70	825.20 ± 608.79
VLF (ms^2/Hz)	376.24 ± 460.82	481.39 ± 593.28	358.45 ± 268.01
LF (ms^2/Hz)	184.48 ± 156.94	282.26 ± 290.73	345.75 ± 346.76
HF (ms^2/Hz)	7.32 ± 5.20	10.48 ± 14.20	9.56 ± 6.80
LF/HF (n.u.)	22.44 ± 7.69	28.96 ± 12.18	29.78 ± 13.01
SD1 (ms)	53.24 ± 27.12	66.56 ± 45.04	44.05 ± 17.81
SD2 (ms)	86.98 ± 56.48	94.55 ± 57.15	60.72 ± 21.62
SD1/SD2 (n.u.)	0.57 ± 0.13	0.62 ± 0.14	0.61 ± 0.12
S (ms^2)	19049.64 ± 19759.56	27570.69 ± 29731.07	9272.31 ± 5435.06
θ (^{o})	44.67 ± 0.63	43.15 ± 6.48	44.35 ± 0.79
Sh (n.u.)	1.04 ± 0.36	1.08 ± 0.29	1.11 ± 0.40

Table 16 *Minimum (mean value and standard deviation) of the different parameters between 02:00 and 03:00. Significative differences between groups ($p < 0.05$) are marked with $*$ in the case of LR vs. HR, † in the case of LR vs. ICS and ‡ for HR vs. ICS).*

	02:00-03:00		
	LR	**HR**	**ICS**
SDNN (ms)	67.83 ± 30.37	75.76 ± 44.40	72.56 ± 39.68
SDSD (ms)	54.94 ± 24.86	63.69 ± 41.20	81.33 ± 50.00
pNN50 (%)	27.54 ± 16.27	28.06 ± 17.79	39.84 ± 24.01
TP (ms^2/Hz)	706.45 ± 604.20	1006.83 ± 1131.81	826.79 ± 791.76
VLF (ms^2/Hz)	353.41 ± 321.20	482.79 ± 559.97	288.00 ± 213.60
LF (ms^2/Hz)	172.18 ± 143.96	229.66 ± 248.27	463.24 ± 554.58
HF (ms^2/Hz)	7.23 ± 4.91	9.16 ± 11.92	10.50 ± 9.92
LF/HF (n.u.)	23.32 ± 8.62	26.58 ± 12.78	34.56 ± 17.09
SD1 (ms)	52.73 ± 22.52	68.82 ± 42.18	46.02 ± 13.83
SD2 (ms)	92.92 ± 40.62	100.34 ± 60.04	73.66 ± 23.60
SD1/SD2 (n.u.)	0.55 ± 0.11	0.60 ± 0.11	0.59 ± 0.06
S (ms^2)	18472.32 ± 16092.59	30453.45 ± 32198.18	11799.76 ± 6768.57
θ (^{o})	44.81 ± 0.32	43.19 ± 6.49	44.81 ± 0.34
Sh (n.u.)	1.09 ± 0.33	1.12 ± 0.30	1.18 ± 0.29

Table 17 *Minimum (mean value and standard deviation) of the different parameters between 03:00 and 04:00. Significative differences between groups ($p < 0.05$) are marked with $*$ in the case of LR vs. HR, † in the case of LR vs. ICS and ‡ for HR vs. ICS).*

	03:00-04:00		
	LR	**HR**	**ICS**
SDNN (ms)	66.52 ± 19.99	75.45 ± 42.53	75.66 ± 40.88
SDSD (ms)	59.83 ± 25.34	74.85 ± 53.73	73.57 ± 40.42
pNN50 (%)	31.45 ± 17.15	31.66 ± 21.10	35.68 ± 18.10
TP (ms^2/Hz)	632.69 ± 326.07	912.13 ± 954.64	893.55 ± 818.76
VLF (ms^2/Hz)	310.23 ± 180.23	398.12 ± 432.19	326.52 ± 245.81
LF (ms^2/Hz)	199.79 ± 153.35	338.40 ± 412.46	366.56 ± 411.18
HF (ms^2/Hz)	7.21 ± 4.25	12.16 ± 14.88	10.34 ± 9.88
LF/HF (n.u.)	24.76 ± 14.82	27.03 ± 16.33	27.53 ± 14.12
SD1 (ms)	54.85 ± 18.79	70.45 ± 40.75	53.43 ± 18.52
SD2 (ms)	84.50 ± 23.87	93.52 ± 47.38	83.79 ± 24.92
SD1/SD2 (n.u.)	0.56 ± 0.13	0.64 ± 0.11	0.58 ± 0.12
S (ms^2)	16373.23 ± 9128.82	26370.09 ± 25600.41	15589.11 ± 9195.81
θ (^{o})	44.86 ± 0.27	45.02 ± 0.20	44.95 ± 0.04
Sh (n.u.)	1.01 ± 0.28	1.14 ± 0.41	1.02 ± 0.22

Table 18 *Minimum (mean value and standard deviation) of the different parameters between 04:00 and 05:00. Significative differences between groups ($p < 0.05$) are marked with $*$ in the case of LR vs. HR, † in the case of LR vs. ICS and ‡ for HR vs. ICS).*

	04:00-05:00		
	LR	**HR**	**ICS**
SDNN (ms)	52.23 ± 18.79	53.19 ± 32.30	70.50 ± 35.17
SDSD (ms)	46.21 ± 20.88	49.41 ± 40.89	70.35 ± 33.45
pNN50 (%)	20.57 ± 13.48	16.80 ± 16.44	32.57 ± 14.81
TP (ms^2/Hz)	375.88 ± 226.77	435.65 ± 450.88	773.01 ± 637.07
VLF (ms^2/Hz)	140.37 ± 61.62	165.20 ± 143.09	219.18 ± 174.65
LF (ms^2/Hz)	122.34 ± 111.96	162.83 ± 233.87	289.46 ± 252.81
HF (ms^2/Hz)	4.27 ± 2.64	6.55 ± 9.92	8.90 ± 6.08
LF/HF (n.u.)	16.92 ± 9.26	18.87 ± 7.61	22.36 ± 10.73
SD1 (ms)	41.04 ± 18.08	46.26 ± 36.95	36.56 ± 14.40
SD2 (ms)	62.42 ± 17.81	66.67 ± 36.85	59.84 ± 20.91
SD1/SD2 (n.u.)	0.43 ± 0.10	0.43 ± 0.12	0.46 ± 0.10
S (ms^2)	9521.33 ± 6474.81	14201.46 ± 16911.71	8159.03 ± 5966.24
θ (^{o})	39.22 ± 11.73	41.02 ± 4.99	43.64 ± 1.03
Sh (n.u.)	0.71 ± 0.19	0.73 ± 0.17	0.77 ± 0.09

Table 19 *Maximum (mean value and standard deviation) of the different parameters between 23:00 and 00:00. Significative differences between groups ($p < 0.05$) are marked with $*$ in the case of LR vs. HR, † in the case of LR vs. ICS and ‡ for HR vs. ICS).*

	23:00-00:00		
	LR	**HR**	**ICS**
SDNN (ms)	77.84 ± 22.50	95.10 ± 39.53	97.48 ± 30.65
SDSD (ms)	76.13 ± 26.28	83.49 ± 51.73	89.72 ± 33.12
pNN50 (%)	44.60 ± 17.14	39.76 ± 23.29	50.86 ± 13.16
TP (ms^2/Hz)	896.89 ± 571.90	1462.02 ± 1018.35	1525.40 ± 809.52
VLF (ms^2/Hz)	458.90 ± 302.97	837.50 ± 647.08	787.97 ± 504.52
LF (ms^2/Hz)	313.84 ± 186.42	425.64 ± 425.48	493.77 ± 319.66
HF (ms^2/Hz)	12.49 ± 6.94	15.68 ± 18.49	14.19 ± 8.81
LF/HF (n.u.)	34.16 ± 13.95	40.76 ± 17.50	43.28 ± 23.74
SD1 (ms)	90.04 ± 37.98	90.77 ± 48.67	98.33 ± 39.32
SD2 (ms)	120.82 ± 35.65	133.32 ± 55.78	130.66 ± 40.65
SD1/SD2 (n.u.)	0.82 ± 0.13	0.76 ± 0.22	0.80 ± 0.14
S (ms^2)	36971.65 ± 26010.56	44879.91 ± 33443.41	43340.92 ± 29002.11
θ (^{o})	84.74 ± 78.71	86.63 ± 101.66	71.61 ± 70.06
Sh (n.u.)	1.70 ± 0.43	1.67 ± 0.83	1.66 ± 0.51

Table 20 *Maximum (mean value and standard deviation) of the different parameters between 00:00 and 01:00. Significative differences between groups ($p < 0.05$) are marked with $*$ in the case of LR vs. HR, † in the case of LR vs. ICS and ‡ for HR vs. ICS).*

	00:00-01:00		
	LR	**HR**	**ICS**
SDNN (ms)	90.49 ± 31.58	102.24 ± 46.38	100.15 ± 23.88
SDSD (ms)	80.73 ± 32.20	88.52 ± 49.76	107.20 ± 35.84
pNN50 (%)	44.55 ± 19.25	41.07 ± 21.10	56.35 ± 12.17
TP (ms^2/Hz)	1179.92 ± 786.32	1723.72 ± 1444.93	1417.65 ± 621.87
VLF (ms^2/Hz)	658.92 ± 485.32	997.93 ± 847.23	665.07 ± 280.39
LF (ms^2/Hz)	350.48 ± 213.30	478.85 ± 449.28	616.69 ± 342.73
HF (ms^2/Hz)	13.34 ± 8.46	15.14 ± 15.20	19.08 ± 10.54
LF/HF (n.u.)	32.33 ± 13.87	38.77 ± 15.34	40.02 ± 22.85
SD1 (ms)	96.54 ± 39.23	104.75 ± 61.88	77.35 ± 28.48
SD2 (ms)	131.71 ± 49.01	147.58 ± 65.88	117.48 ± 42.72
SD1/SD2 (n.u.)	0.86 ± 0.27	0.75 ± 0.14	0.74 ± 0.18
S (ms^2)	41493.51 ± 25036.43	59809.49 ± 56830.70	29823.80 ± 21936.93
θ (^{o})	109.81 ± 108.73	59.07 ± 50.58	83.25 ± 100.86
Sh (n.u.)	1.74 ± 0.63	1.63 ± 0.60	1.58 ± 0.56

Table 21 *Maximum (mean value and standard deviation) of the different parameters between 01:00 and 02:00. Significative differences between groups ($p < 0.05$) are marked with $*$ in the case of LR vs. HR, † in the case of LR vs. ICS and ‡ for HR vs. ICS).*

	01:00-02:00		
	LR	**HR**	**ICS**
SDNN (ms)	89.57 ± 39.31	97.45 ± 50.25	116.49 ± 54.33
SDSD (ms)	78.95 ± 33.43	83.02 ± 51.76	123.45 ± 55.92
pNN50 (%)	42.84 ± 18.59	39.19 ± 19.13	58.82 ± 16.09
TP (ms^2/Hz)	1221.45 ± 1102.43	1591.74 ± 1606.98	2463.85 ± 3252.77
VLF (ms^2/Hz)	672.99 ± 648.76	936.85 ± 1068.55	1153.01 ± 1698.08
LF (ms^2/Hz)	332.05 ± 236.04	418.83 ± 415.81	858.35 ± 675.63
HF (ms^2/Hz)	12.84 ± 7.43	15.51 ± 17.36	21.05 ± 13.24
LF/HF (n.u.)	28.38 ± 8.60	38.01 ± 11.63	42.01 ± 17.70
SD1 (ms)	83.47 ± 40.45	114.35 ± 66.43	68.02 ± 34.01
SD2 (ms)	122.73 ± 52.46	148.45 ± 69.62	99.98 ± 38.15
SD1/SD2 (n.u.)	0.78 ± 0.29	0.78 ± 0.17	0.77 ± 0.16
S (ms^2)	34233.75 ± 25379.96	65201.09 ± 60284.05	24515.00 ± 23406.25
θ (^{o})	83.34 ± 97.53	79.88 ± 86.77	83.09 ± 100.93
Sh (n.u.)	1.63 ± 0.70	1.60 ± 0.55	1.76 ± 0.52

Table 22 *Maximum (mean value and standard deviation) of the different parameters between 02:00 and 03:00. Significative differences between groups ($p < 0.05$) are marked with $*$ in the case of LR vs. HR, † in the case of LR vs. ICS and ‡ for HR vs. ICS).*

	02:00-03:00		
	LR	**HR**	**ICS**
SDNN (ms)	90.17 ± 37.90	106.71 ± 50.59	111.38 ± 60.15
SDSD (ms)	79.10 ± 32.95	90.01 ± 54.65	105.68 ± 62.16
pNN50 (%)	43.58 ± 15.21	41.99 ± 19.56	51.43 ± 18.95
TP (ms^2/Hz)	1229.23 ± 1095.85	1861.73 ± 1502.33	2453.36 ± 3287.70
VLF (ms^2/Hz)	668.91 ± 617.76	1062.69 ± 1025.00	1224.75 ± 1686.06
LF (ms^2/Hz)	329.12 ± 235.56	466.16 ± 441.78	703.63 ± 741.52
HF (ms^2/Hz)	11.46 ± 7.45	17.38 ± 17.41	15.13 ± 13.00
LF/HF (n.u.)	34.55 ± 16.71	40.17 ± 13.75	41.67 ± 17.64
SD1 (ms)	86.23 ± 52.40	127.84 ± 63.20	68.66 ± 27.42
SD2 (ms)	128.33 ± 64.78	166.32 ± 67.63	94.91 ± 28.46
SD1/SD2 (n.u.)	0.71 ± 0.18	0.81 ± 0.14	0.75 ± 0.11
S (ms^2)	40734.00 ± 48563.71	75494.78 ± 51266.46	21904.72 ± 15083.64
θ (^{o})	45.24 ± 0.45	65.89 ± 74.84	45.13 ± 0.30
Sh (n.u.)	5.37 ± 14.75	1.56 ± 0.49	1.56 ± 0.45

Table 23 *Maximum (mean value and standard deviation) of the different parameters between 03:00 and 04:00. Significative differences between groups ($p < 0.05$) are marked with $*$ in the case of LR vs. HR, † in the case of LR vs. ICS and ‡ for HR vs. ICS).*

	03:00-04:00		
	LR	**HR**	**ICS**
SDNN (ms)	106.65 ± 36.83	104.49 ± 46.95	109.89 ± 21.31
SDSD (ms)	82.42 ± 28.02	91.55 ± 55.44	106.11 ± 43.72
pNN50 (%)	44.53 ± 16.49	43.06 ± 20.32	56.44 ± 19.79
TP (ms^2/Hz)	2354.53 ± 3342.09	1784.41 ± 1397.44	1643.07 ± 932.22
VLF (ms^2/Hz)	1402.59 ± 2127.52	928.73 ± 796.20	842.75 ± 470.93
LF (ms^2/Hz)	341.41 ± 190.55	484.64 ± 477.57	646.95 ± 510.57
HF (ms^2/Hz)	12.53 ± 6.06	18.03 ± 16.62	16.98 ± 9.41
LF/HF (n.u.)	35.92 ± 17.19	38.93 ± 14.39	38.87 ± 15.75
SD1 (ms)	137.57 ± 107.64	112.42 ± 59.78	139.87 ± 121.06
SD2 (ms)	197.41 ± 139.69	156.45 ± 70.06	213.71 ± 176.95
SD1/SD2 (n.u.)	0.76 ± 0.14	0.80 ± 0.17	0.70 ± 0.14
S (ms^2)	1.25e5 ± 2.03e4	65099.20 ± 51552.04	149596.88 ± 269583.86
θ (^{o})	45.31 ± 0.51	86.69 ± 101.38	45.15 ± 0.28
Sh (n.u.)	5.49 ± 14.71	1.62 ± 0.78	1.36 ± 0.28

Table 24 *Maximum (mean value and standard deviation) of the different parameters between 04:00 and 05:00. Significative differences between groups ($p < 0.05$) are marked with $*$ in the case of LR vs. HR, † in the case of LR vs. ICS and ‡ for HR vs. ICS).*

	04:00-05:00		
	LR	**HR**	**ICS**
textbf{SDNN (ms)}	144.24 ± 55.89	240.13 ± 396.73	131.36 ± 34.70
SDSD (ms)	95.16 ± 30.81	240.42 ± 489.62	127.82 ± 46.61
pNN50 (%)	52.38 ± 14.76	48.21 ± 20.05	64.85 ± 16.47
TP (ms^2/Hz)	4120.81 ± 4089.49	231689.84 ± 825884.69	2449.10 ± 1336.10
VLF (ms^2/Hz)	2635.06 ± 2635.16	121604.96 ± 433181.31	1346.69 ± 675.91
LF (ms^2/Hz)	463.38 ± 226.80	1347.62 ± 2508.45	943.22 ± 612.18
HF (ms^2/Hz)	18.18 ± 6.00	46.65 ± 83.21	24.82 ± 14.10
LF/HF (n.u.)	46.78 ± 18.71	46.16 ± 13.59	48.10 ± 21.08
SD1 (ms)	1183.18 ± 3565.86	315.40 ± 488.01	1986.45 ± 4873.05
SD2 (ms)	1238.21 ± 3529.88	399.60 ± 634.01	2015.92 ± 4830.94
SD1/SD2 (n.u.)	0.90 ± 0.11	0.95 ± 0.18	0.86 ± 0.13
S (ms^2)	4.10e7 ± 1.47e8	1288462.06 ± 4.12e6	7.59e7 ± 2.00e8
θ (^{o})	185.61 ± 118.63	208.63 ± 118.02	182.00 ± 129.94
Sh (n.u.)	5.37 ± 14.75	1.56 ± 0.49	1.56 ± 0.45

Table 25 *Median (mean value and standard deviation) of the different parameters during the whole night. Significative differences between groups ($p < 0.05$) are marked with $*$ in the case of LR vs. HR, † in the case of LR vs. ICS and ‡ for HR vs. ICS).*

	Whole night		
	LR	**HR**	**ICS**
SDNN (ms)	73.83 ± 16.06	83.09 ± 41.78	88.76 ± 29.90
SDSD (ms)	66.77 ± 22.46	78.96 ± 51.13	89.08 ± 34.11
pNN50 (%)	37.83 ± 16.01	35.43 ± 21.34	48.46 ± 12.00
TP (ms^2/Hz)	741.87 ± 264.60	1129.21 ± 1017.87	1121.10 ± 645.50
VLF (ms^2/Hz)	367.23 ± 122.42	564.42 ± 554.75	445.08 ± 210.40
LF (ms^2/Hz)	237.55 ± 129.23	363.77 ± 370.37	478.07 ± 373.76
HF (ms^2/Hz)	8.44 ± 3.68	12.90 ± 16.09	12.74 ± 7.59
LF/HF (n.u.)	27.77 ± 9.21	33.82 ± 10.08	34.73 ± 14.16
SD1 (ms)	66.05 ± 15.81	74.23 ± 46.51	83.46 ± 30.23
SD2 (ms)	97.25 ± 12.76	106.23 ± 48.38	112.20 ± 32.34
SD1/SD2 (n.u.)	0.66 ± 0.09	0.67 ± 0.11	0.76 ± 0.14
S (ms^2)	20921.01 ± 7203.24	30925.63 ± 29341.83	32173.24 ± 19323.46
θ (^{o})	45.00 ± 0.01	45.02 ± 0.06	83.46 ± 101.76
Sh (n.u.)	1.29 ± 0.14	1.27 ± 0.22	1.17 ± 0.05

Table 26 *Iqr (mean value and standard deviation) of the different parameters during the whole night. Significative differences between groups ($p < 0.05$) are marked with $*$ in the case of LR vs. HR, † in the case of LR vs. ICS and ‡ for HR vs. ICS).*

	Whole night		
	LR	**HR**	**ICS**
SDNN (ms)	36.69 ± 11.36	35.05 ± 11.23	31.45 ± 7.66
SDSD (ms)	24.57 ± 12.82	26.84 ± 17.89	33.35 ± 19.45
pNN50 (%)	18.07 ± 5.16	15.92 ± 5.22	19.32 ± 4.80
TP (ms^2/Hz)	792.09 ± 319.72	946.58 ± 584.14	793.95 ± 346.49
VLF (ms^2/Hz)	519.13 ± 197.02	647.62 ± 467.33	473.59 ± 220.40
LF (ms^2/Hz)	159.00 ± 86.96	211.58 ± 197.86	322.51 ± 238.65
HF (ms^2/Hz)	6.72 ± 3.93	7.25 ± 7.10	7.69 ± 5.40
LF/HF (n.u.)	11.44 ± 5.85	11.72 ± 4.56	11.42 ± 7.34
SD1 (ms)	41.76 ± 23.04	34.29 ± 17.81	39.20 ± 22.84
SD2 (ms)	62.66 ± 17.09	66.83 ± 17.39	54.33 ± 16.98
SD1/SD2 (n.u.)	0.23 ± 0.09	0.22 ± 0.10	0.19 ± 0.03
S (ms^2)	24897.93 ± 11043.88	26994.14 ± 13077.98	26866.20 ± 10138.10
θ (^{o})	0.35 ± 0.75	20.89 ± 74.83	38.74 ± 101.97
Sh (n.u.)	0.52 ± 0.31	0.51 ± 0.26	0.45 ± 0.16

Table 27 *Minimum (mean value and standard deviation) of the different parameters during the whole night. Significative differences between groups ($p < 0.05$) are marked with $*$ in the case of LR vs. HR, † in the case of LR vs. ICS and ‡ for HR vs. ICS).*

	Whole night		
	LR	**HR**	**ICS**
SDNN (ms)	31.76 ± 12.67	40.58 ± 29.01	33.23 ± 11.00
SDSD (ms)	24.63 ± 12.49	34.80 ± 32.07	29.15 ± 10.66
pNN50 (%)	5.56 ± 6.35	10.40 ± 13.34	9.03 ± 6.24
TP (ms^2/Hz)	144.36 ± 104.98	256.70 ± 335.97	151.83 ± 90.77
VLF (ms^2/Hz)	54.96 ± 27.95	60.66 ± 47.91	43.40 ± 22.03
LF (ms^2/Hz)	38.49 ± 35.86	95.29 ± 158.39	50.34 ± 39.04
HF (ms^2/Hz)	1.75 ± 1.11	4.07 ± 6.44	2.07 ± 1.09
LF/HF (n.u.)	12.15 ± 7.27	11.66 ± 4.48	12.99 ± 6.07
SD1 (ms)	21.59 ± 13.49	32.73 ± 33.09	27.22 ± 15.21
SD2 (ms)	39.84 ± 13.67	46.44 ± 24.66	44.05 ± 19.21
SD1/SD2 (n.u.)	0.32 ± 0.07	0.34 ± 0.10	0.40 ± 0.10
S (ms^2)	3472.95 ± 3517.01	7656.03 ± 11731.34	5067.11 ± 4974.62
θ (^{o})	27.95 ± 15.61	35.95 ± 9.36	35.78 ± 6.89
Sh (n.u.) ‡	0.55 ± 0.16	0.47 ± 0.15	0.62 ± 0.10

Table 28 *Maximum (mean value and standard deviation) of the different parameters during the whole night. Significative differences between groups ($p < 0.05$) are marked with $*$ in the case of LR vs. HR, † in the case of LR vs. ICS and ‡ for HR vs. ICS).*

	Whole night		
	LR	**HR**	**ICS**
SDNN (ms) †	158.27 ± 48.83	265.87 ± 389.20	164.91 ± 52.89
SDSD (ms) †	113.52 ± 29.82	257.03 ± 485.20	155.35 ± 41.08
pNN50 (%)	60.48 ± 10.95	59.05 ± 19.05	73.88 ± 10.40
TP (ms^2/Hz)	4693.55 ± 3734.60	232891.48 ± 825524.67	4700.95 ± 4379.92
VLF (ms^2/Hz) †	2916.59 ± 2381.18	122581.45 ± 432889.72	2511.79 ± 2387.22
LF (ms^2/Hz)	629.95 ± 268.22	1483.78 ± 2485.93	1252.10 ± 608.32
HF (ms^2/Hz)	29.02 ± 12.57	54.25 ± 82.08	35.14 ± 9.12
LF/HF (n.u.)	54.25 ± 18.00	60.27 ± 21.91	55.83 ± 24.11
SD1 (ms)	2052.78 ± 4404.69	466.78 ± 621.16	1920.47 ± 2986.38
SD2 (ms)	2095.29 ± 4367.42	555.66 ± 722.36	1967.86 ± 2979.26
SD1/SD2 (n.u.)	1.09 ± 0.19	1.08 ± 0.15	1.07 ± 0.22
S (ms^2)	6.96e7 ± 1.76e8	2.09e6 ± 4.75e6	3.58e7 ± 6.27e7
θ (^{o})	293.37 ± 74.32	291.22 ± 78.89	243.85 ± 134.83
Sh (n.u.)	5.49 ± 14.71	1.62 ± 0.78	1.36 ± 0.28